Landslide Susceptibility Mapping Using Statistical Approach: A Case study in Burji - Maddale Area, Southern Ethiopia

Dibora Hailu Mamo

A Thesis Submitted To the Department of Applied Geology

School of Applied Natural Science

Office of Graduate Studies

Adama Science and Technology University

November, 2024

Adama, Ethiopia

Landslide Susceptibility Mapping Using Statistical Approach: A Case study in in Burji - Maddale Area, Southern Ethiopia

Dibora Hailu Mamo

Advisor: Matebie Meten (Ph.D.)

Co- Advisor: Shankar Karuppannan (Ph.D.)

A Thesis Submitted To the Department of Applied Geology

School of Applied Natural Science

Presented in Partial Fulfillment of the Requirement for the Degree of Master's

In Egineering Geology

Office of Graduate Studies

Adama Science and Technology University

November, 2024

Adama, Ethiopia

Declaration

I hereby declare that this Master Thesis entitled **"Landslide Susceptibility Mapping Using Statistical Approach: A Case study In Burji-Maddale Area, Southern Ethiopia"** is my original work. That is, it has not been submitted for the award of any academic degree, diploma or certificate in any other university. All sources of materials that are used for this thesis have been duly acknowledged through citation.

Dibora Hailu ______ ______________________ ______________

Name of student Signature Date

Recommendation

We, the advisors of this thesis, hereby certify that we have read the revised version of the thesis entitled **"Landslide Susceptibility Mapping Using Statistical Approach: A case study in Burji –Maddale Area, Southern Ethiopia"** prepared under our guidance by **Dibora Hailu** submitted in partial fulfillment of the requirements for the degree of Mater's of Science in **Engineering Geology**.

Therefore, we recommend the submission of revised version of the thesis to the department following the applicable procedures.

Matebie Meten (PhD)	_____	__________________
Major Advisor	Signature	Date
Shankar Karuppannan(PhD)	__________________	________________________
Co-advisor	Signature	Date

Approval Page

We, the advisors of the thesis entitled **"Landslide Susceptibility Mapping Using Statistical Approach: A Case study In Burji-Maddale Area, Southern Ethiopia"** and developed by Dibora Hailu, hereby certify that the recommendation and suggestions made by the board of examiners are appropriately incorporated into the final version of the thesis.

Matebie Meten (PhD)	____________________	____________________
Major Advisor	Signature	Date
Shankar Karuppannan (PhD)	____________________	____________________
Co-advisor	Signature	Date

We, the undersigned, members of the Board of Examiners of the thesis by Migartu Abdissa Tukku have read and evaluated the thesis entitled **"Landslide Susceptibility Mapping Using Statistical Approach: A Case study In Burji-Maddale Area, Southern Ethiopia"** and examined the candidate during open defense. This is, therefore, to certify that the thesis is accepted for partial fulfillment of the requirement of the degree of Master of Science in Engineering Geology.

____________________	____________________	____________________
Chairperson	Signature	Date
____________________	____________________	____________________
Internal Examiner	Signature	Date
____________________	____________________	____________________
External Examiner	Signature	Date

Final approval and acceptance of the thesis is contingent upon submission of its final copy to the Office of Postgraduate Studies (OPGS) through the Department Graduate Council (DGC) and School Graduate Committee (SGC).

____________________	____________________	____________________
Department Head	Signature	Date
____________________	____________________	____________________
School Dean	Signature	Date
____________________	____________________	____________________
Office of Postgraduate Studies, Dean	Signature	Date

Acknowledgments

First and foremost, I want to express deep gratitude and praise to the Almighty Lord, who has supported, helped, and guided me throughout my research work and personal life.

My Golden acknowledgement proceed to appreciate and gratitude to my thesis advisors, Dr. Matebie Meten from Addis Ababa Science and Technology, for his invaluable academic and intellectual guidance throughout this research. His consistent feedback and encouragement greatly contributed to the successful completion of this thesis. Additionally, I would like to express my profound thanks to my co-advisor Dr.Shankar Karuppannan, Associate Professor , School of Applied Natural Science, ASTU, for his timely and enlightening advice. His continuous support and insightful direction were instrumental in shaping this work. Their knowledge, tolerance, and commitment have motivated me to strive for greatness in my studies.

I am greatly grateful to my family, who have inspired and supported me academically and personally with their constant prayers, and sacrifices. Specially my mother, Selamawit Gabre and my sister Samrawit Hailu.

I extend my heartfelt gratitude to Adama Science and Technology University for their sponsorship and the provision of all essential resources, from the beginning of my coursework to the successful completion of this study.

.

Table of Contents

Contents Pages

List of Figures

Content Page

List of tables

Content page

List of Plates

List of Abbreviations and Acronyms

AHP	Analytical Hierarchy Process
AUC	Area under Curve
DEM	Digital Elevation Model
EBCS	Ethiopian Building code Standard
GIS	Geographical Information System
GSE	Geological Survey of Ethiopia
IDW	Inverse Distance weighted
IV	Information Value
LDI	Landslide Density Index
LRM	Logistic Regression Model
LSI	Landslide Susceptible Index
LULC	Land use Land cover
NASA	National Aeronautics and Space Administration
ROC	Receiver Operating Characteristic
R- Index	Relative landslide density index
SE	Standard Error
USGS	United States Geological Survey
UTM	Universal Transverse Mercator
VIF	Variance Inflation Factor

ABSTRACT

Landslides are one of the most widespread geohazards in hilly and mountainous terrains, which often cause huge injury and loss of human life and damage to property. The present study was conducted in the Burji to Maddale area. The main objective of this study is to prepare a landslide susceptibility map for the Burji to Maddale area using the Information value and logistic regression method. A comprehensive landslide inventory of 265 landslides were created from the study area using Google Earth image interpretation. To develop the model and validate, the landside inventory map was randomly split into two sets i.e., 70% for training and 30% was used for testing. Eight landslide causative factors, including slope, aspect, lithology, distance to stream, distance to lineament, rainfall, curvature, and land use/land cover, were integrated with training landslide to determine the weight of each landslide causative factor using the models. The landslide susceptibility index maps were then produced by summing the weights of all the landslide factors using the raster calculator of the spatial analyst tool in ArcGIS. The final landslide susceptibility map was reclassified into very low, low, moderate, high, very high in both models based on the natural break method. The information value model indicates that the landslide susceptibility map was divided into very low, low, moderate, high and very high susceptibility classes accounting for 14.5%, 15.56%, 19.74%, 19.71% and 30.37% of the area respectively, similarly, the logistic regression model result accounts for, 19.90%, 7.98%, 16.04%, 20.40% and 35.65% of the area respectively. The relative landslide density index (R-index), landslide susceptibitlity index(LDI) and area under the curve (AUC) of the receiver operating characteristic curves were calculated using the training and testing of landslide data sets in order to assess the performance of the information value and logistic regression models for landslide susceptibility modelling. The information value model has a success rate of 88.6% and a prediction rate of 86.4%, whereas the logistic regression model has a success rate of 89.4% and a predictive rate of 87.1%.

Key words: *Landslide, density, information, logistic, susceptibility, training.*

CHAPTER 1

1. INTRODUCTION

1.1 Background of the study

Landslides are one of the most serious geohazards that affect most parts of the world (Achour et al., 2017; Wubalem and Meten, 2020). This geohazard often results from complex geology, unstable soil cover, high rainfall, topography, and uncertain hydrologic conditions that cause significant damage to property and human life, resulting in financial losses and disasters (Ayalew and Yamagishi, 2004; Chimidi et al., 2017; Firomsa and Abay, 2018; Beza, 2021;).

Numerous researchers have examined the phenomenon of landslides from various perspectives. A landslide can be defined as the downslope movement of rock and soil near the earth's surface under the influence of gravity (Cruden, 1991). It could manifest in different forms, including rock falls, rockslides, debris flow, soil slides, rock avalanches, and mudflow. Gariano and Guzzetti, (2016), defined a landslide as a type of mass-wasting process that occurs on both natural and human-induced slopes.

Landslides are becoming more frequent globally, driven by factors like climate change, urban expansion, deforestation, and geological changes. This rise in landslide has for reaching consequences for people's quality of life, the economy, and the environment (Kirschbaum et al., 2015).

Landslide occurrence have been documented in various region across Africa and these incidents are becoming increasingly common due to a combination of natural and human induced factors. For instance landslide reported in Kenya, Uganda, Sierra leone and Tanzania (Maina et al., 2013; Kursah et al., 2021).

Communities that are living in hilly and mountainous regions have a concern due to the heightened risks landslides pose to these areas from geoenvironmental processes, including geological, meteorological, and human factors leading to significant landslide hazards, thereby limiting development in both developed and developing countries (Woldearegay, 2013; Wubalem and Meten, 2020). The Ethiopian highlands were frequently experiencing various geohazards(Woldearegay, 2008). Landslides are the most frequently occurring problem in Ethiopia, mainly in highland areas in most parts of the country's north, south, and western regions and parts of the rift valley escarpment (Ayalew, 1999). In Ethiopia, Landslide caused significant damage, demolishing over 200 houses, closing 500km of highways, and causing 300 deaths, limiting urbanization, infrastructure development and most operations carried out on or near slopes (Abebe et al., 2010).

Minimizing a landslide hazard requires a comprehensive understanding of the contributing factors and the implementation of effective strategies. Landslides damage can be minimized by evaluating factors that are responsible for landslides such as geology, land use, rainfall, seismicity, and manmade activities, and identifying landslide-susceptibility-prone areas for strategic planning and mitigation measures (Anbalagan, 1992; Raghuvanshi et al., 2014; Girma et al., 2015; Shano et al., 2020).

Landslide susceptibility maps are crucial tools for engineers, earth scientists, and planners to select appropriate sites for agriculture, construction, other development and land use management, utilizing various methods and approaches(Meten, et al., 2015). Several methods and approaches have been proposed and used in the past for landslide susceptibility mapping. These techniques are widely classified as quantitative, semi-quantitative, and qualitative (Guzzetti et al., 1999; Kanungo et al., 2006; Shano et al., 2020). All of these approaches take into account different elements and use distinct methods for factor analysis and evaluation. Each method has unique qualities and can have advantages or disadvantages over others when compared.

Effective land use planning and management practices can reduce social and economic loss due to landslide. As it causes extensive property and human life loss globally, it is necessary to assess the landslide analysis to provide decision-makers, planers, and stakeholders with comprehensive and reliable information to understand, mitigate and manage the risk associated with highly susceptible and landslide-prone areas. Therefore, it is crucial to assess and predict the landslide susceptibility areas through a selection of appropriate methods and techniques. In order to overcome the limitations of each technique used, a combined approach of bivariate (Information value) and multivariate statistical (logistic regression) models was employed in this work in order to determine the extremely susceptible places and the most important conditioning factors that are responsible for landslide occurrence in the study area.

The current study area is prone to landslides. Its terrain consists of rift margins and highlands that are prone to sliding. The research area experiences increased slope failure.

However, the purpose of the landslide study was to provide solutions for these issues in the current study region. Property damage and fatalities are frequent outcomes of the landslide problem for many years. The goal of the current study is to produce the landslide susceptibility maps of the area so that remedial measures can be taken by the community and administrative bodies in order to avoid landslide disasters in the future.

1.2 Statement of the problem

Landslides are a common geoenvironmental problem in Ethiopia, mainly in highland areas in most parts of the country's north, south and western regions and parts of the rift valley escarpment (Ayele et al., 2014). One of the most important environmental issues affecting Ethiopia's growth is the landslide risk, which limits urbanization and infrastructure development, and most operations are carried out on or near slopes (Abebe et al., 2010).

The hilly and mountainous terrains of the Ethiopian highlands are frequently affected by rainfall-induced landslides of different types and sizes (Woldearegay, 2013). The southern Ethiopian highlands, including the current study area Burji – Maddale area is called Amaro horst is characterized by extremely deep valleys, gorges with high, steep slopes, and river incisions (where many springs are emanating) are characterized by complex surface and groundwater interaction, is affected by very complex geology, and is subjected to heavy precipitation.

The study discusses the geological features of the study area, particularly the East Africa Rift (EAR), and their impact on the stability of the slope. It is observed that Tertiary volcanic units, formed during the Tertiary period, become older outcopping and consisit highly deformed as they move northward along the rift and Amaro Horst axis(Abraham, 1989; Davidson, 1983). This suggests subsidence and basin formation, which have shaped the landscape (WoldeGabriel et al., 1991). Subsidence can destabilize slopes, cause fractures, and make areas more prone to landslides, especially during heavy rainfall or seismic events.

Lineaments such as faults, fractures, and other structural characteristics significantly destabilize a slope. These faults form steep escarpments that define the horst’s edges and indicate active tectonic processes related to the East African Rift’s extensional regime. The area’s structural geology is further complicated by cross-cutting fault systems and jointing within the bedrock, resulting from multiple phases of deformation during the region's tectonic evolution (Ebinger, 1989).

As stated by Girma et al., (2015) there were several lands over a few decades where deforestation has led to a large increase in soil erosion and runoff. These made the landslide process greater. Moreover, the study area is characterized by cultivated land, which can accelerate the dissolution of alluvium and eluvium materials present in the area. This dissolution, combined with the percolation of heavy rainfall, can lead to increased pore water pressure within the slope, further reducing its stability. The combination of active extensional tectonics and intense volcanism due to the East African Rift System suggests a high likelihood of geological hazards, particularly landslides, seismic activity, and volcanic eruptions. The rift-related morphology, seasonal rainfall patterns, and human activities, such as deforestation or land modification, further contribute to the risk of landslides and slope instability(Martínek et al., 2021).

Therefore, the study area is located in the southern Ethiopian highland with mountainous and fragile geological formations, which are affected by geological structure and heavy annual rainfall. This causes frequent large-scale landslides, as evidenced by the landslide inventory map of the area from Google Earth Image that created challenging conditions for the local population in this area, which demands a thorough engineering geological investigation of the conditioning and triggering factors and failure types and mechanism to take corrective measures. Understanding these factors is crucial for developing effective mitigation strategies and land use planning to reduce the risk posed by slope instability in the region.

1.3 Research Question

This study will address the following research questions.

- What are the key causative factors contributing to landslide occurrence in the study area?
- Which parts of the study area are highly prone to landslides?
- How can we generate the landslide susceptibility maps?
- How accurately does the landslide susceptibility model predict areas prone to landslides?
- What are the possible remedial measurements to minimize landslide occurrence?

1.4. Objectives

1.4.1. General objective of the study

The main objective of this research is to prepare the landslide susceptibility maps of the study area using Information value and logistic regression models.

1.4.2. Specific objective of the study

This study's specific objectives are aimed to:

- Identify the high-risk areas with respect to landslide occurrence.
- Prepare the causative factor maps for the area's landslide susceptibility analysis.
- Assess the correlation between landslide occurrence and causative factors in the area.
- Validate the modeled landslide susceptibility map.
- Suggest remedial and mitigation measures to reduce the landslide hazard and risk in the study area.

1.5. Significance of the study

The study area is frequently subject to the pervasive influence of landslide hazards. As such, the primary objective of this research is to prepare the landslide susceptibility map of the study area using Information value and Logistic regression models by combining landslide inventory with causative factors. Additionally, it aims to classify the factors responsible for slope failure- related issues in engineering and natural slopes are common challenges for researchers and professionals. In construction areas, instability may result from rainfall, an increase in groundwater table, or a change in stress conditions. This investigation will enhance our comprehensive understanding of the landslide and the factors that contribute to it. Moreover, it will provide valuable information on potential landslide hazards for the future maintenance of infrastructure stability, such as roads. Furthermore, it will offer concrete statistics and data demonstrating how human activities can exacerbate and increase the risk of landslides. Consequently, it can be utilized to educate the public on effective strategies for reducing socioeconomic losses and preserving the local ecosystem from the devastating effects of landslides.

1.6 Limitation

The primary challenge in the current study was the limited availability of data, including a lack of discontinued records of rainfall data from NMEA, challenges in accessing certain areas because of environmental safety concerns, and difficulties in obtaining time series images of landslide events. Although landslide maps were generated using Google Earth images, these issues constrained the study's depth.

1.7 Organization of the Thesis

This study is organized into seven chapters. Chapter One introduces landslides, describes the Burji - Maddale area in Southern Ethiopia, presents the problem statement, outlines the research objectives, highlights the significance of the study, and discusses its limitations. Chapter Two reviews literature on landslides, factors influencing landslide occurrence and their impacts (particularly in southern Ethiopia), landslide classification, components, types of landslide maps, techniques for landslide susceptibility mapping,

Chapter Three details the methods and materials employed for collecting and processing data, as well as the development of a landslide inventory tailored to the study area. Chapter Four gives a comprehensive overview of the study area, including an in-depth analysis of its geological features. Chapter Five investigates the factors influencing landslides and assesses their distribution in relation to regional geology and prior research on landslides in Ethiopia. Chapter Six analyzes the link between landslide occurrences and causative factors, creates a landslide susceptibility map using Information Value (IV) and Logistic Regression (LR) techniques, and validates the model. Lastly, Chapter Seven summarizes the study’s conclusions and provides recommendations based on the findings.

CHAPTER TWO

2. LITERATURE REVIEW

2.1 An overview of landslide

Landslides are a prevalent Geohazard in hilly and mountainous terrains, which often cause significant damage to property and human life and their hazard probability of a potentially damaging phenomenon occurring within a given period and a specific area (Girma et al., 2015; Du et al., 2017). Despite this fact, there are several methods for defining landslide hazards. According to Woldearegay, (2013), a landslide occurs when soil and rock slide downslope due to the influence of gravity without the primary assistance of a fluid-transporting agent.

Landslides, also known as slope failures, are a serious risk that might have a catastrophic impact on economies and people. Despite advances in science and technology that have improved our understanding of these risks, landslides continue to occur in developed and developing countries, with differing degrees of devastation (Guzzetti et al., 1999; Woldearegay, 2013). Woldearegay (2013), highlighted the potential for significant reduction in economic losses due to slope failures, indicating that these hazards are fairly predictable. However, Guzzetti et al. (1999), pointed out that while developing nations may experience larger casualties, industrialized countries often face severe economic losses due to landslides.

The predictions for continued landslide activities in the 21st century, as mentioned by Schuster (1995), are based on several key factors. First, increased urbanization and development in landslide-prone areas increase the potential for more frequent and severe slope failures. The combination of factors such as urbanization, deforestation, soil erosion, runoff process, and climate change suggests that the threat of slope failures is persistent and likely to increase in the coming years(Girma et al., 2015). As populations continue to grow and urban areas expand, the pressure on natural landscapes can lead to destabilization and increased vulnerability to landslides. Additionally, continued deforestation of landslide-prone areas further make this risk, as the removal of vegetation can destabilize slopes and increase the likelihood of failure.

Finally, changing climatic conditions, including increased precipitation, can also contribute to the occurrence of landslides. As climate change continues to alter weather patterns, areas may experience heavier and more frequent rainfall, which can trigger slope failures. This is a cause for concern as landslides can have wide-ranging and far-reaching impacts. Understanding and addressing the underlying causes of slope failures, such as urbanization, deforestation, and climate change, will be essential in mitigating the potential consequences of these hazards.

2.2 Types of landslide

According to Varnes (1978), a landslide can be classified into different types on the basis of the type of movement and the type of material involved. The material in a landslide mass is either used as criteria for identification and classification as a type of movement (fall, topple, slide, spread, or flow***)***, kind of material (Rock, Earth, Soil, Mud, and Debris), rate of movement, the geometry of the area of failure and the resulting deposit and many others Table (1) and Figure(1).

Table 1. Classification of slope movement (Varnes, 1978)

<table>
<tr><td colspan="2" rowspan="3">TYPE OF MOVEMENT</td><td colspan="3">TYPES OF MATERIAL</td></tr>
<tr><td rowspan="2">BEDROCK</td><td colspan="2">SOILS</td></tr>
<tr><td>Predominately coarse</td><td>Predominately fine</td></tr>
<tr><td colspan="2">Falls</td><td>Rockfall</td><td>Debris fall</td><td>Earth fall</td></tr>
<tr><td colspan="2">Topples</td><td>Rock topple</td><td>Debris topple</td><td>Earth topple</td></tr>
<tr><td rowspan="2">Slide</td><td>Rotational</td><td rowspan="2">Rock slide</td><td rowspan="2">Debris slide</td><td rowspan="2">Earth slide</td></tr>
<tr><td>Translational</td></tr>
<tr><td colspan="2">Lateral spreads</td><td>Rock spread</td><td>Debris spread</td><td>Earth spread</td></tr>
<tr><td colspan="2">Flows</td><td>Rock flow
(deep creep)</td><td>Debris flow Earth flow
(soil creep)</td><td>Earth flow
(deep creep)</td></tr>
<tr><td colspan="2">Complex</td><td colspan="3">Combination of two or more principle types of movements</td></tr>
</table>

- **Fall**; will occur if soil or rock separates from a steep slope without significant shear displacement. Subsequently, the detached material descends rapidly through the air by falling, bouncing, or rolling. In cases where the displaced mass has been undercut, the falling process is preceded by slight sliding movements that detach the material from the undisturbed mass (Cruden, 1991).

- **Toppling**: The forward rotation of a unit or units about some distinguish toppling failures pivotal point, below or low in the unit, under the actions of gravity and forces exerted by adjacent units or by fluids in cracks (Varnes, 1978).

- **Slide**: is a downslope movement of a soil or rock mass occurring on surfaces of rupture or on relatively thin zones of intense shear strain.

A, Rotational slide: This is a slide in which the surface of rupture is curved concavely upward and the slide movement is roughly rotational about an axis that is parallel to the groundsurface and transverse across the slide (Varnes, 1978).

B, Translational slide: The mass in a translational landslide moves out, down, and outward along a relatively planar surface with little rotational movement or backward tilting. This type of slide may progress over considerable distances if the surface of the rupture is sufficiently inclined, in contrast to rotational slides, which tend to restore the slide equilibrium (Highland and Bobrowsky, 2008).

- **Lateral spread**: usually occur on very gentle slopes or essentially flat terrain, especially where a stronger upper layer of rock or soil undergoes extension and moves above an underlying softer, weaker layer. Such failures are commonly accompanied by some general subsidence into the weaker underlying unit. Under certain conditions, the softer, weaker unit may squeeze upward into fractures that divide the extending layer into blocks (Highland and Bobrowsky, 2008).
- **Flows**: is a spatially continuous movement in which the surfaces of shear are short-lived, closely spaced, and usually not preserved. According to (Varnes, 1978), there are five basic categories of flows that are divided: debris flow, debris avalanche, creep, earth flow, and mudflow.

- **Complex**: Combining two or more of the above types is a complex landslide (Varnes, 1978).

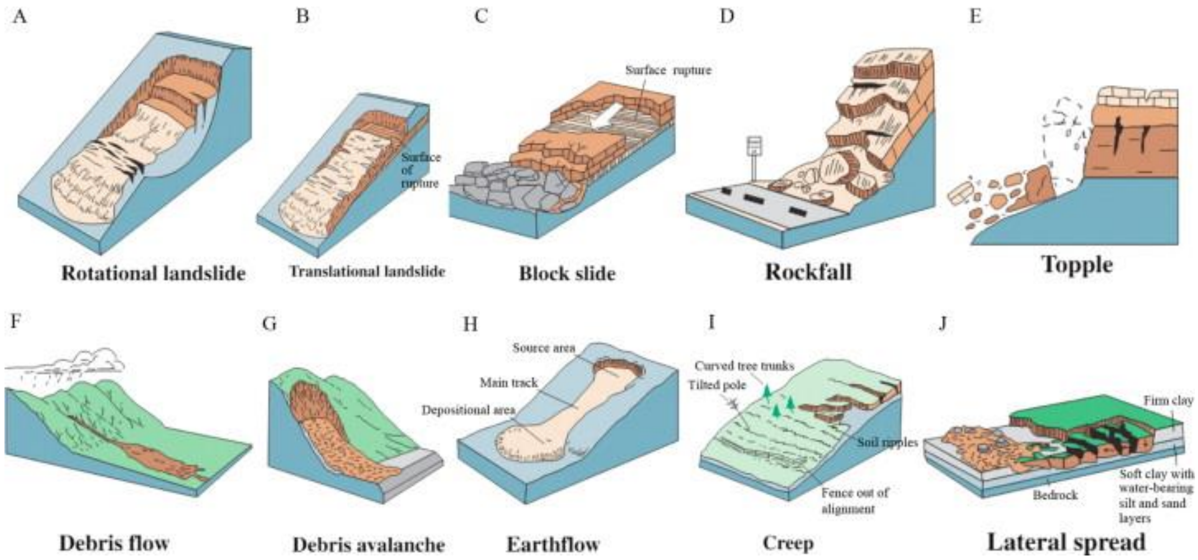

Figure 1.Types of landslide ((Mersha and Meten, 2020a))

2.2 Landslide study in Ethiopia

The actual and catastrophic effects of landslides in Ethiopia's highlands have been highlighted by numerous studies over time, despite the difficulties involved in conducting landslide research in the nation. For example, landslide occurrences in these regions have been observed by researchers including (Abebe et al., 2010; Girma et al., 2015; Shano et al., 2020; Tesfa and Woldearegay, 2021; Mebrahtu et al., 2021; Kebeba et al., 2024)

Abebe et al., (2010): studied the landslide in the Ethiopian highland and rift margin that have been widely studied due to the region's unique topography and geological features.

Girma et al., (2015); Conducted an evaluation of landslide hazards in the Ada berga district in the central Blue Nile (Abay) basin in central Ethiopia. During field investigation and GIS- based inventory, 45 landslides were found. These studies incorporate eight causative factors for LSM including, lithology, land use/ land cover, soil type, aspect, curvature, elevation, and groundwater condition was compiled. They use GIS techniques to map by combining statistical and probabilistic approaches.

Shano et al., (2020): study on the Gamo highlands used the frequency ratio model to map vulnerability and inventory of landslides, revealing 1,554 historical sites. The research, which considered nine parameters, provided valuable information on landslide distribution and initiators. The study also created a landslide susceptibility map, verified using a ROC curve.

Mebrahtu et al., (2021): issued in Ethiopia northwestern plateaus, particularly in the Debre sina area. Landslide problems are caused by complex geological settings and rugged topography.

Tesfa and Woldearegay, (2021): Landslides in Ethiopia, especially in steep areas like the Wabe Shebelle Gorge, cause damage to roads, farmlands, and infrastructure. Factors influencing slope failures include slope angle, aspect, lithology, slope curvature, elevation, and land use. Mitigation measures include proper drainage and retaining structures.

Kebeba et al., (2024): The study conducted in the Maze watershed of southern Ethiopia employed frequency ratio and analytic hierarchy process (AHP) techniques to evaluate landslide susceptibility. Through a combination of remote sensing and field investigations, 793 landslide polygons were identified. The landslide inventory data was divided into training and validation datasets, and the study analyzed various factors such as slope, aspect, curvature, lithology, land use, vegetation index, and proximity to faultlines.

2.3 Landslide causative factors

Landslide poses a significant hazard in the highlands of Ethiopia, impacting human life, infrastructures and the environments. The research done by Das et al. (2012); Bhutia et al. (2020); Mersha and Meten (2020a) have highlighted the destructive nature of landslides in this area. It is essential to understand the controlling factors that contribute to landslide occurrence in the region to effectively assess landslide risks, mitigate their impacts, and plan for land use to minimize the land (Dai et al., 2001). Variables that increase a slope's susceptibility to movement without directly producing it and putting it in danger of instability are known as landslide-influencing variables. These elements create the conditions for possible landslides. However, a slope that was previously in a marginally stable state begins to move when a triggering element is applied. The dynamics of landslides in highland areas of Ethiopia require an awareness of the difference between triggering and influencing factors. Woldearegay (2013) emphasizes the importance of identifying both influencing and triggering factors to predict and prepare the future landslide susceptibility effectively.

2.3.1 Geological factor

The geological factors play a significant role in influencing landslides. The types of rock and soil represented in the area, as well as their structural properties and permeability, can determine the susceptibility of the area to landslides. The lithology, or sorts of rocks, differs in composition and structure, which adds to the material's strength. As a result, stronger rocks are less likely to have landslides than weaker rocks because they can withstand greater driving pressures (Kanungo et al., 2006).

Lithology/ Geological structure

The physical properties of geological features significantly influence the occurrence of landslides. Faults and lithology are two kinds of these geological formations. Each type of geological unit has its own distinct characteristics, specifically in terms of the rock and mineral composition (lithology). For example, large and solid rock formations, such as granite or basalt, are typically very strong and do not erode easily. This means they are more resistant to processes like weathering or erosion that would break down weaker rocks more quickly(Anbalagan and Singh, 2001). Slope material movement is more common in locations close to fault lines than it is in areas farther away. The permeability, strength, and deformation of slope engineering might exhibit anisotropy due to the impact of discontinuities and material nature.

2.3.2 Slope gradient

It is well-established that gravity is the primary force causing slope movements. Previous studies have indicated that most reported cases of debris/earth slides/flows and rockslides occur on slopes with angles between 15 and 45 degrees. Research by Ayalew and Yamagishi, (2004a); Ayenew and Barbieri, (2005); and Woldearegay, (2005) suggest that the low probability of landslides on gentler slopes is due to the higher factor of safety, requiring a higher water table to trigger failure. Conversely, the rare of major debris/earth slides and flows on slopes steeper than about 50 degrees is attributed to the minimal or nonexistent thickness of unconsolidated deposits, as these steeper terrains are typically composed of slightly to moderately weathered rocks.

2.3.3 Slope shapes

The influence of slope shape on landslide occurrence and behavior is a critical aspect of geomorphology. The slope shape can affect the stability of soil and rock on a hill or mountain, impacting factors such as water drainage, soil saturation, and the types of materials involved in a potential landslide. As slope shape controls the distribution of water on a slope, it substantially impacts the occurrence and dynamics of landslides. Plan curvature controls soil-water content and converging/diverging flow by indicating concentration or divergence of flow (Anderson and Burt, 1978a). In Ethiopia, planar terrain is not immune to landslides, typically occurring in concave places. Concave locations have more sensitivity to subsurface erosion, convergent water flows, and thicker unconsolidated deposits, all of which increase the risk of landslides caused by rainfall (Woldearegay, 2013).

2.3.4 Slope modification

Slope modification is essential in areas where human activities or natural processes, can significantly influence the stability of slopes and the occurrence of landslides. Activities such as cutting into a slope can reduce the overall stability by removing material that supports the slope. According to Varnes, (1978), slope cutting alters the natural conditions of the slope, which may increase the likelihood of landslides. In Ethiopia's highlands, the majority of the rainfall that has resulted in landslides happened in locations close to streams, topographic fractures, or places where gully erosion is actively occurring (Ayalew, 1999; Woldearegay, 2005). Modification of natural drainage patterns can increase water saturation in slope materials, leading to landslides. The structures can create impermeable surfaces, reducing slope shear strength and triggering landslides in Ethiopia's highlands, due to land degradation and erosional processes (Woldearegay, 2013).

2.3.5 Hydrological factor

Landslides in Ethiopia are triggered by prolonged and heavy rainfall, mainly at the end of the rainy season. Factors such as high groundwater table, pore water pressure, drainage patterns, and river erosion are all factors that can increase the risk of slope instability and landslides. The significant rainfall-triggered landslides in the Ethiopian highlands are thought to be caused by a combination of (a) elevated groundwater levels reducing the effective stress within slope materials, making the soil more susceptible to failure, and (b) pore-water pressure also affects slope stability as it increases the pore spaces between soil particles, making it weaker and more prone to landslides (Woldearegay, 2013). Poor drainage patterns can saturate the soil, increasing its weight and reducing its shear strength. River erosion can also weaken the foundation of slopes, increasing the likelihood of landslides.

2.3.6 Human induced factor

Landslides are caused by various human activities, including undercutting during construction, overloading, clearing trees, deforestation, urbanization, agricultural practices, road construction, and dam construction. These activities weaken the stability of slopes, increase soil erosion, and disrupt natural drainage patterns. Urbanization also increases surface runoff and soil saturation, further exacerbating landslide risks. Agricultural practices, such as terrace construction, excessive irrigation, and improper land management, along with infrastructure projects like road and dam construction on hilly terrains, can significantly increase landslide risks. For instance, road construction frequently involves cutting into slopes using mechanical methods or blasting, often carried out without sufficient planning (Ermias et al., 2017). The loose material from excavation is frequently deposited downslope, leading to the formation of unstable slope masses. (Raghuvanshi et al., 2014a). Similarly, cultivation practices on steep hill slopes contribute to instability; to prepare land for farming, steep slopes are often regraded into gentler slopes, altering the natural slope geometry and increasing the potential for landslides. By understanding and addressing these influences, we can work towards a safer and more sustainable environment.

2.3.7 Vegetation cover factor

While vegetation changes the mechanical and hydrological characteristics of the soil, it has a major impact on slope stability. Its root systems contribute to the strength and cohesiveness of the soil by binding soil particles together (Greenway, 1987). Additionally, forests are essential for slope stability because they lessen the effects of climatic agents on natural masses. Because of deforestation and ground degradation, landslides are more common in Ethiopia in areas with scant vegetation and shallow roots. Slopes become more susceptible to erosion and landslides as they lose their canopy cover and shielding roots. Slope sustainability can be increased, and landslide dangers can be decreased by encouraging deeper roots and protecting forests.

2.3.8 Seismicity Hazard

According to Highland and Bobrowsky (2008) suggest that earthquakes that occur in steep landslide-prone areas significantly increase the probability of landslides. This increased likelihood is attributed to several factors, including ground shaking from the earthquake, liquefaction of susceptible sediments, and shaking-induced dilation of soil materials, which can lead to rapid water infiltration. The damage caused by earthquake-induced landslides is substantial, as it can result in the destruction of homes and other structures, blockage of roads, and damage to utilities(Hasegawa et al., 2009).

Landslides triggered by seismic activity generally exhibit similar internal dynamics and morphology to those caused by non-seismic factors, but they tend to be more sudden and widespread. The most frequent types of earthquake-induced landslides are rockfalls and rock fragment slides, which typically occur on steep slopes(Jibson et al., 1994).

2.4 Techniques for Landslide Susceptibility Mapping

Landslide hazard mapping deals with dividing a terrain into zones that are basically characterized by the spatial and temporal probability of landslide occurrence, including a description of location, volume, and prediction of future landslide occurrence in an area. in order to evaluate and zone the area for potential landslides, landslide hazard evaluation and zonation techniques may be applied (Anbalagan, 1992). The landslide susceptibility mapping techniques can be classified as Qualitative, semi-quantitative and Quantitative approaches (Shano et al., 2020).

2.4.1 Qualitative Approach

This approach includes distribution analysis or inventory, geomorphic analysis, and expert (heuristic) evaluation techniques (Shano et al., 2020). A landslide inventory map is the method used to identify past landslides and compile and record the details of each data on location, dimensions, causative factors, and frequency of occurrence (Dai et al., 2001, 2002; Girma et al., 2015). Whereas expert (heuristic) techniques are where the experts identify judgments or make decisions on the types and degree of hazard for each area by using a direct or indirect approach (Dai et al., 2002; Girma et al., 2015; Shano et al., 2020). The landslide hazard is an evaluator based on quasi-static variable. This simple method is based on data primarily from the field and well supported by the judgement and experience of an expert (Raghuvanshi et al., 2014a,).

The direct methods of mapping the landslide hazard and susceptibility are geomorphic analysis approaches. These methods depend on the investigator's capacity to calculate both actual and prospective slope failure (Guzzetti et al., 1999) . The majority of information about the many causes of landslides comes from remote sensing; in-person field research is rarely used to collect information for these purposes. Using aerial photos, the geomorphic mapping of landslide risk is completed.

2.4.2 Multi-criteria decision analysis methods

These methods are semi-quantitative approaches that play a crucial role in the evaluation of landslide susceptibility (Erener et al., 2016) and hazard zonation studies(Bera et al., 2019).

These methods are particularly valuable when dealing with complex phenomena such as landslides, where various factors and criteria need to be considered simultaneously. The methods categorized under multi-criteria decision analysis are favored for their ability to integrate different factors and criteria in a systematic and structured way. These methods include analytical hierarchy process, fuzzy set-based analysis, weighted linear combination, and ordered weighted average(Shano et al., 2020).

Analytical Hierarchy Process (AHP) is used method for decision-making and problem-solving, particularly in the field of landslide susceptibility evaluation and hazard zonation studies (Shano et al., 2020). It allows for the systematic structuring of complex problems into a hierarchical format, where the various factors and criteria can be compared and analyzed in a consistent manner. The fuzzy set-based analysis is a semi-quantitative method used in landslide susceptibility evaluation and hazard zonation studies to handle uncertainties and vagueness in data assessment. It helps researchers make informed decisions based on available information. Weighted linear combination is a simple yet effective method for integrating multiple criteria in landslide susceptibility evaluation, providing a transparent and systematic approach to assessing the overall hazard.

2.4.3 Quantitative Approach

These techniques include statistical approach, deterministic, probabilistic, and artificial intelligence (Shano et al., 2020).

2.4.3.1 Statistical approach

These types of quantitative techniques are commonly used for landslide susceptibility and hazard zonation (Girma et al., 2015; Shano et al., 2020). These approaches are based on numerical value driven by the relationship between spatial distribution and landslide-controlling factors (Guzzetti et al., 1999; Girma et al., 2015; Mengistu et al., 2019) . The main challenge of statistical methods is gathering data on the distribution of landslide and the elements that contribute to them over extensive regions over extended periods of time (Van Westen et al., 1997; Girma et al., 2015). Statistical methods can be classified into bivariate and multivariate.

Bivariate statistical analysis

In bivariate statistical analyses, each individual factor is compared to the landslide inventory. The weighted value of the classes used to categorize every parameter is determined on the basis of landslide density in each class. For landslide studies,, it is generally assumed that the combination of various causative factors may lead to a landslide in a given area. Consequently, assessing the factors and their relationship to previous landslides in the area may serve as the basis for estimating potential areas where landslides may occur (Shano et al., 2020). This method includes various statistical techniques: Frequency ratio, weighted overlay model, weight of evidence model, information value model, and fuzzy log methods.

Multivariate statistical method

The Multivariate method evaluates all relevant factors, weighting their relative contribution to landslide susceptibility and hazard zonation based on their relationship to total landslide susceptibility in the area (Dai et al., 2001; Getachew and Meten, 2021). The data layer on the presence or absence of landslides is developed using statistical analysis and methods for landslide susceptibility analysis, which is used to calculate the percentage of landslides for each pixel. For landslide susceptibility and hazard zonation, multivariate statistical techniques such as logistic regression model, multiple regression models, and Discriminant analysis are commonly used (Guzzetti et al., 1999; Kanungo et al., 2006; Shano et al., 2020).

2.4.3.2 Deterministic approach

This technique is a kind of quantitative approach. As stated by Girma et al., (2015), this technique determines the hazard in terms of the probability of failure or the factor of safety by taking into account a variety of internal and external trigger variables. These techniques are useful for mapping large-scale hazards for construction sites, requiring knowledge of geological and geotechnical aspects, potential failure modes, and factors like slope geometry, discontinuity characteristics, groundwater conditions, and surface drainage (Raghuvanshi et al., 2014a; Girma et al., 2015; Shano et al., 2020). These techniques are time-consuming and are limited to small areas at the scale of a single slope.

2.4.3.3. Probabilistic approach

Landslides significantly threaten to human lives and infrastructure, making it essential to assess a given area's susceptibility and hazard zonation. One method used to evaluate landslide susceptibility and hazard zonation is to establish the degree of relationship between past landslide distribution and the causative factors. This relationship is then converted to a value based on a probability distribution function. Using a probabilistic approach, researchers can predict landslide distribution's spatial and temporal probability in a particular area. This approach allows for a comprehensive assessment of the potential for landslides in specific locations and provides valuable information for land use planning and risk mitigation strategies. This model is supposed to determine landslide hazards at the basin scale, predicting where landslides will occur, how frequently they will occur, and how large they will be (Guzzetti et al., 1999).

2.5 Role of GIS technologies to the mapping of Landslide susceptibility

GIS application is in landslide susceptibility mapping by providing powerful tools for data integration, analysis, visualization, and decision-making for spatially referenced data (Guzzetti et al., 1999). The use of geographic information systems (GIS) for landslide susceptibility modeling has become more common due to the development of commercial systems and rapid access to data obtained through global positioning systems and remote sensing techniques(Chen et al., 2016). To minimize the risk associated with landslide susceptibility, the use of modern and emerging techniques like high-resolution satellite data, digital elevation model (DEM 30*30m), and spatial analysis using geographic information systems (GIS) are essential in determining the landslide susceptible zones, hazard analysis, and risk assessment. These technologies include data acquisition and integration, terrain analysis, spatial data modeling, risk assessment and prediction, and decision support systems. By incorporating historical data, monitoring information, and environmental factors, geospatial technologies help develop predictive models that estimate future landslide probabilities, prioritizing mitigation efforts and land-use planning. By leveraging geospatial technologies, researchers and practitioners can effectively analyze and map landslide susceptibility, thereby supporting better understanding, planning, and mitigation of landslide hazards.

Literature on the southern Ethiopia identifies steep slopes, complex geology, and intense rainfall as key factors increasing landslide risk (Woldearegay, 2013). Studies emphasize slope inclination, soil type, and tectonic activity, worsened by human activities like deforestation (Ayalew and Yamagishi, 2004). GIS-based and statistical models have been widely used to map susceptibility zones, aiding in hazard assessment. These findings highlight critical factors and tools for effective landslide mitigation in Southern Ethiopia (Girma et al., 2015).

CHAPTER 3

3. MATERIALS AND METHODS

3.1 Data type and source

The methods employed for achieve research include desk-based review, data collection, processing, and analysis. Data collection involved primary data obtained from google Earth image including landslide inventory mapping, geological mapping. Secondary data sources from different organization, and analyses from core samples, were also utilized. This combined data was processed and analyzed using Information Value and Logistic Regression models to assess landslide susceptibility, allowing for a comprehensive evaluation and presentation of the findings.

Table 2.Data types and source

Data type	**Map**	**Data format**	**Source**
Inventory data	Landslide inventory map	Vector	-Digitize from Google Earth Pro
Geology	Lithology map	Vector	-Digitize from a geological map of Agree Mariam provided by GSE at 1:250,000
DEM	Slope,aspect, curvature map	Raster	-Derived from 30m DEM using ArcGIS.
Hydrology	Distance to stream map	Vector	-Digitize from the topographic map at a scale of 1:50,000 and buffering using distance to Euclidian
Climate data	Rainfall map	Vector	- NASA power https://power.larc.nasa.gov/data-access
Google Earth Image	Distance to lineament map Land use land cover map	Vector	-Extract from Google Earth Pro and buffering using distance to Euclidian -Extract from Google Earth Pro

3.2 Materials and Software's

3.2.1 Materials

Materials are essential resources and instruments used to research and address landslide issues. They play a crucial role at every stage of the research process, including gathering and analyzing data and interpreting findings. A laptop, topographic maps, and stationery supplies like notebooks, and pens are among the materials used in this study. Throughout the investigation, the laptop was used to execute a variety of activities, and stationery was used to collect and organize data and observations. From the beginning to the end of the study, these tools made completing the tasks at hand easier.

3.2.2 Software's

There are some software used for this study.

- ArcGIS 10.8: is primarily used for creating and analyzing the thematic maps and for creating a landslide susceptibility map by using information value and logistic regression. Geostatistical tools are also used to identify the relationship between landslide occurrence and environmental factors.
- Surfer 18.1and Global mapper: used to create 3D models from elevation data, helping visualize the terrain and identify potential landslide areas.
- IBM Spss 22: statistical analysis used to develop predictive models using regression and test model accuracy.
- Microsoft Excel: data management is useful for organizing rainfall data before importing it to ArcGIS software.
- Microsoft Word: This is used to write whole papers.
- Google Earth Pro: used to extract geological features and analyze past events (landslide polygon) and land use of the study area.

3.3 Data collection

3.3.1 Primary Data

A highly effective Google Earth image was used to build the landslide inventory map. The maps showing the causal factors and the landslide inventory for the research areas were largely validated due to this data. Thus, Google Earth Pro was used to produce the main data for the landslide inventory. The following tasks were finished during the investigation phase. Google Earth Pro was used to obtain pertinent information on the locations, processes of failure, and sizes of previous landslides. Google Earth Pro produced a map of land cover land use. Google Earth Pro was used to locate lineaments.

3.3.2 Secondary Data

During this stage, different secondary data were collected from various organizations and sources, including topographic maps, Digital Elevation Models (DEM) (30 m ×30 m resolution), geological maps of the study area with scale of 1:250,000, reports, maps, and meteorological data. These have provided essential information about the study area's elevation, terrain, geological composition, historical and contextual information, and climatic conditions. Meteorological data have been collected from the Ethiopian National Meteorological Agency and NASA to assess weather patterns and the influence of climate change, Ethiopian Space Science and Geospatial Institute of Ethiopia, United States Geological Survey (USGS), Ethiopian Geological Survey (GSE), and Google Earth image provide high-resolution satellite imagery for detailed visual information.

3.4 Landslide Inventory Data

Landslide susceptibility mapping starts with creating a landslide inventory map, as outlined by Ayalew and Yamagishi, (2004). Inventory mapping is a critical first step in assessing areas prone to landslides serving as the foundation for identifying potential hazard zones. Guzzetti et al., (2000) highlighted the inventory maps prepared by different methods depending on the extent of the study area, the scale of base maps, and the resource availability. Digitalized versions of the landslide inventory map were obtained via Google Earth for inaccessible landslide locations such as gorges, valleys, high cliffs, and river banks, and from high-resolution tracking using GPS during field surveying where the area is accessible to locate landslides. The landslide inventory map using Google Earth image interpretation was digitalized for this investigation.

The landslide inventory map serves as the most crucial data source as it provides detailed information on the exact locations where landslides have occurred. The type of landslide, its level of activity, and, if feasible, the date it occurred and the extent of the damage it caused should all be recorded in the data about landslides.

3.5 Landslide Susceptibility Mapping Methods

3.5.1 Information value method

The information value model (IV) is a bivariate statistical method that is commonly applied for landslide susceptibility mapping. The information value method has emerged as a popular approach for spatial landslide prediction and zonation and has been employed by many researchers (Yin and Yan, 1988; Achour et al., 2017; Mengistu et al., 2019; Wubalem and Meten, 2020). Information value is to predict the spatial relationship between landslides and landslide factor classes (Wubalem and Meten, 2020).

- Information values of causative factors can help identify potential landslide areas, aiding in landslide hazard zonation. This is crucial for assessing the potential susceptibility of an area to landslide, allowing for better risk management and mitigation.
- This method is particularly effective in calculating the weight for each factor class by comparing each class's landslide density to the area's total landslide density according to Yin and Yan (1988), which was later defined by Van Westen (1993).

The information value can be determined based on the presence or absence of the causative factor classes within the past landslide (Shano et al., 2020). The method for determining factor classes within past landslides is by combining landslide maps with causative factor maps. This approach allows for the identifying and categorizing of causative factors that contribute to landslide occurrence. By overlaying the causative factor map on the landslide inventory map, the researchers can determine the landslide density in specific areas (Mengistu et al., 2019). According to Yin and Yan (1988), positive information values indicate a strong relationship with landslide occurrence.

This work identifies the causative factors contributing to slope instability in a specific area. The selected causative factors including lithology, slope, aspect, rainfall, curvature, distance to lineament, distance to stream, and land use land cover, were chosen based on their relative importance in inducing slope instability, which was determined through the nature of the study area, literature as there are no universal guidelines regarding the selection of factors in landslide susceptibility mapping.

The information value can be computed using Yin and Yan (1988), as shown in

$$\mathrm{IV} = \log(\text{ conditional probability}/\text{prior probability}) \quad \text{…….(Eq. 1).}$$

$$I(H, Xi) = \log \frac{\text{Npix(Si)/Npix(Ni)}}{\Sigma \text{ Npix(Si) } /\Sigma \text{ Npix(Ni)}} \ldots \ldots \ldots \ldots \ldots \ldots \ldots \ldots \ldots \ldots \text{(Eq. 2)}$$

Whereas I(H, Xi) is the information value of a factor class, Npix(Si) is the number of Pixels of a landslide within class I; Npix (Ni) is the number of pixels within class I; Σ Npix (Si) is the number of pixels of a landslide within the entire study area; Σ Npix (Ni) is the number of pixels within the entire study area. Therefore, the landslide susceptibility Index (LSI) for each pixel will computed by summing the information values of each factor class as follows:

$$LSI = \text{ IV lithology } + \text{ IV elevation } + \text{ IV slope } + \text{ IV aspect } + \text{ IV LULC } + \text{ IV proximity to road} + \text{ IV proximity to stream} ---- \text{(Eq. 3)}$$

Where; IV = information value

3.5.2 Multicollinearity diagnosis

Logistic regression evaluations cannot be computed correctly in cases where the predictive variables have a perfect linear connection. When two or more predictors in the logistic regression model are associated, multicollinearity occurs, producing redundant response variable information (Hosmer and Lemeshow, 2000). Thus, this redundancy must be addressed in this study before doing logistic regression. Utilizing SPSS, multicollinearity was assessed via the Variance Inflation Factor (VIF) and Bivariate Pearson correlation, two highly recommended and adaptable techniques for multivariate analysis.

3.5.3 Logistic regression method

The logistic regression model is among the multivariate statistical methods most commonly applied for spatial prediction of landslide susceptibility maps. It has been recognized as one of the most mature, well-adopted, and reliable approaches proposed for assessing and predicting landslide susceptibility. The logistic model determines the most landslide-influencing factor.

- This method is capable of predicting a binary response variable, such as the presence or absence of landslides through categorical and continuously scaled predictors(Pradhan, 2010; Wubalem and Meten, 2020).
- One of the advantages of logistic regression is its ability to convert a binary dependent variable into a logit variable, which enables the establishment of a

multivariate regression relationship between the variables. (Hosmer and Lemeshow 2000).

By connecting the range of real numbers to the 0–1 range, the logistic regression model is a kind of generalized linear model that expands on the linear regression model (SPSS, 2007). To explain the fluctuation in the dependent variable concerning its binary condition of the presence or absence of landslides, it employs the independent variables in a linear combination(Dai et al., 2002).

$$P = 1/ (1 + \exp\wedge \{-z\} \dots\dots\dots\dots\dots\dots\dots\dots\dots\dots\dots\dots\dots . \dots\dots\dots \text{ (Eq. 4)}$$

Where: P is the probability of landslide that estimated values from 0 to 1.

exp ^ {-z} = exponential function, where exp is a number (approximately 2.718281828) and z is landslide causal factor and assumed as a linear combination which is expressed as Xi=(i=1,2…n)

$$z = b0 + b1X1 + b2X2 \dots + bnXn \dots\dots\dots\dots\dots\dots\dots\dots\dots\dots\dots\dots\dots .. \dots .. \text{(Eq. 5)}$$

Where; b0 is the intercept; b1, b2… bn is the coefficient value for each independent variable indicating its contribution and strength of relation with the dependent variable, whereas X1 X2… Xn is the predictor variables.

3.6 Data Processing and Analysis

The data from primary and secondary were systematically grouped and analyzed using different techniques and computer programs.

- Landslide inventory polygons were created by Google Earth images for accessible and inaccessible areas.
- Thematic map layers of causative factors maps were prepared using secondary and primary data in Arc GIS v 10.8, and parameters responsible for past landslides were evaluated.
- Then, landslide susceptibility index maps were generated.
- Finally, Validation was done for the landslide susceptibility maps obtained from training landslides and the factor maps from the two models using validation Landslides. The accuracy of the results of the two models was evaluated through the ROC curve of the analysis tool in SPSS software and the R-index. The AUC value was obtained in the end to select the optimal model.

3.7 Methods

Inorder to achieve the objective of study the following procedure.

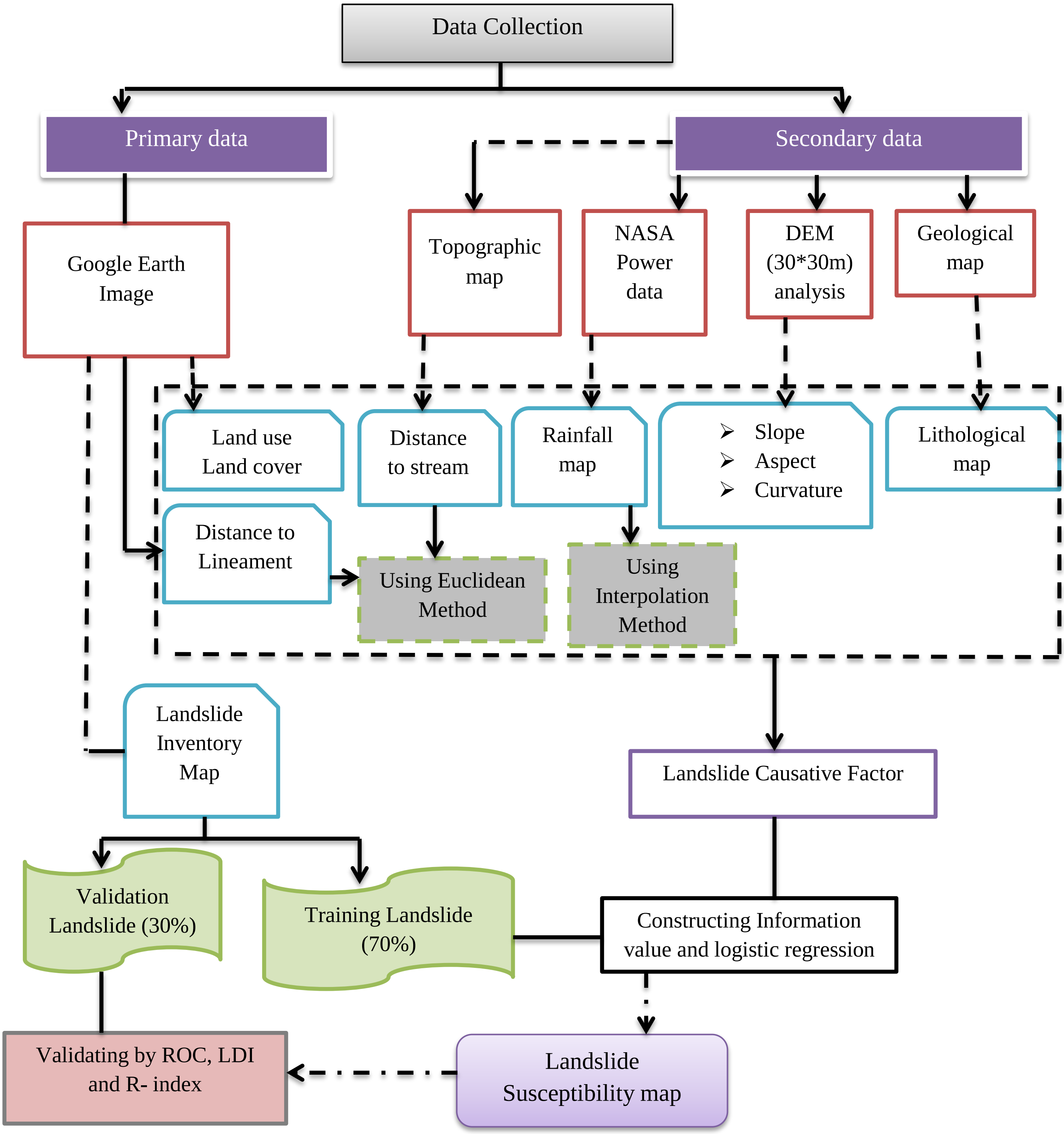

Figure 2.Flow charts of methods

CHAPTER 4

4. DESCRIPTION ABOUT THE STUDY AREA

4.1 Location of the study area

The present study area is located in a part of South Regional state of Ethiopia, which is 262km from Hawassa and 536km from Addis Ababa the capital city of Ethiopia with an area coverage of 250 km^2. It is geographically defined by coordinates between 5°31'03" to 5°41'01" N and 37°42'50" to 37°50'26" E. The study area (Figure 2) is a mountainous area that is characterized by mountain peaks, deep gorges (valleys), plateaus, and undulating topography with minimum and maximum altitudes of 909 m and 2769 m.

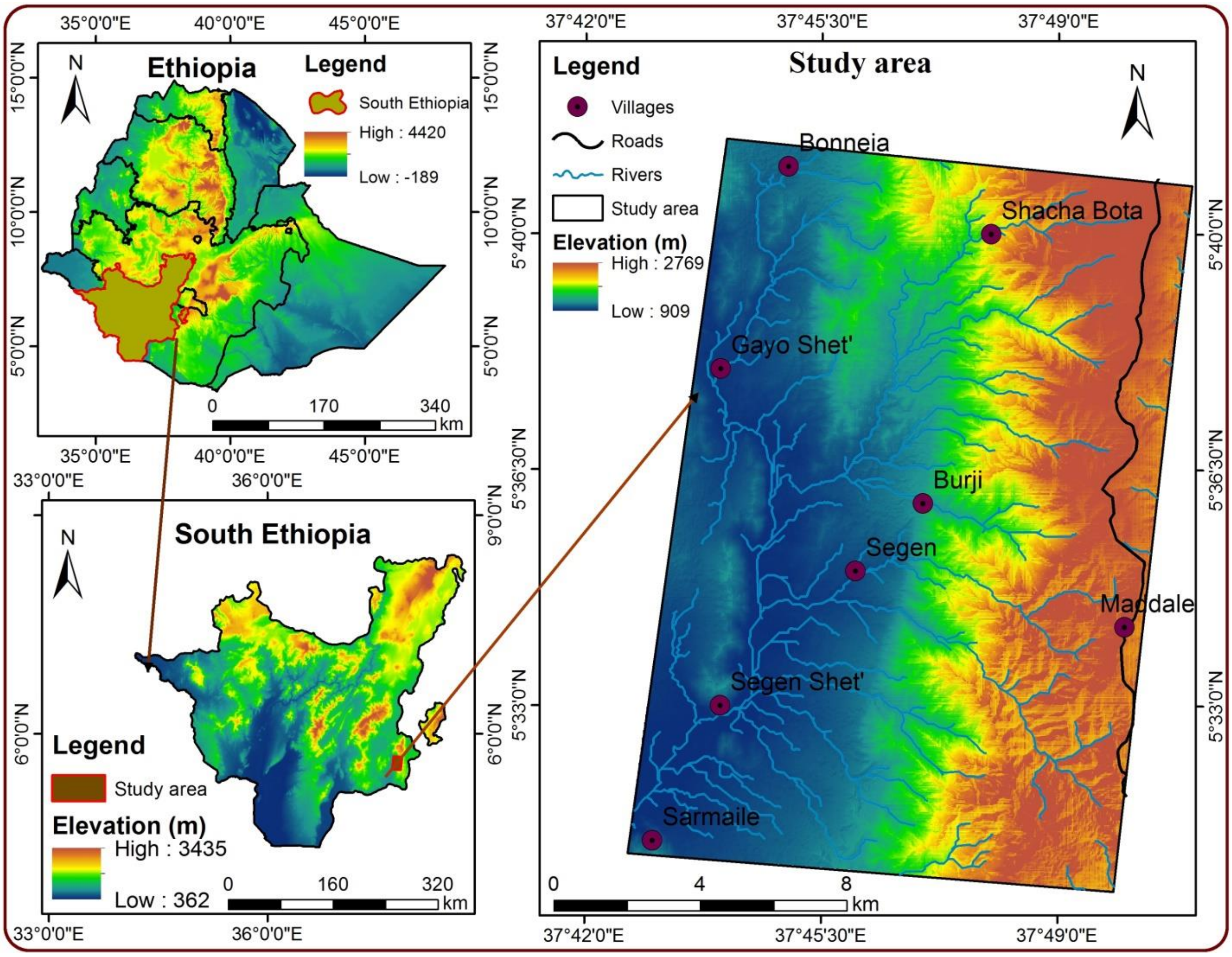

Figure 3.Study area locations

4.2 Physiography and Drainage Pattern

The study area is located in the southeastern part of the Ethiopian plateau, predominantly covered by volcanic formations. Southeastern Ethiopia is affected by the southern part of the Ethiopian Rift, which consists of a mix of narrow and wide ridges and valleys. The study area(Figure 3), ranges from the lowest peak elevation of 909m to the highest peak elevation of 2769m. The study area has a significant elevation difference of over 1500m. The Amaro horst, rising majestically above its surroundings, is an uplifted block that extends from the northern edge of the Gayo sheet southwards to the Segen River, which is gradually decreasing in elevation. To the west, it is bordered by the Chamo and Segen valleys, and to the east by the Gelana Valley. The main river that flows continuously is the Gelana River which moves towards the north. The physiography of Amaro Horst is characterized by mountain peaks, deep gorges (valleys), plateaus, and undulating topography. There are also many rivers and streams which cross the study area. These streams and rivers start from the North and Northeast part of the study area and drain to the west and finally to the Galena River(Figure 4).

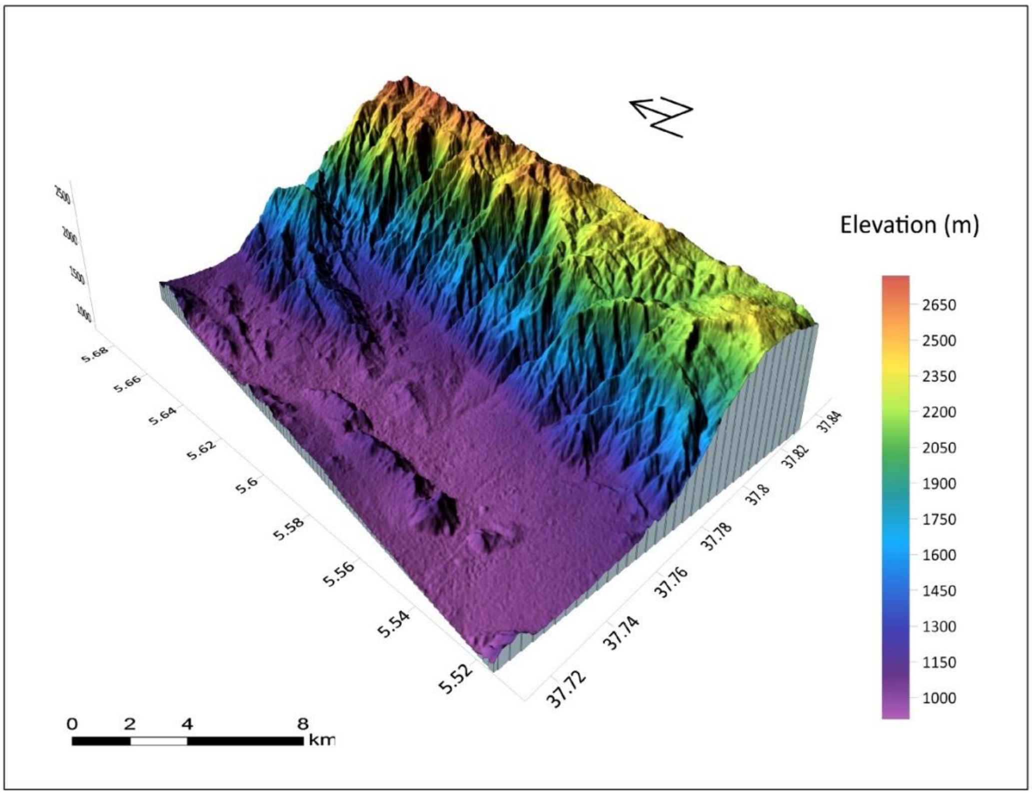

Figure 4.Physiographic map of the study area

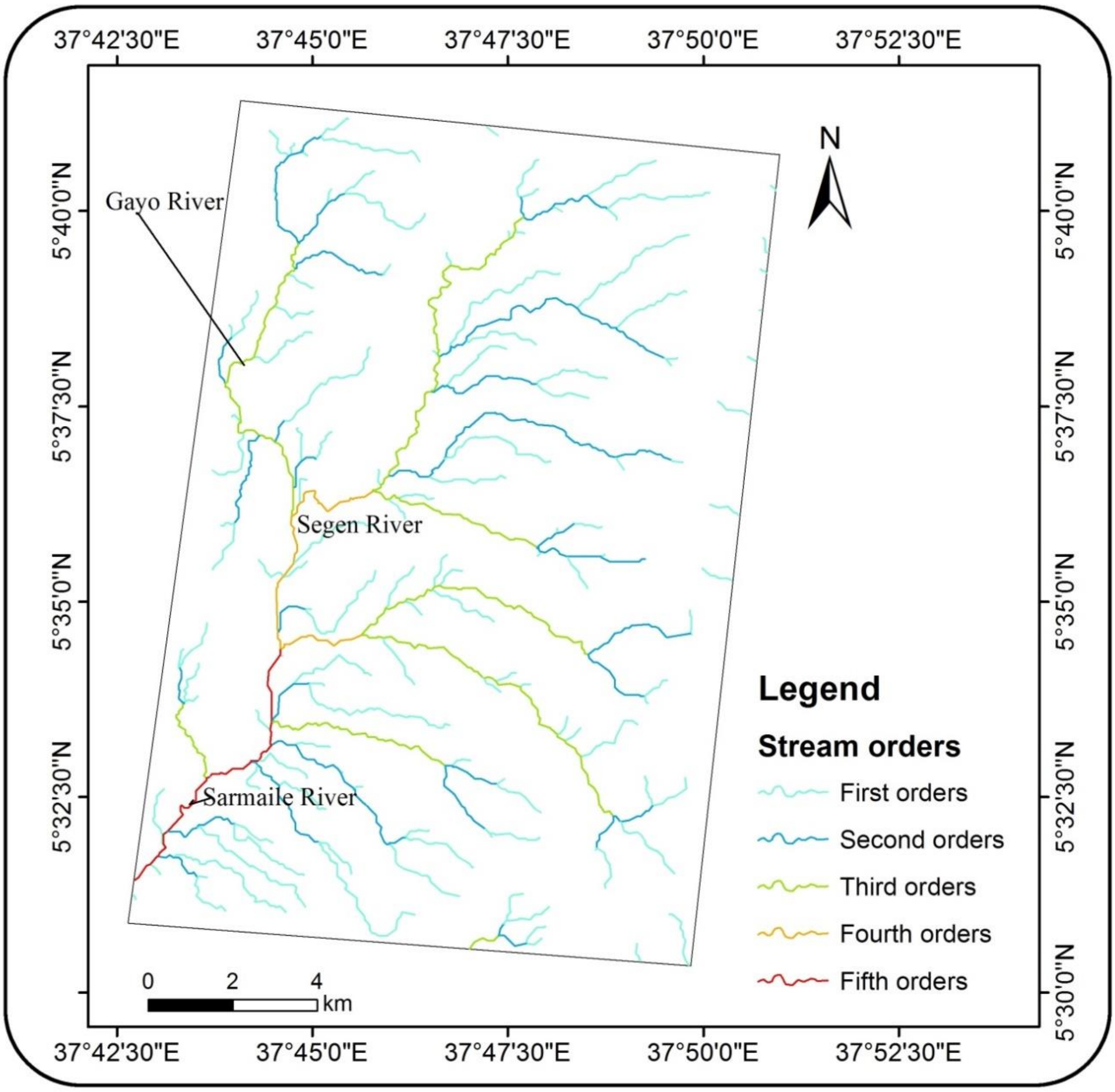

Figure 5.Drainage map of the study area

4.3 Climate Characteristics of the Area

This study analyzed 12 years of rainfall data from NASA power larc to understand the average annual and monthly rainfall patterns in the Ethiopian highlands, an area known for high rainfall variability. High rainfall variability is common in the Ethiopian highlands. The mean annual rainfall varies from 500mm to 2000mm (Woldearegay, 2013). The study area is characterized by extreme variation in topography. The study area lies in the humid to semiarid areas, which are classified as having an average annual rainfall (Figure 5b). The highest monthly average precipitation in the study area was 310.36 mm, which occurred in April. This indicates that April marks the beginning of a period of heavy rainfall in the region. The area experiences two distinct rainy seasons: the first spans from

April to June, during which significant precipitation is observed, with April being the wettest month. The second rainy period occurs from September to November, further contributing to the overall annual rainfall. In contrast, the region receives comparatively lower rainfall during the remaining months, which reflects a marked seasonal pattern (Figure 5a).

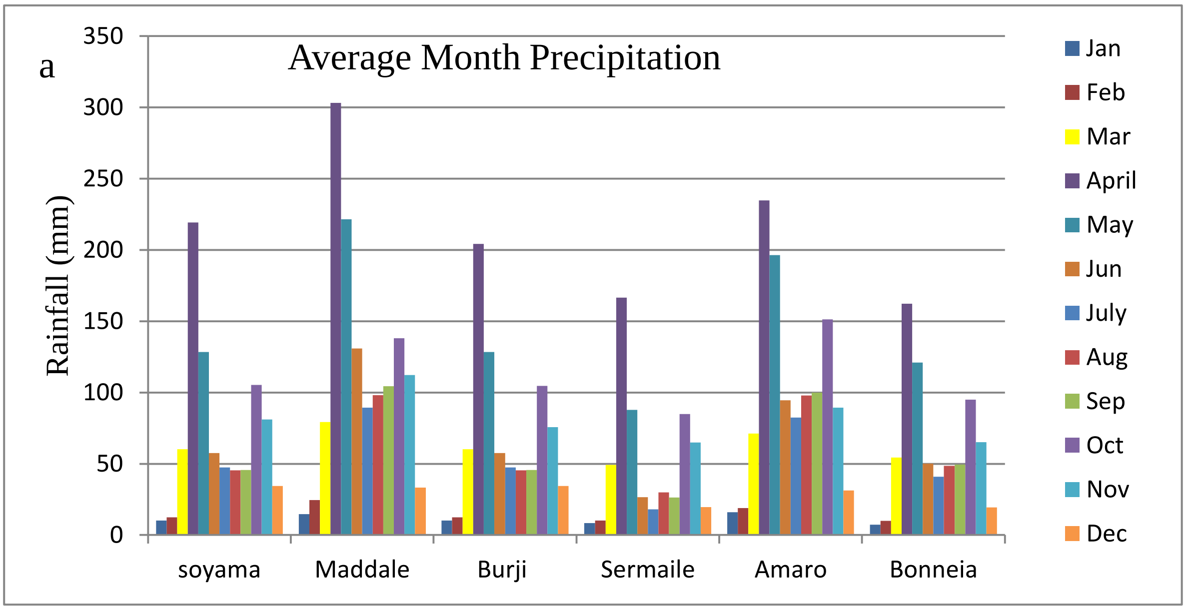

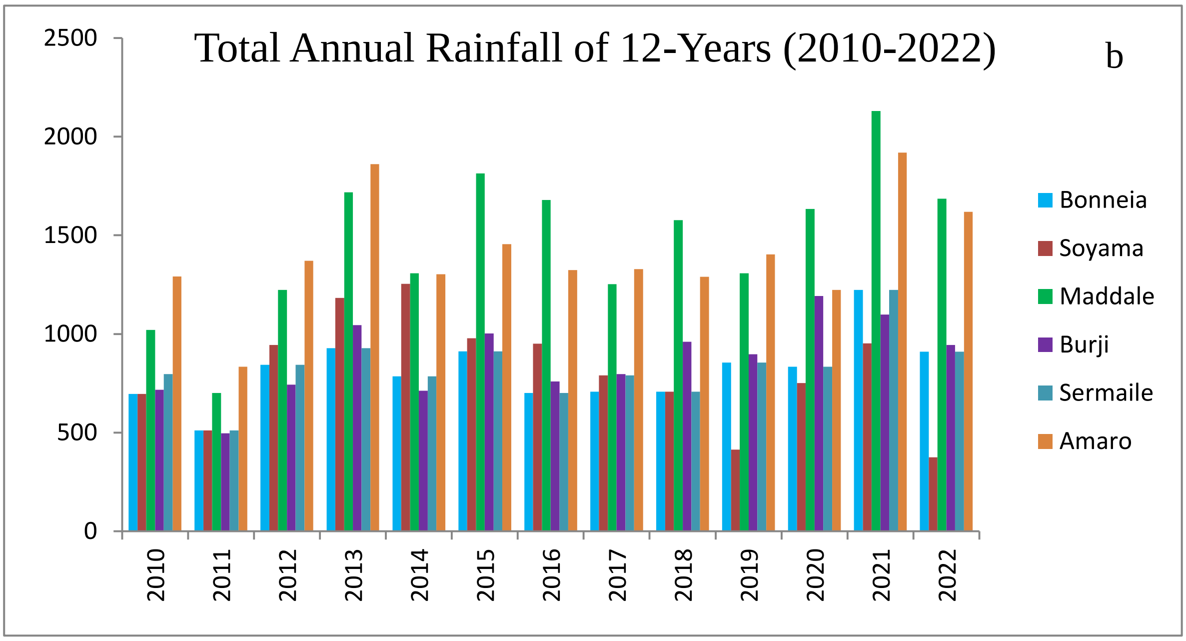

Figure 6.a) Average monthly precipitation b) Average annual rainfall

4.4 Seismicity of the Study Area

In the context of the present study area, it is important to note that the seismic hazard map indicates that the area falls within zones 0 and 1, characterized as seismic-free and associated with minor damage (Figure 6). This would imply that the study area, spanning from Burji to Maddale, is situated in a zone with no seismic hazard. However, it is also mentioned that the area may still be affected by minor hazards despite of falling within these supposedly low-risk zones.

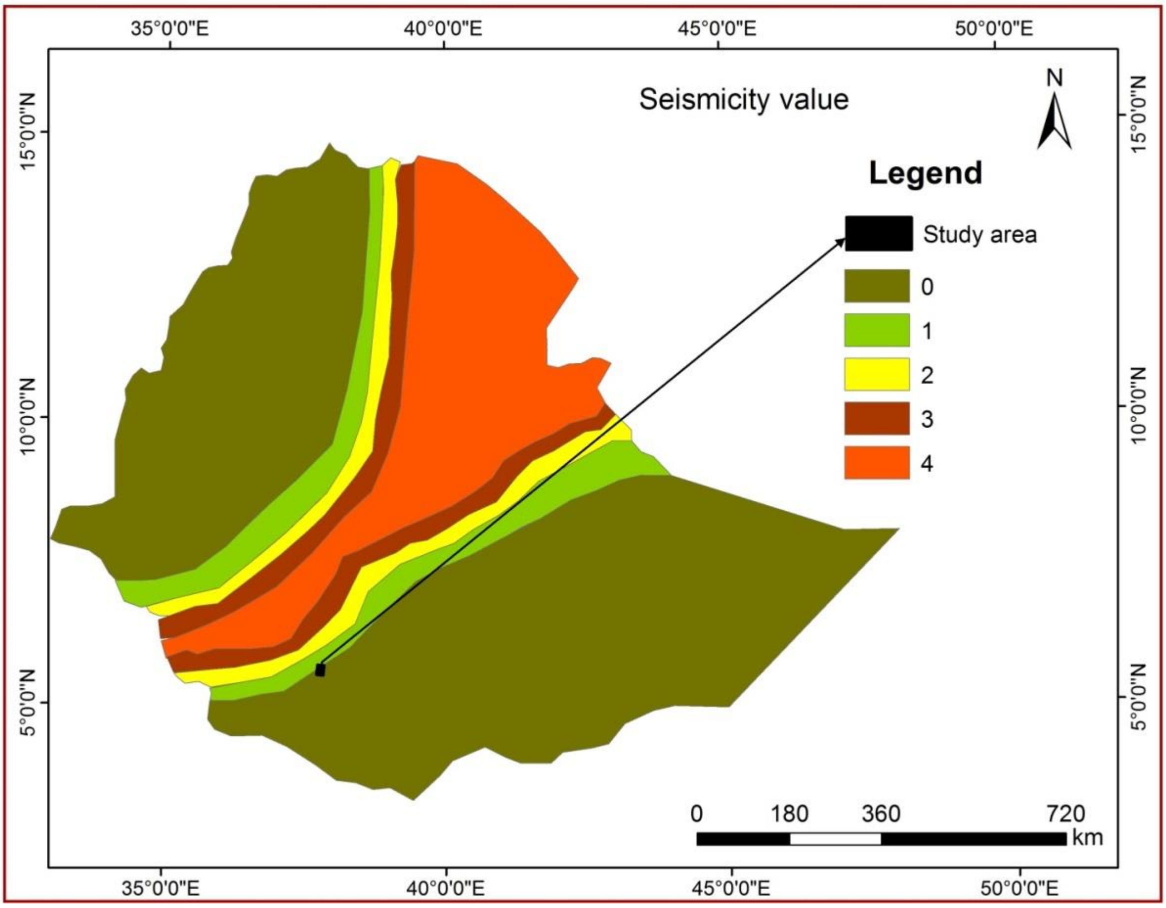

Figure 7.Seismic map of Ethiopia (EBCS, 1995)

4.5 Regional geology

The Mozambique belt is a significant geological feature that extends from Mozambique to Ethiopia, It is classified as an orogenic belt due to its formation from tectonic plate collisions and subsequent mountain-building processes. The composition of the Mozambique belt consists mainly of high-grade gneisses and migmatites. These rocks within the Mozambique belt have undergone extensive metamorphism and deformation, indicating a complex geological history. A north-south tendency and a structural fabric orientated in the same direction are its defining characteristics ages of the rocks within the belt range between 1300 and 480 million years ago, reflecting multiple episodes of geological activity over a significant period(Cahen et al., 1984). In addition to gneisses and migmatites, the Mozambique belt also contains folded schists, marbles, and amphibolites (Almond, 1983).

The southern main ethiopian volcanic activity is divided into three major episodes: (a) Eocene to Oligocene pre-rift volcanic activity (~45 to 27 Ma), (b) Miocene syn-rift volcanic activity (~22 to 8 Ma) and (c) Pleistocene post-rift volcanic activity(~1.6 to 0.5Ma). The pre-rift Amaro-Gamo sequence and related basic vulcanite exhibit a minimum thickness of approximately 600 meters and are dominated by tholeiitic to alkaline basalt lava. This indicates a long history of volcanic activity in the region, with different phases contributing to the formation of the geological features observed today (Banda and Wickham, 1986). The Miocene syn-rift volcanic formations consist of basalts, felsic volcanic rocks, and volcaniclastic deposits, including rhyolite lava, minor ignimbrites, trachyte lava flows, and associated pyroclastic materials. These units primarily belong to the Getra and Kele sequences, which also feature Mimo trachyte. The products of post-rift volcanic activity from the Pleistocene to Holocene period consist of bimodal volcanic rocks and volcaniclastic materials. These include massive Nech Sar basalts, rhyolites, highly welded rhyolitic ignimbrites, and various other pyroclastic deposits (Ebinger et al., 1993; Martínek et al., 2021). The presence of fossil-bearing sedimentary strata suggests a rift-related basin developed in the Early to Mid-Miocene time, coincident with the development of the sedimentary basin. The Amaro Horst was uplifted in the post-Mid-Miocene time (WoldeGabriel et al., 1991).

The earliest exposed geological formation in southern Ethiopia consists of a basement made up of plutonic rocks from the Archean to Proterozoic eras, overlaid by extensively deformed gneisses, amphibolites, and granulites (Davidson, 1983). Approximately 70% of the Agere Maryam area in southern Ethiopia is made up of extensively metamorphosed and deformed gneissic rocks. This illustrates how the Mozambique belt, which exhibits a meridional trend and a structural fabric that is similarly aligned, has a significant influence here, suggesting that the two regions have comparable geological origins and tectonic activity. The Mozambique belt, which stretches southward from the Arabian-Nubian Shield into Ethiopia and Kenya, contains low-grade metasedimentary rocks in addition to high-grade gneisses and migmatites. This continuity emphasises the Mozambique belt's (GSE, 1994).

4.6 Local Geology of the study area

The lithological descriptions were derived from the geological map of the Agere Mariam sheet, at a 1:250,000 scale, prepared by the Geological Survey of Ethiopia (GSE, 1994).

Table 3.Area coverage of each lithological unit.

Lithologic unit type	**Area (km^2)**	**Area (%)**
Hornblend-biotite- gnesis	162	63.44
Magnetite	1	0.09
Lower basalt	31	12.11
Eluvium deposit	53	19.70
Alluvium deposit	12	4.66

Hornblende Gnesis

This rock type is predominantly exposed in the western and southern areas along the Amaro horst and the Segen Rivers and small streams drainage. The lithological units covered the study area by 162 km and 63.44% as shown in (Table 3). The presence of migmatitic features in the gneiss suggests that it has undergone partial melting at some point in its history.

Magnetite quartz gnesis In the study area this unit is generally ridge forming. This unit covers 1km and 0.065% of the study area(Table 3). Magnetite is present as disseminated clots form thin bonds parallel to the foliation.

Lower Basalt

Lower Basalt is a dominant volcanic unit found in the northern and western parts of the most widespread unit in the area. The unit covered 31km and 12.11% of the study area (Table.3). The thickness of the Lower Basalt unit varies across different locations within the boundary. In the northern part of the Amaro horst, the Lower Basalt is observed to be particularly thick, with sections ranging from 600 to 700 meters in thickness.

The Eluvium Deposit

Eluvium deposit is loose residual material ranging from accumulations of cobble-sized fragments to soils. In the Segen basins, the eluvium consists of sub-rounded to sub-angular pebbles and cobbles set in a poorly sorted matrix of coarse sand. The lithological units covered the study area by 53 km and 19.70% as shown in (Table 3). The thickness of the eluvium in these basins ranges from 2 to 14 m.

The Alluvium Deposits

According to Table (3) the the lithology units covered 12km and 4.66% of the study area (It is commonly found along river courses with very low gradients. The alluvium in the Segen basin is composed of silty clays with minor detrital feldspar, quartz, and rounded rock fragments. It is also noted that the thickness of layer of alluvium, varies from place to place, with the maximum thickness being 15 meters (GSE ,1994).

4.7 Geological structure of the study area

The Main Ethiopian Rift System, which is currently experiencing seismic and volcanic activity, crosses the elevated Ethiopian plateau around 1000 km south of the Afar Depression and into a wide area of basins and ranges close to the Kenyan border crossing into Ethiopia (Davidson, 1983). The MER begins to broaden south of Lake Abay where the topographic expression of the rift valley broadens into two basins separated (Ebinger et al., 1993). Rock structure, comprising primary and secondary discontinuities such as bedding, joints, foliations, faults, and thrusts, plays a significant role in slope stability. Three critical factors to consider are: the degree of parallelism between the direction of discontinuities and the slope, the steepness of the dip, and the variation in dip or plunge between the discontinuities and the slope's inclination. When discontinuities align more closely with the slope, the risk of slope failure increases(Anbalagan, 1992).

In the study area, the dominant geology structures are Normal faults and lineaments. They are mostly normal faults connected with the formation of graben and horst and lineament are mostly fractures (joints and faults) that were developed during the Cenozoic. The structures that strike general North-South and NorthWest are trending occurring associated with the main Ethiopian rift in the study area(GSE, 1994).

5. RESULTS AND DISCUSSION

5.1 Landslide inventory

Landslides are one of the most frequent and destructive natural hazards globally, causing significant economic losses and loss of life. A landslide inventory map forms the basis for most susceptible and hazard mapping techniques. In recent years, Geographical information and field-based mapping techniques have significantly improved landslide inventory mapping methodologies in remote sensing. A landslide inventory map is a method used to identify past landslides and compile and record details of each data on location, dimensions, causative factors, and frequency occurrence (Dai et al., 2001, 2002; Girma et al., 2015). Identifying and mapping the distribution and location of past and present landslides in a certain area is very important to predict the future probability of landslide occurrence(Guzzetti et al., 1999).

Hazard or risk assessments may be adversely affected by insufficient information about the accuracy of the inventory maps and the dependability of the procedures employed to create these inventories. While there is no consensus on a conventional strategy for constructing landslide inventory maps, researchers apply diverse sampling strategies. These include: (1) using polygon features to map each landslide's main scarp and differentiate it from the rupture zone or accumulation or depletion zone; and (2) utilizing seed cells, a method to represent landslides. (3) Selecting a point in the upper part of the scar based on the computed positions of the landslides (Solaimani et al., 2013). As noted by Yilmaz (2009a), point data in a GIS is represented by a single X, Y coordinate and does not capture the full area impacted by the landslide. This approach is useful in cases where the map scale is too small to accurately represent the full extent of a smaller landslide. A map of the research area’s landslide distribution or inventory was created using Google Earth Image. While Google Earth was utilized to identify landslides in inaccessible areas such as valleys, gorges, high cliffs, and river wall banks, Google Earth version 2021 (Plate 1.2.3).

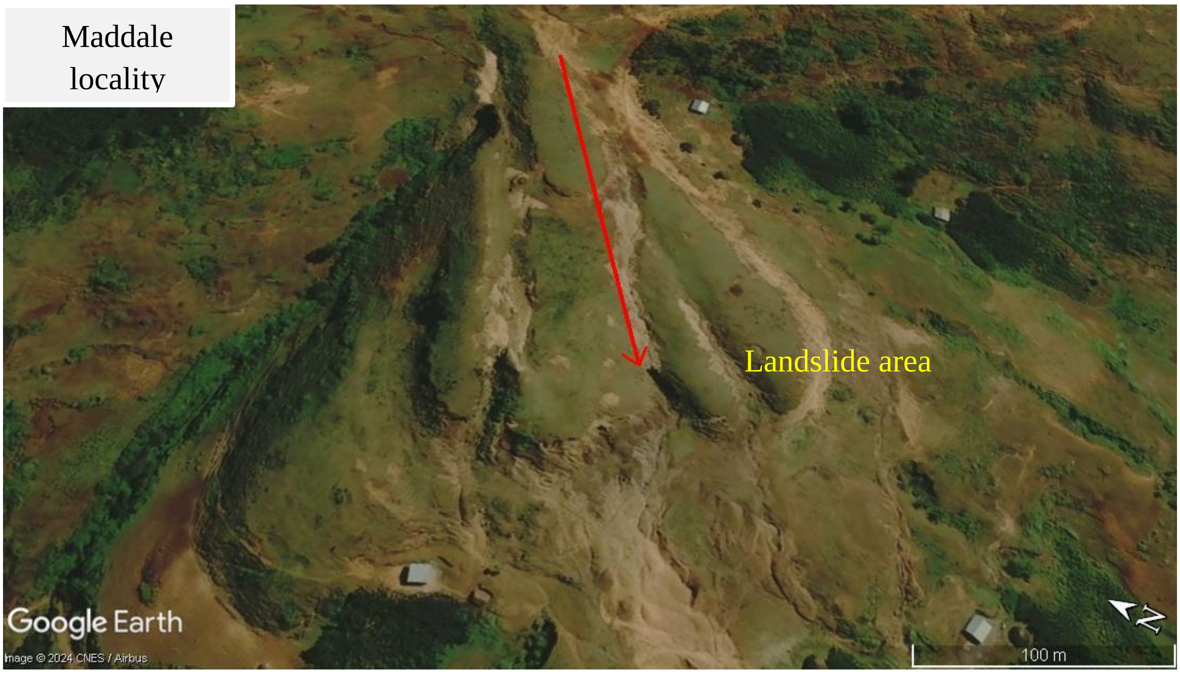

Plate 1.Earthflow along the Escarpment(Google Earth Pro)

The materials move down channel like structure due to gravity and water saturation in Maddale locality.

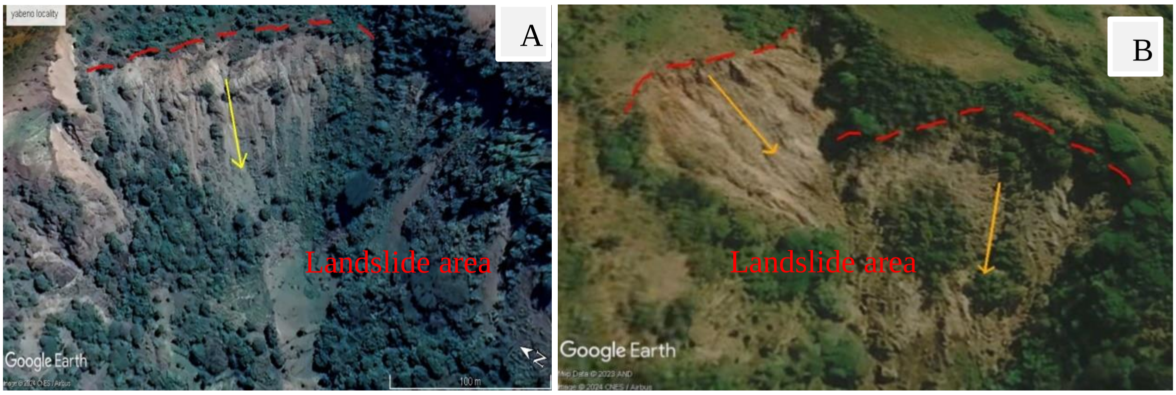

Plate 2.A) Rock unit sliding down, B) creep tyes of landslide (Google Earth Pro) in the Yabeno locality is made up of strongly and weathered basalt and is located close to the foot of a steep slope.

Plate 3. Planar types of landslide showing the direction sliding (Google Earth Pro).

In the present study, an area of 265 active types of landslide were recorded based on the Google Earth image interpretation image techniques. These data give information on the location of slope instability in the study area. This landslide was randomly divided into training data sets for development and testing data sets for validation, predicting image training(70%), and validating(30%) of the area. This inventory landslide area coverage area (Figure 8).

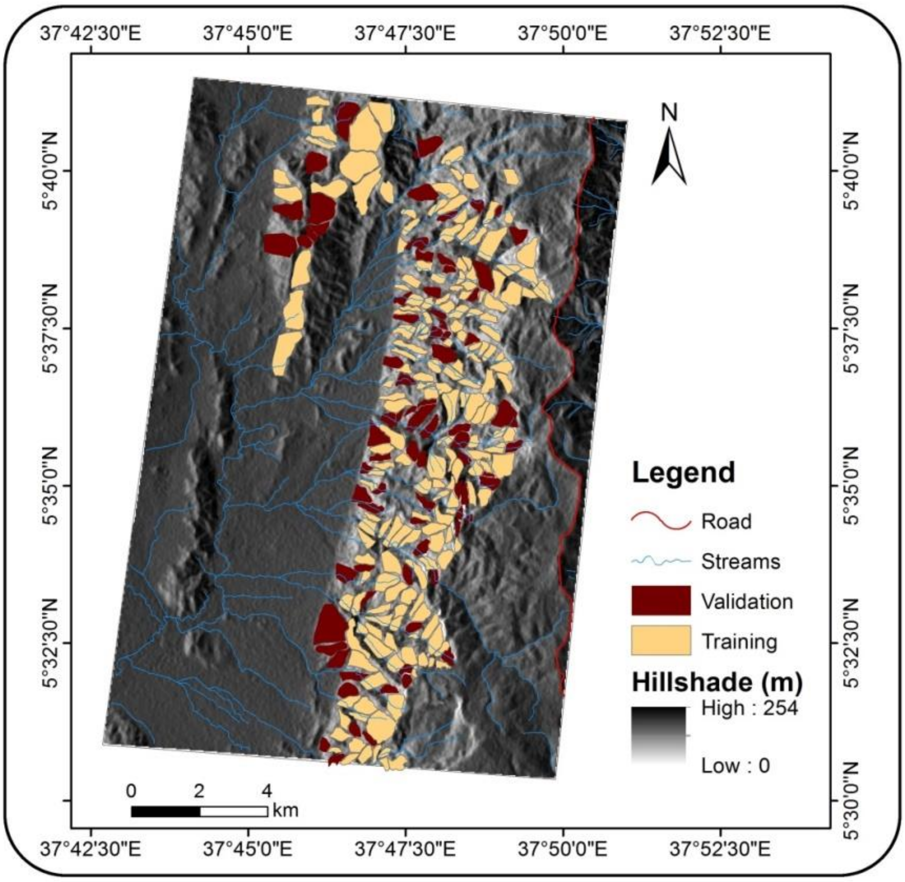

Figure 8. Landslide inventory map of the study area

According to Figure (8) based on time series analysis of Google Earth imagery, the study area has been frequently affected by landslides. The primary causes of these landslides are the high density of lineaments and the rugged terrain with steep slopes.

5.2 Landslide causative factor maps

The intrinsic parameters known as causative factors determine the stability condition of a slope (Girma et al., 2015). Several factors can contribute to the occurrence of landslides, both natural and man-made. Understanding these causative factors is important for effective landslide risk management and mitigation strategies. The selection of suitable parameters was predicated on (a) previous research findings (Ayalew and Yamagishi, 2005b). (b) experience with and understanding of landslide incidents in the study region; and (c) accessibility of data in the study region without universal or standard criteria (Meten, et al., 2015; Wubalem and Meten, 2020). Eight landslide factors were used for landslide susceptibility mapping, including slope, aspect, rainfall, lithology, distance to stream, distance to lineament, curvature, and land use/ land cover. These factors are reclassified into subclasses. A thorough explanation of how each causal element affects the landslide occurrence will be discussed as follows.

5.2.1 Lithology

Lithology is a landslide causative factor used in landslide susceptibility mapping (Dai et al., 2001; Shano et al., 2020). The lithological variation leads to differences in the strength and permeability of rocks and soils (Achour et al., 2017). If the rock unit is loose and fragile, the probability of landslide occurrence will increase. The presence of fractures and faults in the region creates zones of weakness, where water infiltration can destabilize the rock, making landslides more likely. The lithological unit of the study area is digitized from Ageremariam sheet and has been analysized. With ArcGIS10.8, the lithological map of the study area was digitized and categorized using the on-screen digitizing tool. In the study area, kinds of lithological units are predominantly covered by alluvium, eluvium, lower basalt, Hornblende gnesis, and magnetite. The classification result has validated the claim made regarding the rock structure of the mentioned study area (Figure 9).

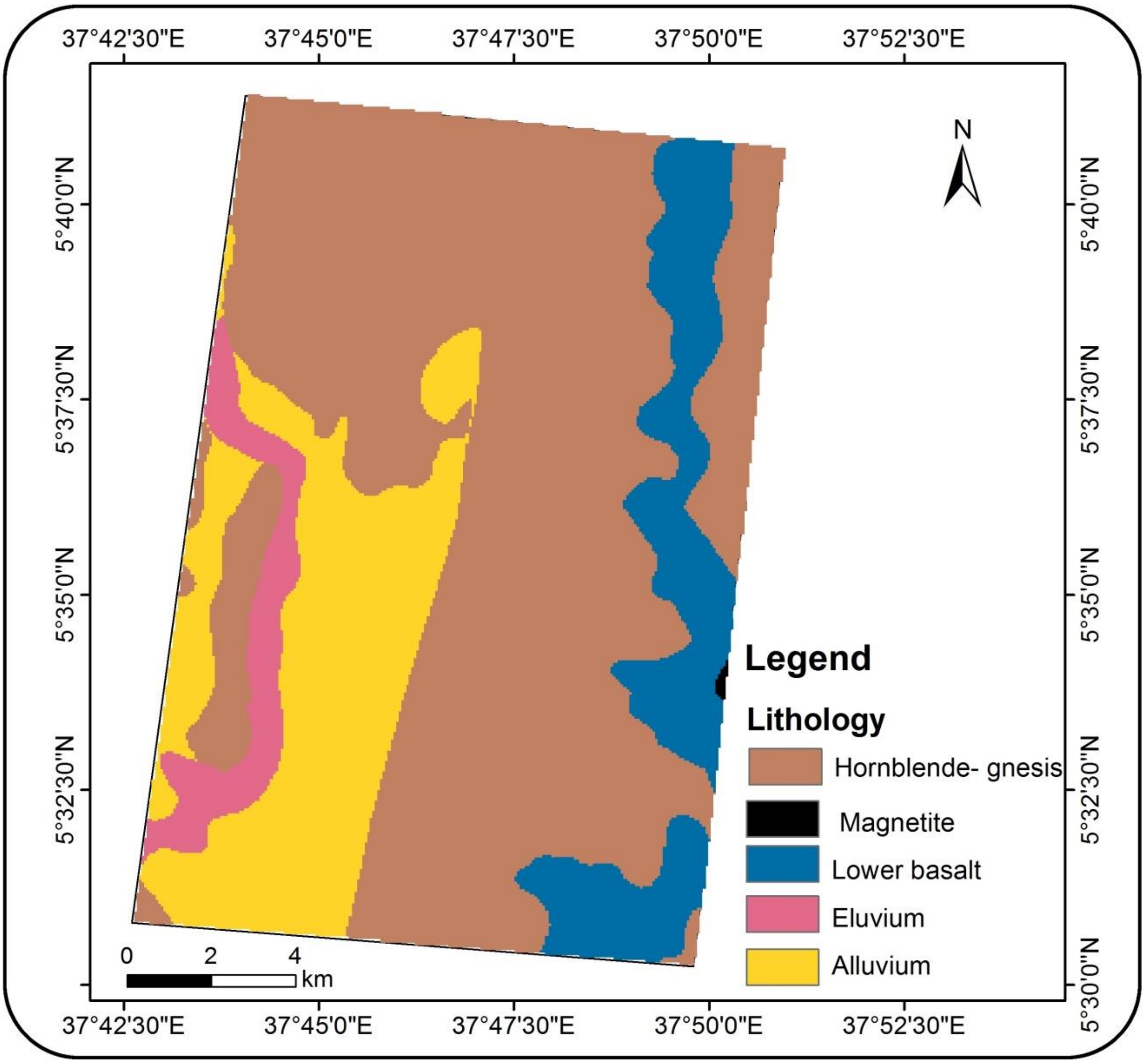

Figure 9. Lithology map of the study area

5.2.2 Slope

The slope is a crucial factor that affects the process of landsliding. If the slope is steep, the mass's tangential component of weight will increase, and its perpendicular component will decrease due to an increase in shear stress (Girma et al., 2015). It is well known that landslides occur more frequently on steeper slopes due to gravity (Mersha and Meten, 2020b). A downslope movement of these masses following steep topography tends to occur by the disintegration of rocks due to weathering, river erosion, incision, groundwater infiltration, or percolation from heavy rainfall events along fractures. Landslides are more common on steep slopes than on moderate and gentle slopes (Meten, et al., 2015). Slope classification according to the geomorphological area reflects specific processes and controls and the frequency of particular slope angles. These maps use the same contour line spacing to split the slope maps' angles into smaller units. Escarpment/cliff, steep, moderately steep, gentle, and extremely gentle slopes are the five classifications selected (Anbalagan, 1992; Mengistu et al., 2019). The slope factor for the study area was prepared from DEM data of 30m*30m resolution. The analysis was done in ArcGIS using surface analysis tools. The slope of the area ranges from slope is 0 to73°, which was classified in Arc-GIS software into five classes: 0-5°, 5-12°, 12-30°, 30-45° and >45° based on the Natural break method (Figure.10). The values were classified according to each class's contribution to the landslide occurrence.

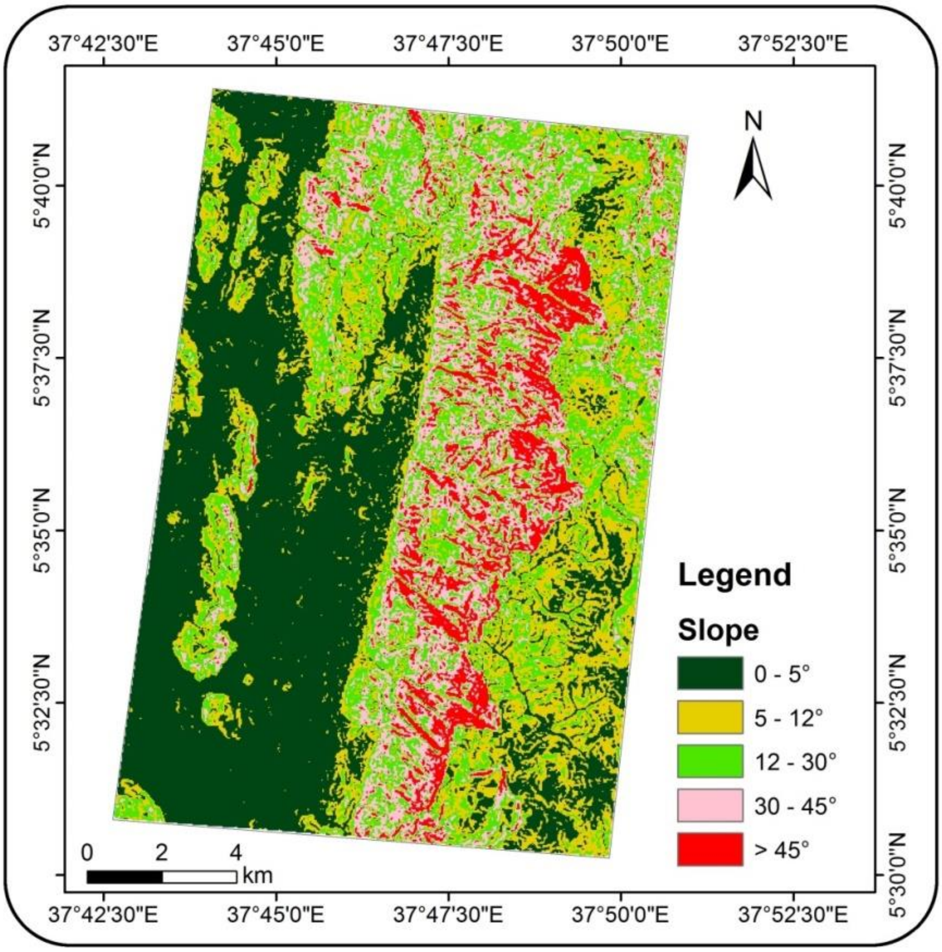

Figure 10.Slope map of the area

5.2.3 Aspect

Aspect refers to the way the slope is facing. The aspect of a slope that ranges from 0 to 360°, is responsible for reducing sunlight to heat the ground and reduce soil moisture content(Shano et al., 2020; Wubalem and Meten, 2020; Tesfa, 2022). This factor was prepared by using ASTER DEM (30m*30m). The surface analysis tool in the ArcGIS environment is used to complete the derivation. The class name was assigned based on the aspect value as utilized and then classified based on the direction they have from the north into nine subclasses using Arc GIS software. It ranges from -1 to 360. Then classified into nine subclasses as flat (-1), north (0–22.5°) and(337.5-360°), north-east (22.5–67.5°), east (67.5–112.5°), southeast (112.5–157.5°), south (157.5–202.5°), southwest (202, 5–247.5°), west (247.5–292.5°) and northwest (292.5–337.5°) by using Natural breaks method according to their influence to landslide (Ayalew and Yamagishi, 2005).

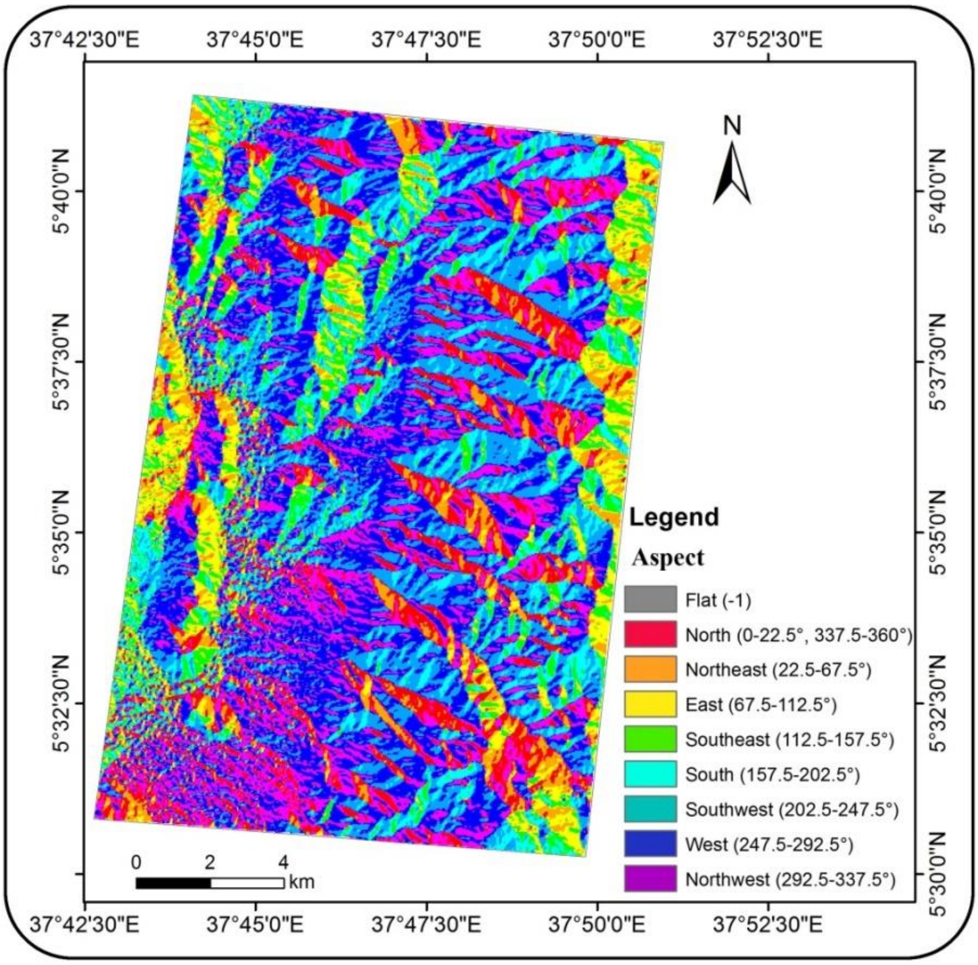

Figure 11.Aspect map of the study area

5.2.4 Curvature

Curvature affects a slope's susceptibility to landslides by controlling the water distribution (surface and subsurface) within the slope. Regarding landslide and hillslope analysis, profile and plan curvatures are utilized (Ayalew and Yamagishi, 2004a). Plan curvature and its impact on hillslope stability in areas where earth flow and earth slide predominate. It is the curvature of a line created when an imagined horizontal plane intersects the ground, or the curvature of the topographic contours(Meten, et al., 2015). Based on plan curvature, hillslopes can be classified as relatively planar areas, hollows, and noses. Regions known as hollows are those where surface water would converge as it travels downslope because the plan curvature of the contours is concave there. Areas known as coves or noses are those where the contours' plan curvature is convex in the downslope direction and surface. Plan curvature values in relatively flat locations are approximately zero. The curvature in the downslope direction along a line created by the junction of the ground surface and an imagined vertical plane is known as the profile curvature. Determining if a curve is concavity or convexity requires understanding of its curvature sign. Positive plan curvature values (convex) indicate divergence and negative plan curvature values (concave) indicate concentration downhill of flow (Anderson and Burt, 1978). The area's vulnerability to landslides is influenced by the combined curvatures of the plan and profile. The area’s curvature map was generated from ASTER DEM (30m*30m) resolution which covers ranges from (-20 to 19.7). It was classified by using the Arc-GIS spatial analysis tool into three curvature classes: Concave (-20 to 0), Flat (0), and Convex (19.7) Figure (12a).

5.2.5 Distance to lineament

The Ethiopian highlands are characterized by significant relief and rugged terrain, featuring deep valleys and gorges with steep slopes, resulting from large-scale Pliocene-Quaternary uplift. As a result, horsts, tectonic depressions, and fault scarps have been created by the intersection of numerous geological features in the area. These structures have an impact on the research area, which is located in the southern of the Ethiopian highlands. Slope failure risk often rises with increasing distance to any structure or lineament; hence, this is an important consideration when determining a site's susceptibility to landslides (Getachew and Meten, 2021).

The rocks close to active faults are weaker due to high shearing, making them more susceptible to landslides (Leir et al. 2004). This has significant implications for hazard assessment and mitigation strategies in areas with active faults. Understanding the relationship between fault proximity and landslide susceptibility is crucial for assessing the potential risks associated with this geological structure. Distance from faults increases the likelihood of landslides (Pradhan and Lee, 2010). Fault and lineaments were digitized from the region's geological map and Google Earth Pro and updated by remote sensing distances to lineament were buffered by a distance of 600m. Which was classified into five classes 0 – 600, 600-1200, 1200- 1800, 1800-2400, and > 2400m based on the Equal interval method (Getachew and Meten, 2021). Manual classification was used to provide a realistic picture of how landslides and escarpments relate to one another (Figure.12b). The past pattern of landslide density increased with decreasing distance to the lineament.

5.2.6 Distance to stream

Streams with multiple drainage networks are more likely to cause landslides because they erode the slope base and saturate the slope, forming materials in the subsurface water section (Akgun and Turk, 2011). This parameter focuses on identifying and mapping surface and subterranean water in a specific region, along with identifying shear zones and weak zones that follow the area's streams and gullies that have eroded the slope near the streams. Because active river incision erodes the toe and increases saturation, the slopes become steeper and more unstable (Getachew and Meten, 2021). Other reasons can also cause landslides to occur far from the Stream River. These landslide-prone locations are usually found on parallel drainage patterns on steep hillslopes where the shear strength of rocks and soils is decreased by increasing pore-water pressure. The stream of the study area was digitized from the topographical map at a scale of 1: 50,000 in Arc GIS. Distance to stream at the study area was classified into five subclasses, with distance values ranging from that range 0 m to greater than 1366m. The distance value of the stream (0- 190, 190-445, 445-760, 760-1220, and >1220m) is classified based on the natural break method (Figure.13b). Manual classification was used to provide a realistic relation of how landslides and escarpments relate to one another.

5.2.7 Rainfall

Ethiopian highlands are known for their highly variable rainfall (Woldearegay, 2013). A landslide occurs when the shear stress within slope materials exceeds their shear strength. The primary cause of landslides is the saturation of slope materials due to heavy rainfall (Getachew and Meten, 2021). Rainfall plays a role in causing slope instability, especially heavy and persistent rainfall is a controlling factor that causes landslides by supplying water, which raises the pore water pressure and subsurface hydrostatic level (Mersha and Meten, 2020b). When these materials become saturated, their shear strength diminishes due to changes in friction and the loss of effective intergranular cohesion. Moreover, the added weight and increased pore water pressure further elevate the shear stress in the saturated slope materials, leading to instability. Provided the annual rainfall data for the study area. The IDW method in ArcGIS was used by some rain gauge stations to interpolate the annual rainfall data (Appendix 1.1). Since IDW is more straightforward and fundamental than Kriging, which is more complex and difficult to understand, IDW is utilized. Kriging involves complex statistical modeling and variation of analysis. The annual rainfall map of the study area is classified into five subclasses based on the Natural break classification method (Figure 13a). Consequently, the study region receives the most rainfall. The average yearly rainfall they will receive ranges from 500mm to 2000mm with significant precipitation. The study area receives a high rainfall of >1,650mm/yr. The classification of the factors depends on the relationship between landslides and escarpments.

5.2.8 Land use/land cover

Land-use change, including intensive farming, deforestation, and overgrazing, significantly influences rainfall-induced landslides due to slope instability, as vegetation bonds to slope materials and affects slope stability (Mersha and Meten, 2020a). Because the natural anchorage of plant roots prevents erosion, the vegetated region is less vulnerable to landslide concerns. The land use map of the study area was prepared by digitizing from Google Earth Pro. This step is crucial in understanding the distribution of land use types in the area and how they contribute to landslide susceptibility. By analyzing ArcGIS's land use factors, seven land use types were identified in the study area. These include Grazing land, Bushland, Dense forest, Sparse forest, Agricultural land, River water, and Settlement (Figure 14a).

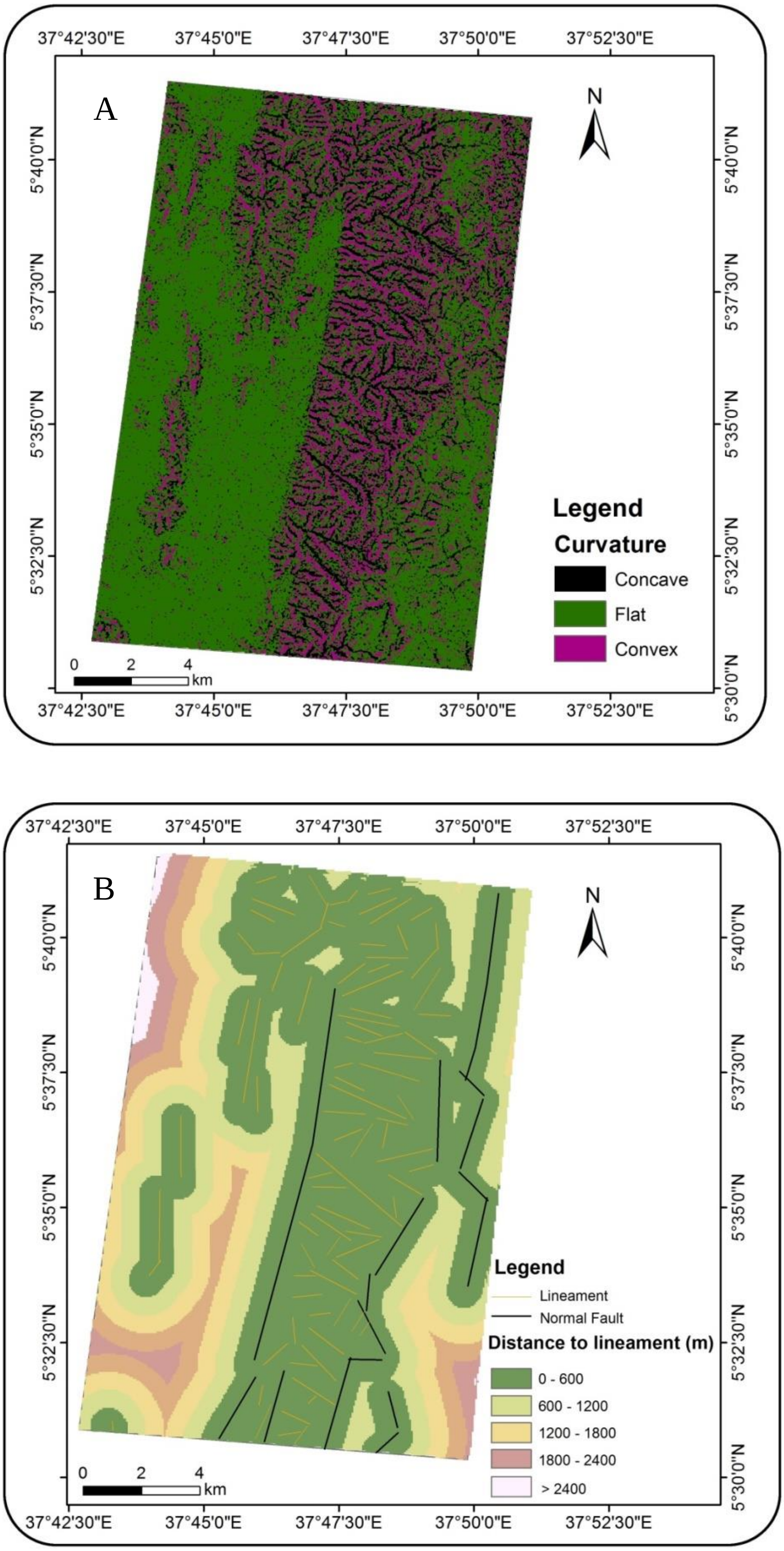

Figure 12.A) Curvature map, B) Distance to lineament

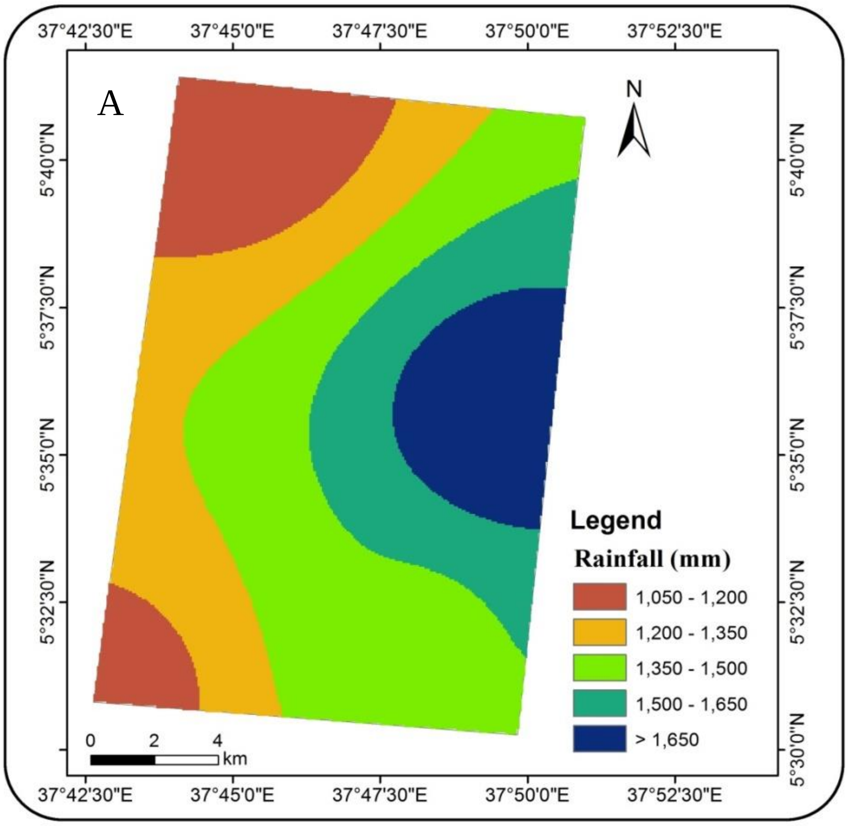

.

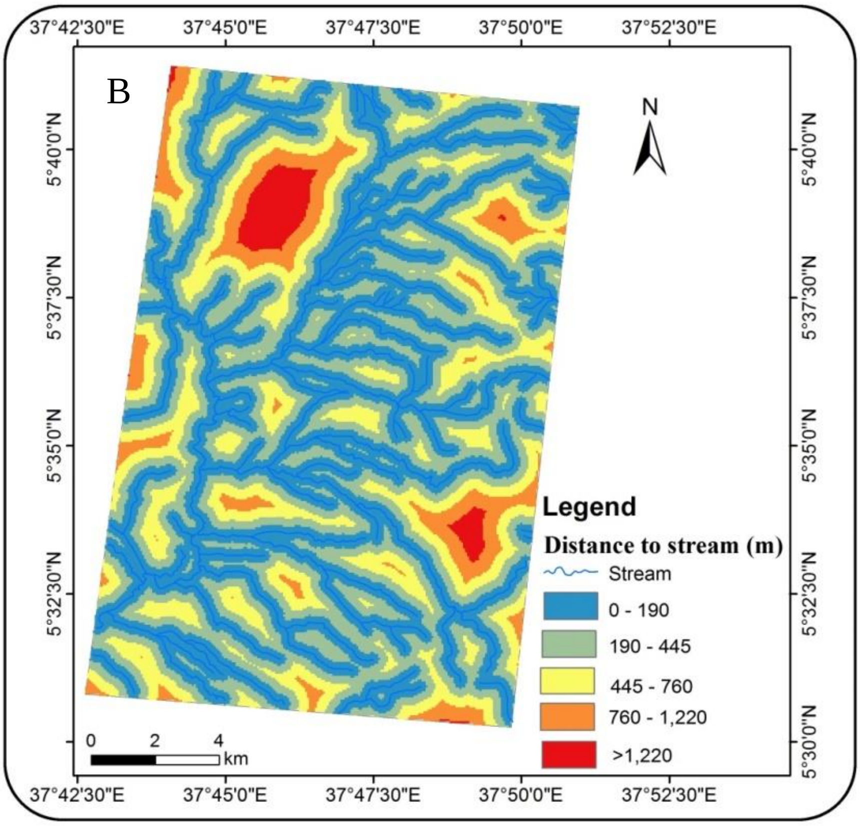

Figure 13.A) Rainfall map, B) Distance to stream map

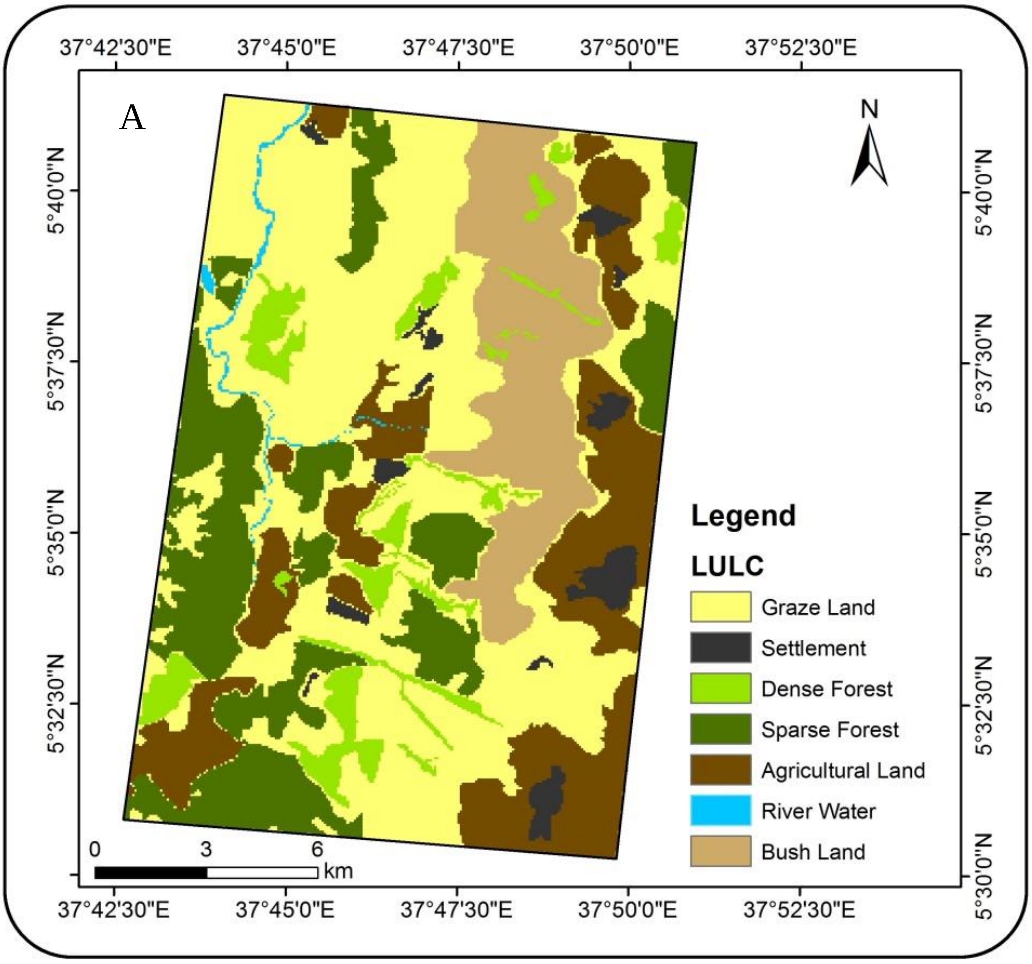

Figure 14.A) Land use Land cover map

,

5.3 Information Value Method Result

5.3.1 Relationship between Causative factors and landslide

This study used the statistical information value (IV) model to evaluate the associations between eight causal factors and the occurrence of landslides. There were forty-four different classes into which the causal factors were split. Table 4 summarizes the numerous classes of the statistical IV model and shows the relative relevance of each causal component. The statistical IV model's weight values show the spatial association between the class contributions of the causative elements and the occurrences of landslides. It is possible for the calculated statistical IV values for the classes to be negative or positive. Positive IV values show that the causal factor can contribute to the occurrence of landslides, whereas negative IV values indicate a reduced probability and signal that the causal component is unlikely to cause a landslide (Yin and Yan, 1988). The IV method values statistically.

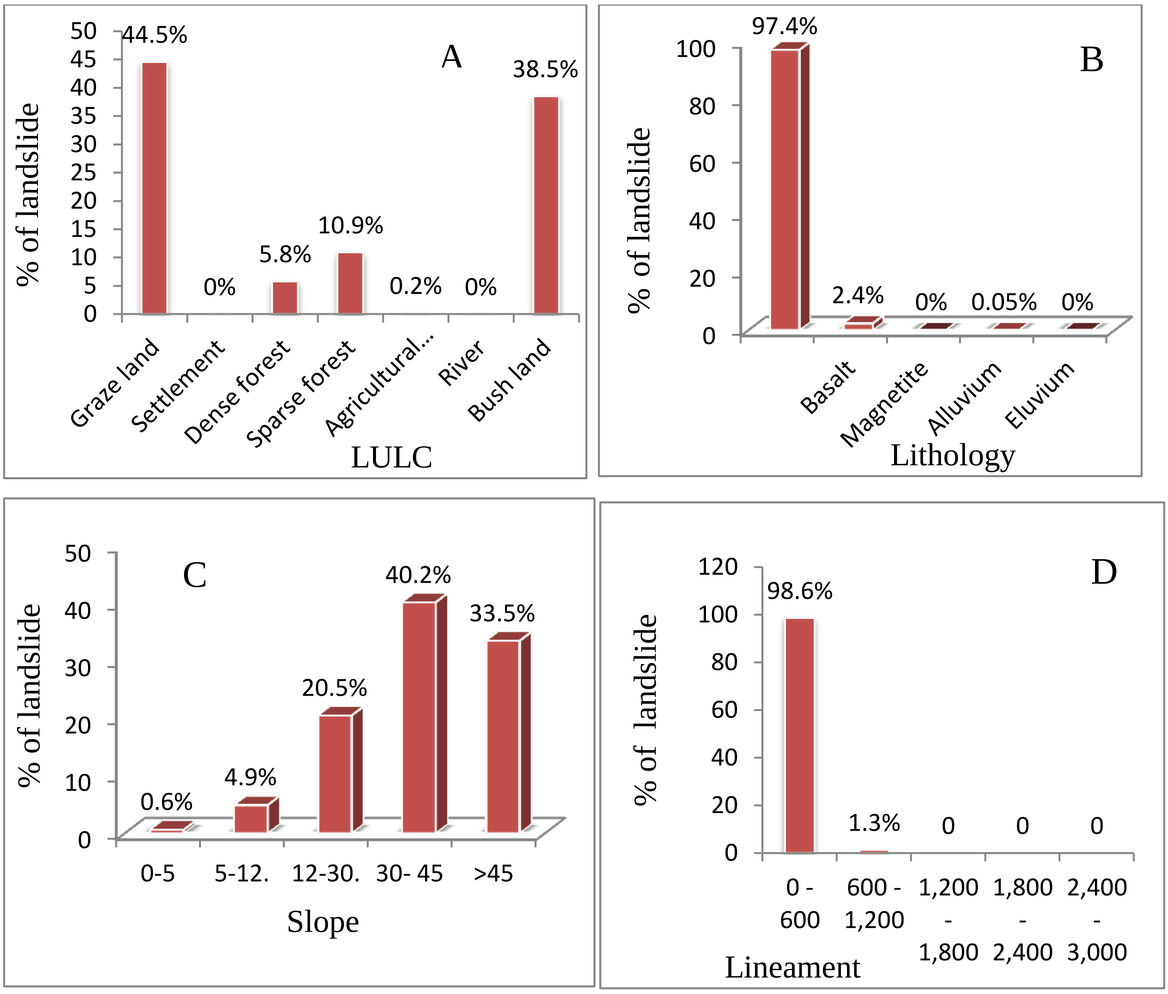

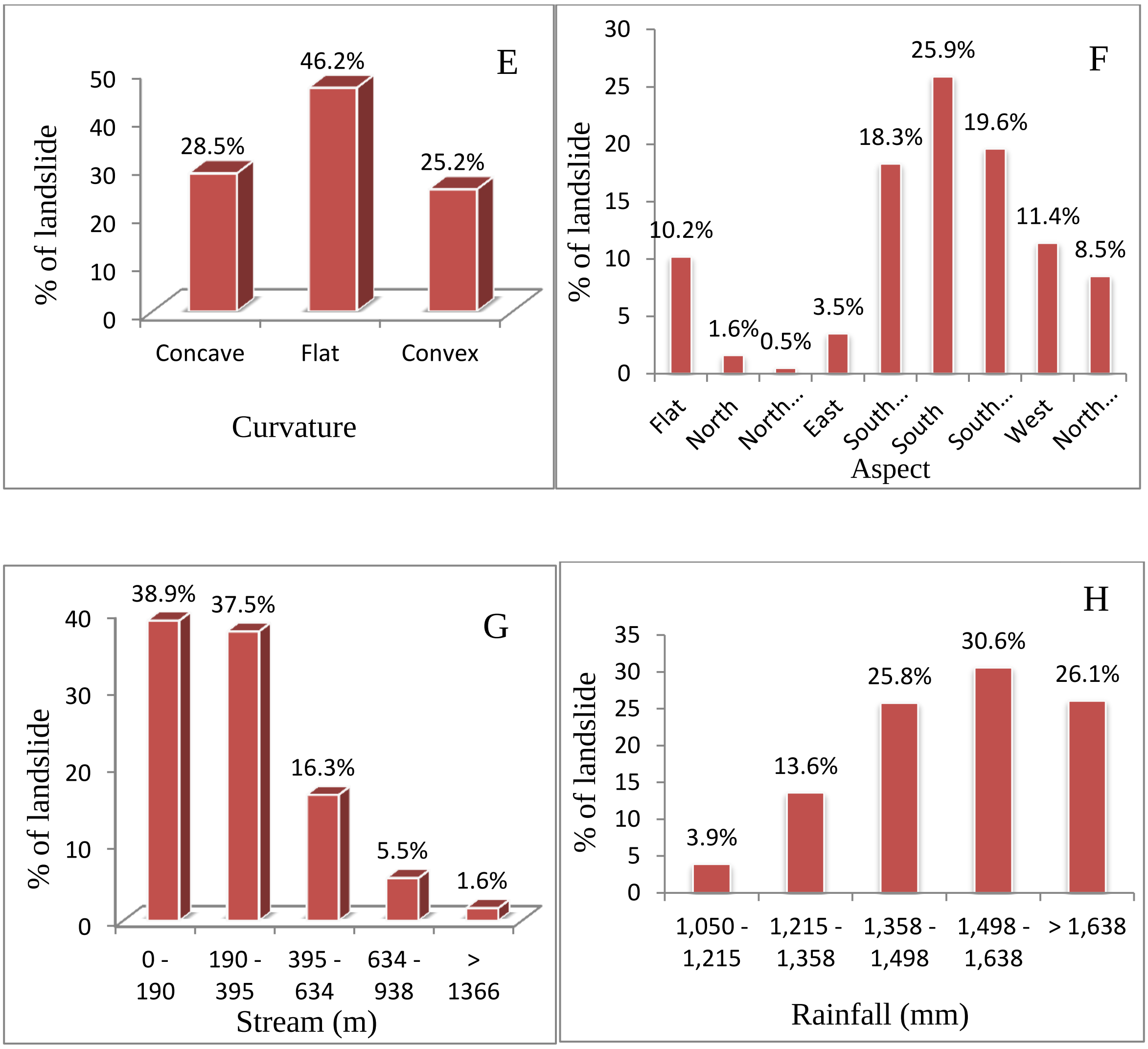

Figure 15. Relationship between the percentage of landslide distribution with causative factor classes, A) Land use land cover, B) Slope, C) Lithology, D) Lineament, E) Rainfall, F) Curvature, G) Aspect and H) Stream

5.3.2 Rating Landslide Factors Using Information Value Model

Based on the features of the research location, an analysis of eight causal factors from previous research was chosen for this study. We chose these parameters for landslide susceptibility mapping because no established standards or principles exist. The selected causative factors include lithology, aspect, slope, curvature, rainfall, distance to stream, distance to lineaments, and land use/land cover (Table 4).

Slope: maps are categorized based on specific slope angles, influenced by the area's geomorphological history and localized processes and controls (Anbalagan, 1992). The study area’s slopes play a significant role in the occurrence of landslides, as indicated by the statistical information values of different subclasses. Five slope classes were used to categorize the study area: 0 – 5°, 5 – 12°, 12 – 30°, 30 –45° and >45° based on the Natural break method (Girma et al., 2015), where landslides occurred at 0.6%, 4.9%, 20.5%, 40.2%, and 33.5% of these classes respectively. The slope classes' statistical information values (IV) are -1.64, −0.52, 0.13, 0.48, and 0.69, respectively. Among slope classes, 0 – 5°, and 5 −12°exhibit negative information values, implying that their contribution to the likelihood of a landslide occurrence is low. Gentle slopes are anticipated to experience a low occurrence of landslide due to the reduced shear stresses that come with a low gradient (Raghuvanshi et al., 2015). On the other hand, the positive information values (IV) for the slope classes 12– 30°, 30– 35°, and >45° contribute highly to landslide susceptibility. Due to the slope being steeper, it will be more prone to instability. The slope classes with these values will slide when subjected to heavy and prolonged rainfall (Wubalem and Meten, 2020). Steep slopes increase the likelihood of slope failure, especially when other instability factors favor sliding compared to gentle slopes in similar conditions (Girma et al., 2015).

The insufficient qualities of the slope material in the positive slope class values cause instability in these slopes. The slope materials are mostly made of weathered basalt rocks and hornblende gnesis material. The slope materials have a high porosity, are comparatively more permeable, and have low shear strength.

Aspect: This frequently impacts a slope's ability to retain moisture and vegetation cover. Aspect is consequently thought to be a significant factor for landslide susceptibility (Raghuvanshi et al., 2015). The aspect classes west, southeast, south, and southwest, northwest facing slopes have the information values of 0.007, 0.25, 0.32, 0.17, and 0.005, which represent the positive value of information value have the highest probability of contribution to a landslide occurrence in the which occurrence 11.4%, 18.3%, 25.9%, 19.6%, and 8.5% of the study area fall on the southeast, south, southwest, west and northwest facing slope aspects respectively which are affected by landslides. The remaining aspect classes covering 18.34% of the study area, have no slope instability problems.

Curvature: The slope curvature of the study area was classified into concave, flat, and convex classes. The finding revealed that the flat area dominated the study area, covering approximately 46.2% while the concave and convex curvature covered about 28.5 % and 25.2%, respectively. In addition to categorizing the slope curvature, the information values were calculated to assess the probability of landslide occurrence in each slope type. The information value in concave, flat, and convex curvatures showed 0.34,-0.10, and 0.35, respectively. Those positive values have the highest probability of causing landslide occurrence. If the slope has a concave and convex curvature,, it significantly impacts landslide occurrence as it impounds water (Wubalem and Meten, 2020). According to topography type, in hilly and mountainous areas, it is higher value, and in flat areas, low.

Distance to stream: The distance to stream classes have the highest probability of landslide occurrence. Streams affect the stability of a slope by eroding the slope and saturating the earth's material to reduce shear strength (Asmare et al., 2023). Water flowing through streams can also increase pore water pressure, reducing the strength of the soil or rocks and increasing the likelihood of landslide occurrence. The distribution of landslide in the distance to stream classes of 0-190, 190- 445, 445-760, 760-1220, and >1220 are 38.9%, 37.5%, 16.3%, 5.5%, and 1.6%, respectively. The information value in the classes of 0-190m, 190- 445m, and 445-760m are 0.03, 0.15, and 0.07 positive values, while others in the distance to stream classes of 760-1220 and >1220 have lower probability landslide occurrence as their information value shows negative value.

Rainfall: Heavy rainfall is the main triggering factor for slope failures that can saturate the soil or rocks (Ayalew, 1999; Abebe et al., 2010). In addition, rainfall adds weight to the slope, contributing to instability, especially in areas with weakened and intense surface runoff. The finding indicates that there is a strong association between rainfall classes and the occurrence of landslides (Tesfa, 2022). Rainfall classes are also supported respectively; landslide occurred at 3.9%, 13.6%, 25.8%, 30.5%, and 26.1%. The statistical information value supports this association, as it shows a high positive value for certain rainfall classes, indicating a higher probability of landslide occurrence. The specific values of 0.102, 0.34, and 0.32 for certain rainfall classes suggest that they have a significantly higher likelihood of causing landslides compared to others. In contrast, the lower probability of landslide occurrence of certain rainfall classes values -0.65 and -0.26, indicating a negative association with landslide.

Distance to lineament: Ethiopian highlands are affected by different structures that give horst, tectonic depression, and fault scarps (Korme et al. 2004) as cited in Getachew and Meten (2021). Landslides are more likely to occur in areas closer to active faults. The presence of faults and lineaments near a slope can create conditions that increase the potential for landslide occurrence. The stress and movements associated with faulting can affect slope stability, making it susceptible to failure. The information value of the study areas 0.31 have positive values that show a high probability of landslide occurrence in which 98.6% of the landslides occur in the first class of 0-600m, respectively.

Lithology: has a significant influence on landslide occurrence. The lithology of the study area includes Hornblend gnesis, lower basalt, magnetite, eluvium, and alluvium deposits. The distribution of past landslides showed that 97.4% occurred within hornblende gneiss, 2.4% in lower basalt, and 0.05% in Alluvium. The information value 0.24 was shown in hornblende gneiss, indicating a positive relation with landslide occurrence. The distribution of higher landslide density was within hornblende in the study area due to the degree of weathering and steep slope. Due to their flat topography, the lower distribution of landslide was on magnetite, lower basalt, alluvium, and eluvium units.

Land use and land cover play a crucial role in influencing the occurrence of landslides. The poorly cultivated areas, including bare land, sparsely vegetated areas, and overgrazed lands, are highly susceptible to soil degradation, mass wasting, and slope instability (Asmare et al., 2023). The Grazing land (overgrazing) and bushland area show the highest probability contribution for landslide occurrence. The distribution of landslide occurrence in the study area with land use type of grazing land and bushland showed 38.5% and 44.5% highest values. The information value of the land use types 0.27 and 0.55 show positive values. The other land use types show low distribution for landslides.

Table 4. Information value for each factor class and landslide

Factor	Class	Nclass	Ncpix%	Nslpix	Nslpix%	con_pro	prior_pro	cp/pp	L. density	IV
Slope(°)	0-5	104938	37.3	231	0.6	0.002	0.097	0.022	0.22	-1.64
	5-12	56580	20.1	1635	4.9	0.0288	0.097	0.297	0.27	-0.52
	12- 30	51576	18.3	6789	20.5	0.1316	0.097	1.35	0.07	0.13
	30- 45	45069	16	13323	40.2	0.295	0.097	3.045	-0.27	0.48
	>45	23157	8.2	11093	33.5	0.4790	0.097	4.934	-0.31	0.69
Stream(m)	0-190	122209	43.1	12877	38.9	0.105	0.097	1.08	0.90	0.03
	190-450	89924	31.7	12413	37.5	0.138	0.097	1.42	1.18	0.15
	450-760	46322	16.3	5400	16.3	0.116	0.097	1.2	1	0.07
	760-1290	18885	6.6	1829	5.5	0.096	0.097	0.99	0.83	-0.001
	>1290	6199	2.1	556	1.6	0.089	0.097	0.923	0.7	-0.03
Lineament(m)	0 - 600	160416	57.3	32168	98.62594	0.201	0.097	0.69	1.71	0.31
	600 - 1,200	56545	19.9	448	1.374065	0.008	0.097	-1.57	0.06	-1.07
	1,200-1,800	34291	11.9	0.00	0.000	0.000	0.097	-2.65	0.00	0.00
	1,800-2,400	20724	7.03	0.00	0.000	0.000	0.097	-2.42	0.00	0.00
	>2,400	11561	3.7	0.00	0.000	.000	0.097	-3.37	0.00	0.00
Lithology	Hornblend gnesis	179862	63.4	30614	97.4	0.1702	0.097	1.753	1.53	0.24
	Basalt	34338	12.1	780	2.4	0.0227	0.097	0.233	0.20	-0.63
	Magnetite	186	0.06	0.00	0.00	0.0000	0.097	0	0	0
	Alluvium	55873	19.7	18	0.05	0.0003	0.097	0.003	0.002	-2.47
	Eluvium	13225	4.6	0.00	0.00	0.0000	0.097	0	0	0
LULC	River	193	0.1	0	0	0	0.097	0	0	0
	Dense forest	55400	19.6	1939	5.8	0.03488	0.097	0.359	0.29	-0.44
	Agriculture	53300	19.0	81	0.2	0.0015	0.097	0.015	0.01	-1.81
	Settlement	1306	0.6	0.00	0.00	0.00	0.097	0.00	0.00	0.00
	Bush land	3683	12.9	12791	38.5	0.347	0.097	3.57	2.98	0.55
	Spare forest	166	0.05	2120	10.9	0.070	0.097	0.728	0.6	-0.13
	Graze land	171653	60.5	15944	44.58	0.1808	0.097	1.8633	1.55	0.27
Curvature	Concave	44435	15.6	9444	28.5	0.212	0.097	2.18	1.82	0.34
	Plan(0)	201425	71.04	15292	46.2	0.075	0.097	0.78	0.65	-0.10
	Convex	37660	13.2	8339	25.2	0.221	0.097	2.28	1.90	0.35
Aspect	Flat	23104	8.2	3378	10.2	0.1462	0.097	-1.506	1.24	-0.17
	North	22316	7.9	560	1.6	0.0250	0.097	0.258	0.20	-0.58
	Northeast	22464	7.9	175	0.5	0.0077	0.097	0.080	0.06	-1.09

	East	24798	8.8	1182	3.5	0.0476	0.097	0.491	0.39	-0.30
	Southeast	34978	12.4	6066	18.3	0.1734	0.097	1.786	1.47	0.25
	South	41988	14.9	8587	25.9	0.2045	0.097	2.106	1.73	0.32
	Southwest	44764	15.9	6504	19.6	0.1452	0.097	1.496	1.23	0.17
	West	38242	13.5	3778	11.4	0.0987	0.097	1.017	0.84	0.007
	Northwest	23104	10.1	3378	8.5	0.0983	0.097	1.013	0.84	0.005
Rainfall	1,050 - 1,200	48348	17.1	1067	3.9	0.0214	0.097	0.221	0.22	-0.65
	1,200 - 1,350	70540	24.9	3732	13.6	0.053	0.097	0.546	0.54	-0.26
	1,350 - 1,500	88609	31.3	7039	25.8	0.0777	0.097	0.801	0.82	0.102
	1,500 - 1,650	41180	14.5	8318	30.6	0.2177	0.097	2.243	2.6	0.34
	> 1,650	33692	11.9	7115	26.1	0.206	0.097	2.126	1.8	0.32

Note; Ncpix= Factor class pixel count, Nslpix= Landslide pixel within factor, Con_prob= conditional probability, Prior_prob= Prior probability, Cp/Pp= Weight of factor classes, IV= Information value

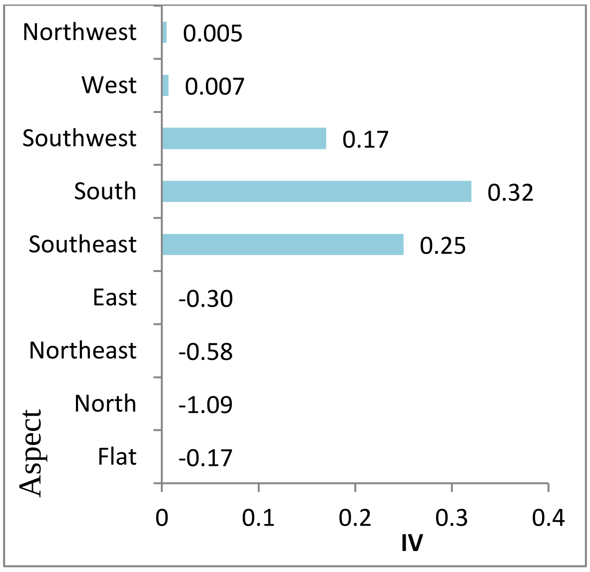

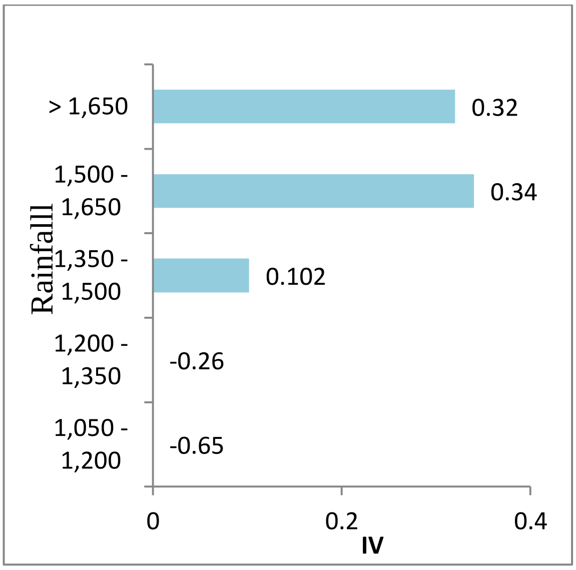

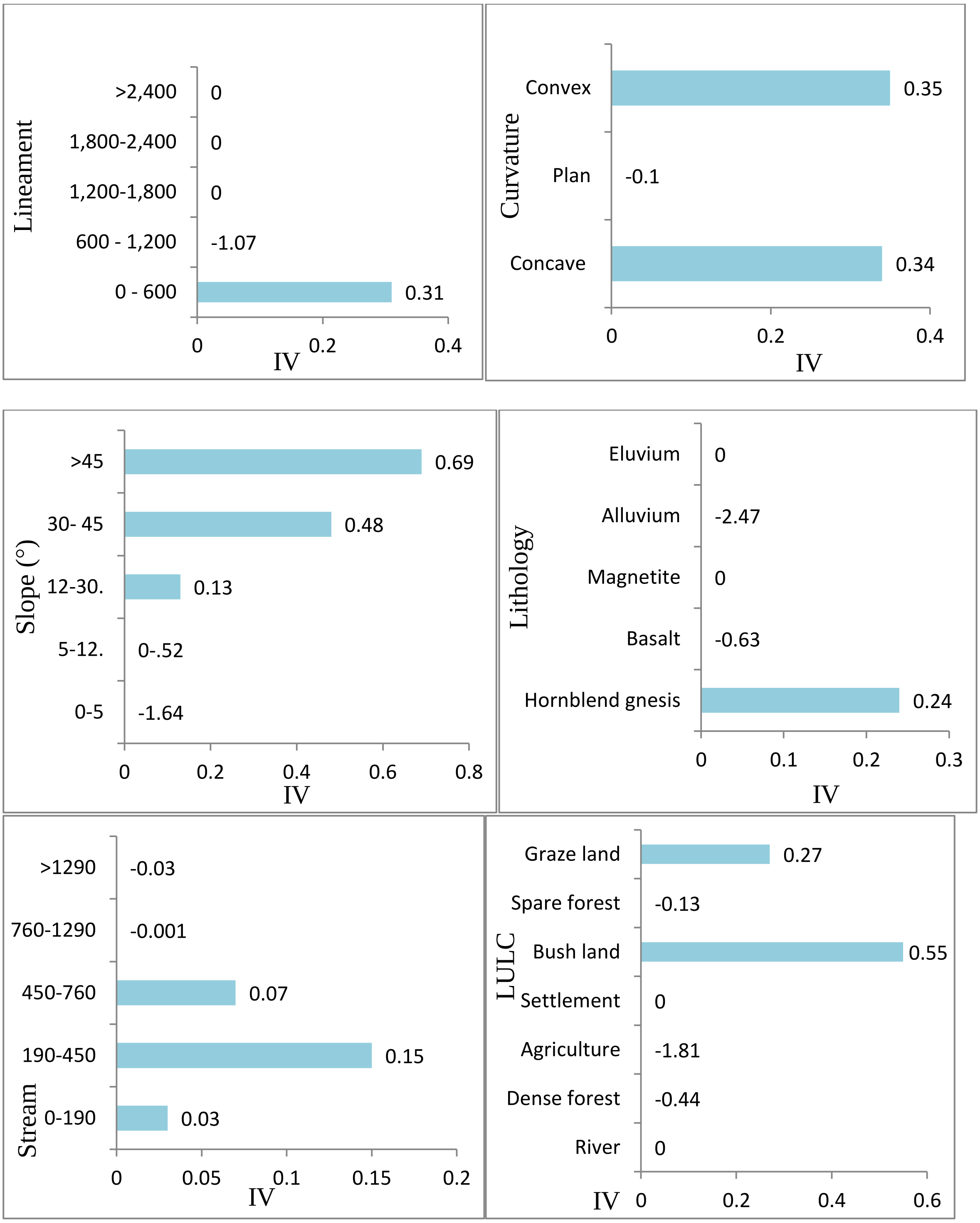

Figure 16.Relationship between causative factors and information value

5.3.3 Significant classes among various causative factor classes

Landslides are a significant geological hazard that can have devastating consequences for both human life and infrastructure. Therefore, understanding the factors contributing to landslides is crucial for effective risk assessment and mitigation strategies. In the current study, eight causal factors were taken into account: aspect, curvature, LULC, lithology, rainfall, slope, and distance to streams and lineament. With the aid of statistical information value, the relational statistical correlation between different causative factors and historical landslide data was analyzed, and the relative importance of different causative factor classes was determined. According to the IV method, the dominant influencing factor for landslide occurrence was slope, followed by LULC, curvature, and rainfall (Table 5 and Figure 17).

Table 5.The highest information value classes

Causative factor	**Classes**	**Information value**
Slope(°)	>35	0.69
Aspect	South	0.33
Curvature	Convex	0.35
Distance to lineament (m)	0 – 600	0.31
Distance to stream(m)	190 –450	0.15
Rainfall (mm)	1500 – 1650	0.34
Lithology	Hornblend – gnesis	0.24
LULC	Bushland	0.55

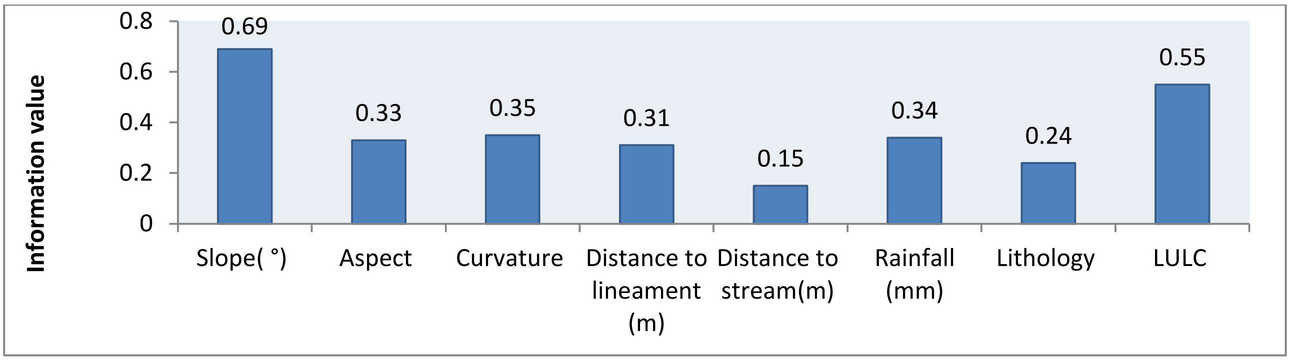

Figure 17. Rating highest information value classes

5.4 Landslide susceptibility mapping using Information value

Landslide susceptibility analysis is a critical component of geohazard assessment and management, aiming to identify areas that are prone to landslides based on various causative factors. The present study utilized the statistical information value method to conduct landslide susceptibility analysis in the study area. The first step in the analysis involves the preparation of thematic factor maps and statistical information value pixels calculation, which was employed in ArcGIS 10.7. Once the weight assigned for causative factor classes was completed, the weight-assigned causative factor map was rasterized using the lookup tool in spatial analysis. The rasterized causative factors maps were used to generate the landslide susceptibility index map. The LSI map of the study area was prepared by summing all information value raster maps by using a raster calculator in the map algebra of ArcGIS.

Using a raster calculator in map algebra, the landslide susceptibility index value for each pixel in the study area was determined by summing all the maps of causal factors. The number ranged from -8.8 to 2.76. The landslide susceptibility index map requires further classification using techniques like natural break, standard deviation, equal interval, manual, and quantile in GIS. Natural breaks are crucial for unevenly distributed data(Meten, et al., 2015).

The study area's landslide susceptibility index map was classified into five classes of very low, low, moderate, high, and very high based on the natural breaks method, showing a correlation between the area's landslide susceptibility and the total area, with a minimum of -8.8 and maximum of 2.76.

Table 6.Landslide susceptibility classes for Information value model

Susceptibility classes	**LSI**	**Pixel**	**Area (km^2)**	**Area (%)**
Very low	-8.83 - -5.28	40527	35.9	14.5
Low	-5.28- -3.30	43316	38.79	15.56
Moderate	-3.30 - -1.27	55042	49.1	19.74
High	-1.27 – 0.61	54856	48.47	19.71
Very high	0.61 - 2.76	84537	78.17	30.37

According to the Table (6) and Figure (19), 35.9km^2 (14.5%) and 38.9km^2 (15.56%) of the study area are classified as being in the very low and low susceptible classes, whereas 49.1km^2 (19.74%) is classified as being in moderate susceptible class. The susceptible class for the last 48.04km^2 (19.71%) and 78.17km^2 (30.37%) fall into the high and very high susceptible classes. Only 74.69km^2 (30.1%) of the study area is classed as low susceptible, whereas 175.3km^2 (69.8%) of the study area is classified as moderate, high, and very high (Figure 18). The plateau part of the study area including the location shacha and burji fall in very high classes.

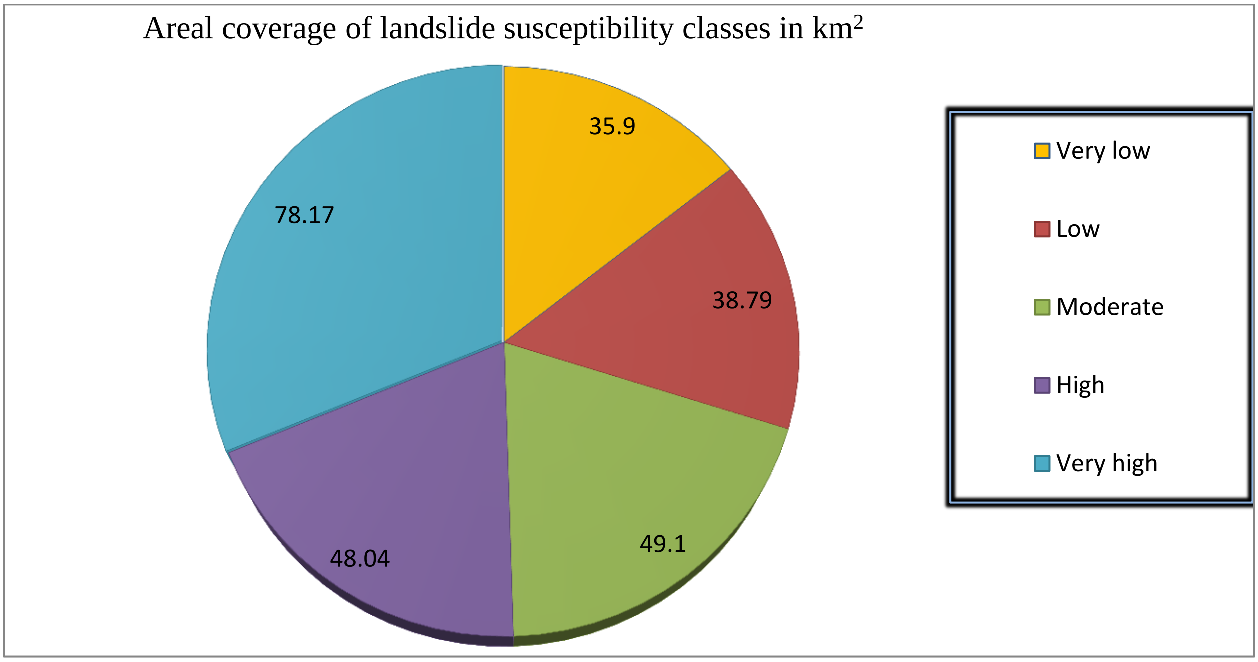

Figure 18.Pie charts indicating landslide susceptibility classes for Information value.

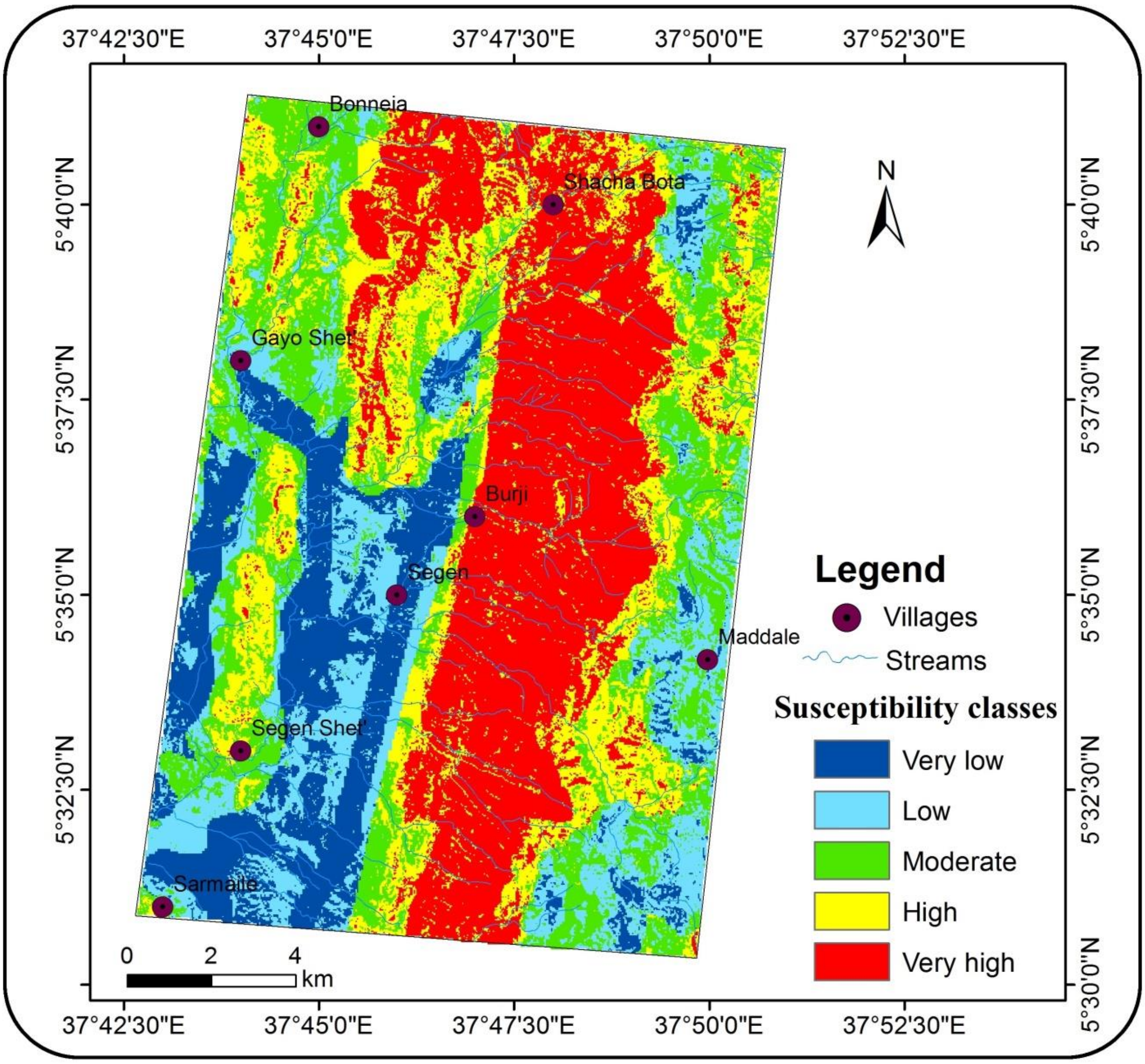

Figure 19.Landslide susceptibility map produced by using the Information value method

5.5 Landslide susceptibility mapping using Logistic Regression model

The logistic regression model is the linear model that extends the linear regression model on SPSS software. This model lies in the sample size selection of dependent and independent variables for susceptibility analysis. There are three ways to sample landslide and non-landslide points. The first way is to use all data from all the study areas. This ways leads to uneven proportions of points of landslide and non-landslide pixels(Guzzetti et al., 1999). The second method that results in less reliability, which uses all landslide pixels with equal non-landslide pixels, is less reliable. It can reduce the sampling bias. The third method uses an equal proportion of landslide and non-landslide pixels (Dai et al., 2002). This was divided into training and testing data, which have two cases. For this model, an equal proportion of both landslide and non- landslide pixel points were used in this study.

The study classified landslides into 70% (186) training landslides and 30% (79) testing landslides. Causative factor maps were calculated and analyzed in ArcGIS. A logistic regression analysis was performed using an input database and eight independent variables. Landslide data was entered into a table, and related variables were extracted. The results were exported into a format for SPSS and used in the logistic regression model (Appendix 1.2 and Table 7). The Backward Likelihood Ratio method was chosen for the logistic regression module.

Table 7.Logistic Regression (LR) Coefficient, Collinearity test and Model statistic

Landslide factors	**LR coefficient(b)**	**Sig**	**S.E**	**Exp(b)**	**Collinearity statistic**	
					Tolerance	**VIF**
Slope	0.283	0.000	0.022	17.906	0.534	1.873
Lithology	0.214	0.000	0.018	16.25	0.793	1.261
Distance to lineament	-0.029	0.347	0.000		0.964	1.037
Rainfall	0.064	0.039	0.000	1.196	0.943	1.060
Aspect	0.314	0.000	0.044	44.28	0.890	1.124
Curvature	0.058	0.437	0.931	3.313	0.821	1.217
Distance to stream	0.275	0.305	0.268	0.001	0.976	1.025
Landuse	0.085	0.000	0.022	17.629	0.652	1.534
Constant	0.557	0.000	0.029	0.151		

Model Statistics	Value
Chi- square	6.14
Cox & Snell R square	0.670
Significance	0.632

The Standard Error (SE) of the estimated coefficients is a crucial metric in logistic regression landslide susceptibility modelling that is used to evaluate the accuracy and dependability of the model's prediction. A smaller SE indicates that the model's estimates are more accurate and less variable, indicating a higher degree of confidence in the relationships between predictor variables and landslide susceptibility. Conversely, a larger Standard error signifies a higher degree of uncertainty (Table 7).

Model significance (Sig.) is the main focus of logistic regression modeling, and null hypothesis tests are employed to assess the model significance. A low p-value (0.05) indicates statistical significance and the model's capacity to explain landslide differences, rejecting the null hypothesis. In logistic regression, the exponentiation of the coefficient (ß) associated with a predictor variable in the model is called Exp(ß). This is also known as the odds ratio (exp(bi)) and is commonly utilized. Each coefficient in the model represents the change in log odds of landslide occurring. The positive coefficient indicates that the likelihood of a landslide occurring increases as the independent variable increases, while the negative coefficient is vice versa. When many predictors in a logistic regression model have a high degree of correlation, it is known as multicollinearity. This allows one predictor to be predicted linearly from the others with a particularly high degree of accuracy (Shano et al., 2020).

This study conducted a multicollinearity analysis using techniques like Variance Inflation Factors (VIF), tolerance, linear and chi-square. To ensure accurate findings, components with collinearity problems were eliminated. A VIF value of less than 10 indicates non-extreme collinearity, while a larger VIF indicates increased collinearity. Variables with a VIF application range of 1-10 are considered suitable factors.

The landslide susceptibility map of the model displays the spatial probability of future landslides. The extracted coefficient values are calculated using an ArcGIS environment raster calculator. The linear combination is converted into a probability value between 0 and 1 through the logistic function (1/1+exp(-z)). Where b0=0.557 (constant), b1=0.283 (regression coefficient of slope), b2=0.214(regression coefficient of lithology), b3=-0.029 (regression coefficient of lineament), b4=0.064 (regression coefficient of rainfall), b5=0.314 (regression coefficient of aspect), b6=0.058 (regression coefficient of curvature), b7=0.275 (regression coefficient of stream), b8=0.085 (regression coefficient for land use). This expressed as P = 1/ (1 + exp^(-(b0 + b1*slope + b2*lithology + b3*lineament + b4*rainfall + b5*aspect + b6*curvature + b7*stream+b8*lulc

Z= 0.557+ 0.283*slope + 0.214 *Lithology + -0.029 * Distance to lineament + 0.064

*Rainfall + 0.314 * Aspect + 0.058 * Curvature + 0.275 * Distance to stream + 0.085* Landuse

In the index map of the study area, the probability values range between 0.199 and 0.893. Using an index map, it is possible to visually interpret how much historical landslides confirm the probability of a landslide occurring. The landslide susceptibility index map was reclassified into five groups by using the natural breaks method (Table.8). The classifications (0.199 -0.3331) fall under very low which cover 19.9 % (49.38km), (0.3331– 0.4175) low covers 7.98% from 19.81km, (0.4175– 0.5169) moderate 16.04 % from 39.8km, (0.5169– 0.638) high 20.40% from 51.6km, and (0.638– 0.893) very classes cover 35.65% from 89.4km susceptible classes.

Table 8. Landslide susceptibility classes for Logistic regression model

Susceptibility classes	**LSI**	**Pixel**	**Area (km^2)**	**Area (%)**
Very low	0.199 – 0.3331	55386	49.38	19.90
Low	0.3331– 0.4175	22541	19.81	7.98
Moderate	0.4175– 0.5169	44765	39.82	16.04
High	0.5169– 0.638	56762	51.6	20.40
Very high	0.638– 0.8934	98824	89.4	35.65

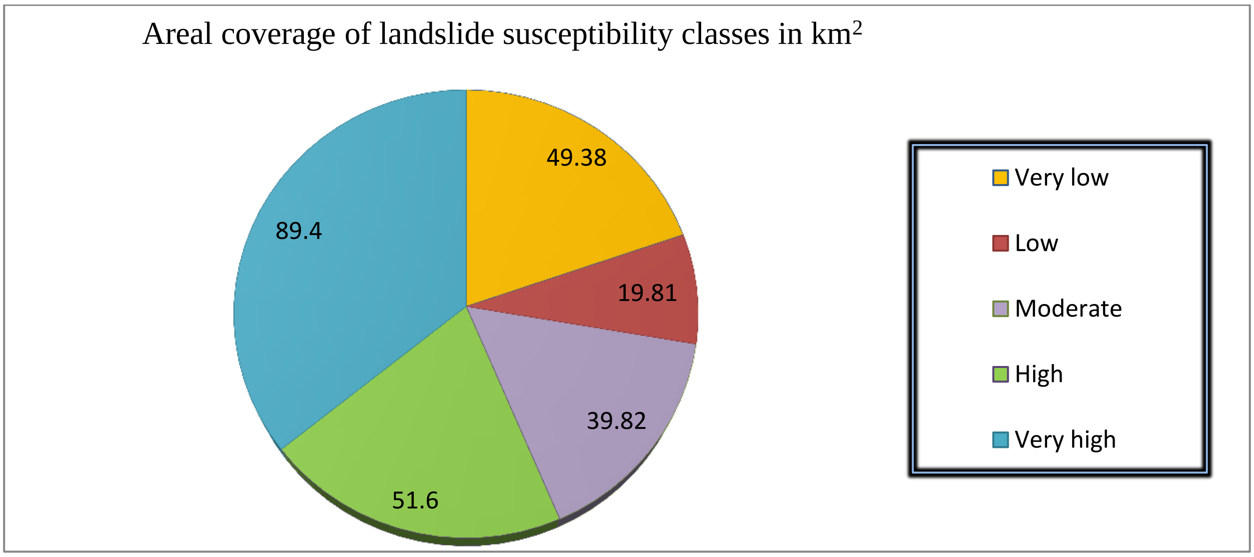

Figure 20.Pie charts indicating landslide susceptibility classes for LR

Figure 19 shows the plateau part of the study area, including the locality of Burji, Shacha bota, segen sheet, and Sermaile show very high and high susceptibility classes. Localities such as Bonneia, Gayo sheet, Maddale, and Segen fall into very low, low, and moderate susceptibility classes. From Figure (21), the areal coverage of landslide susceptibility 89.4 km is covered by very high susceptible classes.

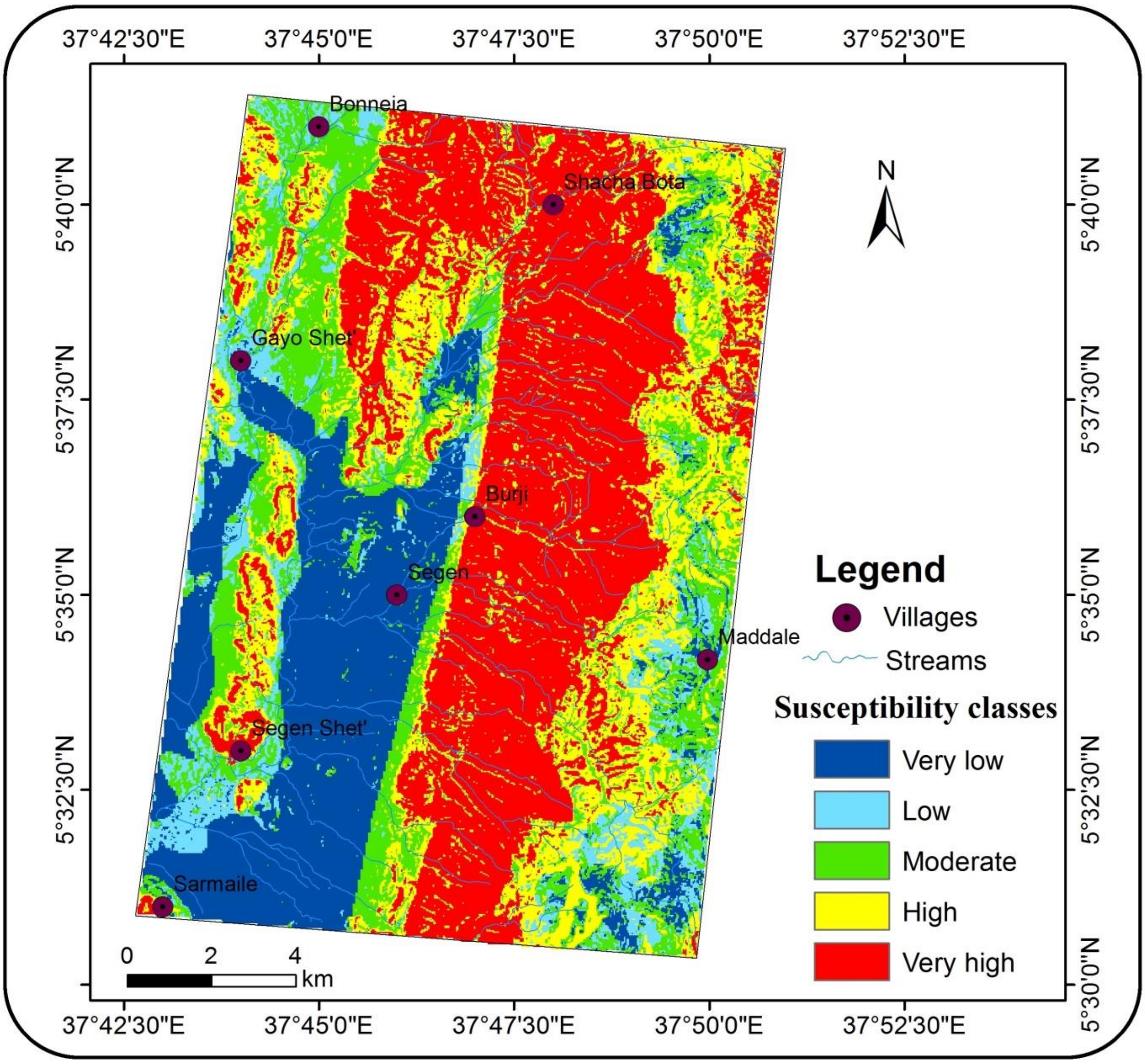

Figure 21.Landslide susceptibility classes produced by using the logistic regression method.

5.6 Verification of landslide susceptibility map

Landslide susceptibility maps are crucial tools for disaster risk management, land use planning, and infrastructure development in regions that are prone to landslides. These maps indicate areas with varying probabilities of landslide occurrence based on analyzing various conditioning and trigger factors. Model validation is the most crucial stage before interpreting the model's output maps. A map prone to landslide without verification means less from a scientific standpoint. This study used three validation methods: receiving operating characteristic (ROC), relative landslide density index (R- index) and landslide density index(LDI).

5.6.1 Validation of model using ROC

The comparison process used the receiving operating characteristic (ROC) curve method. The area under curve (AUC) is calculated to evaluate the success and predictive rate training and testing data set for information value and logistic regression model (Wubalem and Meten, 2020; Asmare et al., 2023). AUC value ranges from 0.5 to 1. When the AUC value is between 0.9 and 1, the model will have excellent performance; if the AUC value is between 0.8 and 0.9, the model will have very good performance. If the AUC value is between 0.7 and 0.8, the model will perform well. If the AUC value is between 0.6 and 0.7, the model will have average performance. However, if the AUC value is between 0.5 and 0.6, the model will have a fair performance, but if the AUC value is equal to or less than 0.5, then the model will have a poor performance (Wubalem and Meten, 2020).

In this investigation, the computed susceptibility index values were sorted in descending order for both training and validation of landslide raster maps. The success rate was obtained by comparing training landslide pixels (70%) with landslide susceptibility maps, and the predictive rate (30%) was obtained by comparing the validating pixel (30%) with the landslide susceptibly maps of both IV and LR models. The success rate and predictive rate from AUC are 0.886 and 0.864, respectively, for the information value model, and for the logistic regression model, these rates are 0.894 and 0.871, respectively. The two current models AUC values for both success and predictive rates fall between 0.8 and 0.9, indicating a very good performance (Figure 22).

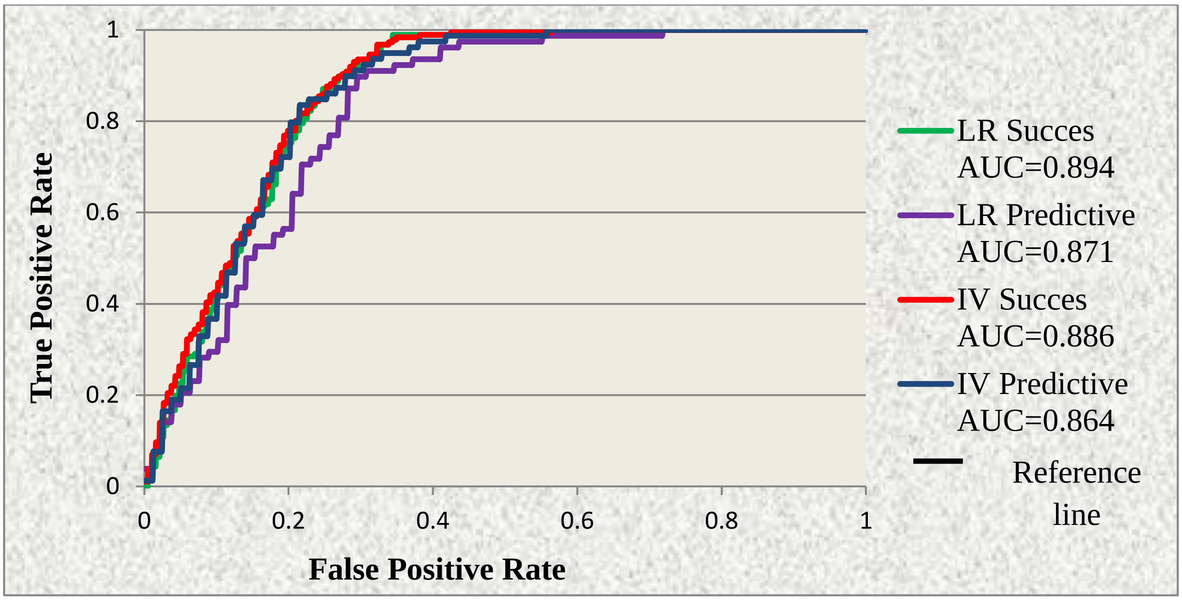

Figure 22.Success and predictive rate curves

5.6.2 Validation of model using LDI and R- index

One such valuable tool in assessing landslide susceptibility is the landslide density index. Landslide density index is a quantitative measure used to evaluate landslides' spatial distribution and concentration within specific regions. The model is valid when a high landslide density index value indicates an area with a higher concentration of landslide signification and elevated susceptibility to landslide events (Pradhan and Lee, 2010). It is typically calculated by dividing the percentage of pixels with landslide susceptibility class by the percentage of pixels with landslide susceptibility classes (Table 9). The LDI value for both models shows an increase from a very low value to a very high landslide susceptibility class (Figure 21).

$$\text{LDI} = \frac{\text{(Percent) observed landslide}}{\text{(Percent) predicted landslide}} \dots\dots\dots\dots\dots\dots (\text{Eq. } 6)$$

Relative landslide density index

The landslide susceptibility models in the current study were validated using a relative landslide density index, which is determined using the following equation.

$$R - index = \sum \frac{\frac{ni}{Ni}}{\frac{ni}{Ni} * 100} \dots\dots\dots\dots\dots\dots\dots\dots (\text{Eq.7})$$

Where ni is the number of landslides in a landslide susceptibility class, Ni is the number of landslide susceptibility class pixels within the class. The increase in R-index values from the very low to the very high landslide susceptibility categories validates the accuracy as well as reliability of the model (Wubalem and Meten, 2020). In contrast to the two methods, the information value method shows a greater R-index value for the high susceptibility class. The logistic regression approach also recorded the very low susceptibility class's lowest R-index (Figure 22 and Table 9).

Table 9. Landslide density index of information value and Logistic regression models

Model	**LS class**	**LSI**	**LSP**	**LSP (%)**	**TLSP**	**R-index**	**TLSP (%)**	**LDI**	**VLP**	**R-index**	**VLP (%)**	**LDI**
Information method	Very low	-8.83 - -5.28	40527	14.5	5	0.1	0.01	0.00	2	0.1	0.00	0.00
	Low	-5.28- -3.30	43316	15.56	23	0.45	0.06	0.003	3	0.14	0.02	0.00
	Moderate	-3.30 - -1.27	55042	19.74	309	5.2	0.93	0.04	120	4.44	0.8	0.06
	High	-1.27 – 0.61	54856	19.71	2881	44.3	8.7	0.45	1860	69.2	13.6	0.69
	Very high	0.61 - 2.71	84537	30.37	29810	305.2	90.25	2.97	11649	281.25	85.4	2.81
	278278				33028		100		13634	100		

Model	**LS class**	**LSI**	**LSP**	**LSP (%)**	**TLSP**	**R - index**	**TLSP (%)**	**LDI**	**VLP**	**R-index**	**VLP (%)**	**LDI**
Logistic regression method	Very low	0.199-0.3331	54867	19.90	5	0.16	0.01	0.00	7	0.25	0.05	0.00
	Low	0.199 – 0.3331	22022	7.98	50	2.13	0.15	0.02	10	0.91	0.07	0.008
	Moderate	0.3331– 0.4175	44246	16.04	319	6.2	0.96	0.12	82	3.74	0.6	0.03
	High	0.4175– 0.5169	56243	20.40	1938	29.80	5.86	2.44	1018	36.5	7.4	0.36
	Very high	0.5169– 0.638	98305	35.65	30713	261.2	92.97	3.7	12517	257.46	91.8	2.5
					33026		100		13634			

All things considered, the analysis shows that the very high landslide susceptibility zone experiences the highest concentration or density of landslides. This suggests that the maps of landslide susceptibility produced by the LR and IV models are dependable and provide important information on the distribution and intensity of landslide susceptibility in the study area.

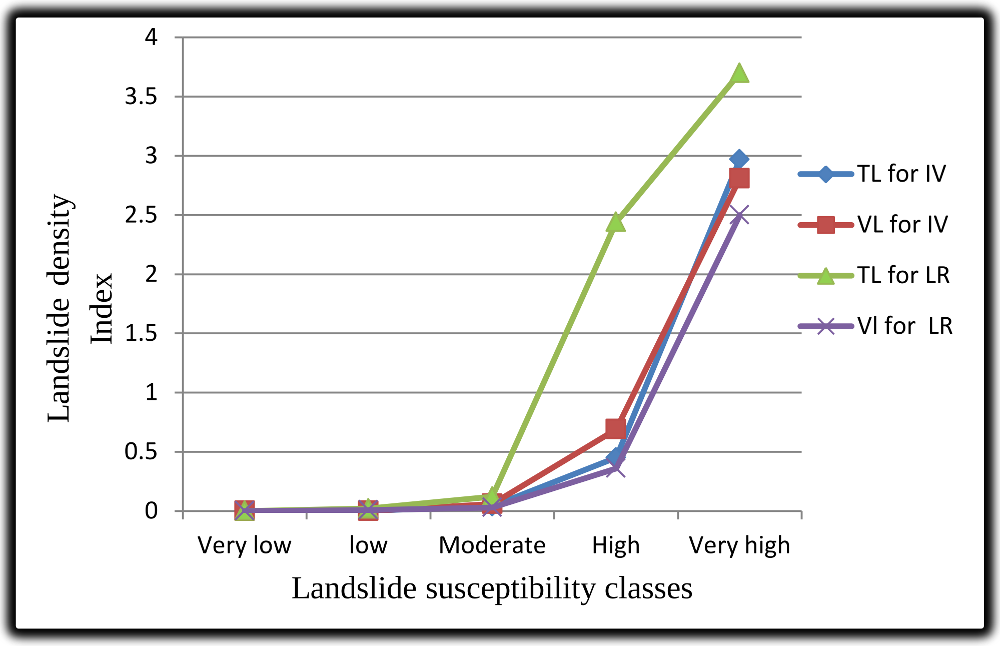

Figure 23. The landslide density index for IV and LR model

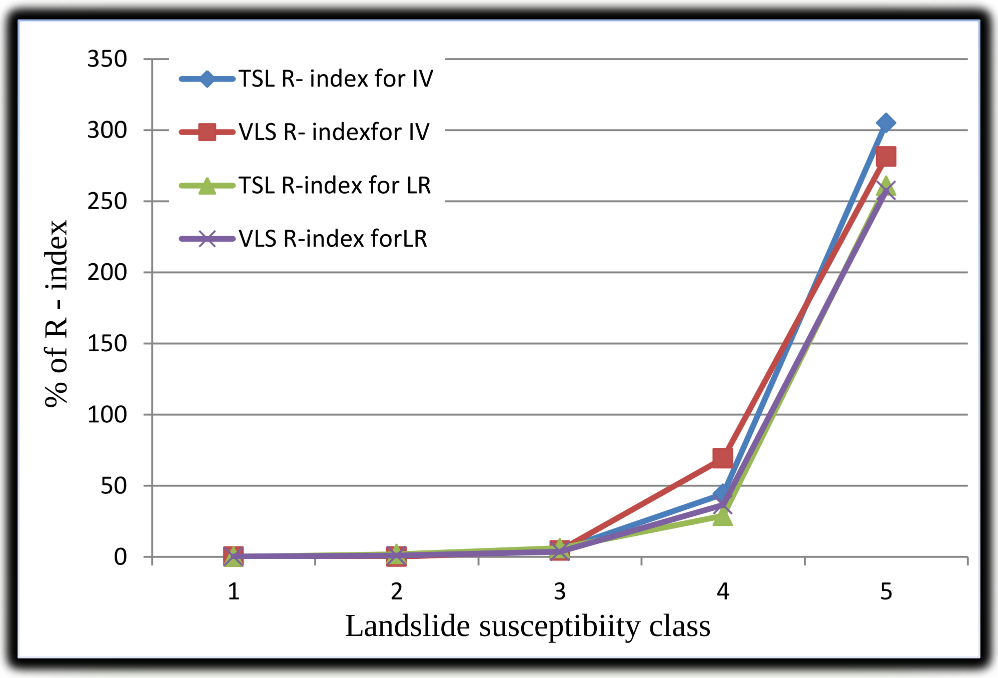

Figure 24. R- Index value

From Table (9) shows the two methods categorized into five susceptibility classes using quantile classification method. The Information value method shows higher R-index for higher susceptibility classes than the logistic regression method. Indicate a stronger relationship between the causative factors and landslide occurrence in those areas. This suggests that the IV method more effectively shows the areas at greater risk of landslides.

5.7 Model comparision

The IV methods offer several advantages, It is beneficial to understand how each factor class influences landslide occurrences. It calculates the contribution of each landslide-conditioning factor by comparing the percentage of landslides occurring in a particular class with the percentage of the total area occupied by that class, As shown in Figure13, while it is possible to predict the likelihood that each factor class will contribute to a landslide event. However, the information value model has some limitations. It does not provide insight into which landslide component has the greatest control. The logistic regression model, which computes the regression coefficients for each landslide factor to establish their significance, can be used to overcome this limitation. However, because the landslide variables have been simplified and generalized, the model also has limits. It typically requires a larger dataset and balanced data for reliable predictions. In cases of data scarcity or imbalance, the model may perform poorly.

According to the success and predictive rate curves, the logistic regression method generally performs better than the information value model in landslide susceptibility mapping (Du et al., 2017). However, in this study, the logistic regression model achieved a higher success rate curve of 89.4% and a predictive rate curve of 87.1%, compared to the information value model's success rate of 88.6% and predictive rate of 86.4%.

6. CONCLUSION AND RECOMMENDATION

6.1 Conclusion

Landslides represent a significant natural hazard that profoundly impacts human life, infrastructure, and the environment. The present study area is located in southern regional state, southeastern Ethiopian highland. Rift margins and highlands contribute to the region, making them particularly vulnerable to landslide event. In this study, the landslide susceptibility map of the study area was created using information value and logistic regression model.

The main objective of this study is to prepare a landslide susceptibility map for Burji to Maddale area using Information value and logistic regression method. The landslide susceptibility map prepared for the area serves as a critical tool for reducing risk, enhancing planning, protecting the environment, and fostering informed decision-making. It helps communities and governments better manage and mitigate the impacts of landslides.

A landslide inventory map was created using Google Earth image interpretation. A total of 265 landslides were identified, of which 70% (186) were utilized to build the model and 30% (79) were used for validation. Eight causative factors were randomly selected such: as slope, aspect, curvature, rainfall, distance to stream, distance to lineament, lithology, and land use land cover. All causative factor maps changed from vector into a raster data format. Then, all thematic maps were reclassified into different classes. When the weights of each class of landslide factor were computed using the information value model. When factor classes of information value exceed 0.1, it will significantly contribute to landslide occurrence in the study area. Based on the results of the IV analysis, the factor classes with information values greater than 0.1include slope (26-35 and >35), aspect (southeast and south), curvature (concave and convex), lithology (Hornblend gnesis), distance to stream (190-450m), rainfall (1498-1688 and >1688 mm), distance to lineament (0-600 m) and land use/ land cover (graze land and bush land).

The logistic regression coefficients for each landslide factor were found from the logistic regression model. The coefficient of the causative factors from logistic regression analysis with a positive value will have an impact on landslide occurrence. From this study, all causative factors without distance to lineament have positive coefficient values that have high contribution to landslide occurrence. In this study, the highest contribution to landslide occurrence is expected from aspect, lithology, slope and distance to stream as their coefficient are higher. Using the natural break classification method, the landslide susceptibility map was reclassified into very low, low, moderate, high, and very high in ArcGIS.

Receiving operating characteristic (ROC) is used in the evaluation of landslide susceptibility models. The curve values quantify the overall ability of the model to determine between landslide-prone and non-landslide areas. The relative landslide density index (R- index) and area under the curve (AUC) of the receiver operating characteristic curves were calculated from the training and testing/validation/ landslide data sets in order to assess the performance of the information value and logistic regression models for landslide susceptibility modelling.

The information value model has an AUC accuracy of 88.6% success rate and 86.4% prediction rate, whereas the logistic regression model has an AUC accuracy of 89.4% success rate and 87.1% predictive rate. From the success rate and predictive rate from ROC, the AUC value is between 0.8 and 0.9 in both models, indicating an acceptable result. Based on the AUC result, the logistic regression model is better than the information value model. For the R-index validation method, the results of the information value method perform better than the logistic method, as the R-index increases from the very low to very high susceptibility classes.

This study was conducted to identify the areas that are prone to landslides and to understand each factor’s and each factor class’s contribution to landslide occurrence. The findings of this study are important for risk management, urban planning, infrastructure development, and disaster mitigation.

6.2 Recommendation

Managing landslide risk issues in a certain region requires a combination of engineering solutions, policy measures, community involvement, and environmental management.

- The government should enforce and implement strict land use planning in the area based on the findings of this study for settlement and infrastructural development purposes.
- Future slope instability issues will likely cause serious concern in areas with high and very high susceptibility classes. A more thorough slope stability analysis using a safety factor is recommended before any future settlements and infrastructure development in these susceptibility classes.

Based on the results of the current study, the relevant land management bodies should propose future landslide interventions in the study area to implement more effective landslide management measures.

REFERENCE

Abebe, B., Dramis, F., Fubelli, G., Umer, M., & Asrat, A. (2010). Landslides in the Ethiopian highlands and the Rift margins. Journal of African Earth Sciences, 56(4–5), 131–138. https://doi.org/10.1016/J.JAFREARSCI.2009.06.006

Abraham, A. (1989). Tectonic history of the pan-african low grade belt of western Ethiopia. Ethiopian Institute of Geological Survey, 305, 22.

Achour, Y., Boumezbeur, A., Hadji, R., Chouabbi, A., Cavaleiro, V., & Bendaoud, E. A. (2017). Landslide susceptibility mapping using analytic hierarchy process and information value methods along a highway road section in Constantine, Algeria. Arabian Journal of Geosciences, 10, (1-16).

Almond, D. C. (1983). The concepts of "Pan-African episode" and "Mozambique Belt" in relations to the geology of east and northeast Africa. Faculty of Earth Sciences Bulletin, King Abdulaziz University, 6(71–87).

Anbalagan, R. & Singh, B. (2001). Landslide hazard and risk mapping. Landslide Hazard and Mitigation in the Hidu-Kush Himalayas.

Anbalagan, R. (1992). Landslide hazard evaluation and zonation mapping in mountainous terrain. Engineering Geology, 32(4), 269–277. https://doi.org/10.1016/0013-7952(92)90053-2

Anderson, M. G., & Burt, T. P. (1978). The role of topography in controlling throughflow generation. Earth Surface Processes, 3(4), 331-344.

Asmare, D., Tesfa, C., & Zewdie, M. M. (2023). A GIS-based landslide susceptibility assessment and mapping around the Aba Libanos area, Northwestern Ethiopia. Applied Geomatics, 15(1), 265–280. https://doi.org/10.1007/s12518-023-00499-7

Ayalew, L. (1999). The effect of seasonal rainfall on landslides in the highlands of Ethiopia. Bulletin of Engineering Geology and the Environment, 58, 9-19.

Ayalew, L., & Yamagishi, H. (2004). Slope failures in the Blue Nile basin, as seen from landscape evolution perspective. Geomorphology, 57(1–2), 95–116.

Ayalew, L., & Yamagishi, H. (2005). The application of GIS-based logistic regression for landslide susceptibility mapping in the Kakuda-Yahiko Mountains, Central Japan.

Geomorphology, 65(1–2), 15–31.

Ayele, S., Raghuvanshi, T. K., & Kala, P. M. (2014). Application of Remote Sensing and GIS for Landslide Disaster Management: A Case from Abay Gorge, Gohatsion–Dejen Section, Ethiopia. 15–32. https://doi.org/10.1007/978-4-431-54871-3_2

Ayenew, T., & Barbieri, G. (2005). Inventory of landslides and susceptibility mapping in the Dessie area, northern Ethiopia. Engineering Geology, 77(1–2), 1–15. https://doi.org/10.1016/J.ENGGEO.2004.07.002

Banda, E., & Wickham, S. M. (1986). The geological evolution of the Pyrenees. Tectonophysics, 129(1–4).

Bera A, Mukhopadhyay BP, D. D. (2019). Landslide hazard zonation mapping using multi-criteria analysis with the help of GIS techniques: a case study from eastern Himalayas, Namchi, South Sikkim. Nat Hazards, 96((2)), 935–959.

Beza, Y. A. (2021). GIS-Based Statistical Analysis for Evaluation of Landslide Susceptibility Mapping: A Case Study in Blue Nile Gorge, Gohatsion-Dejen Road Section, Central Ethiopia.

Bhutia, S. L., Borah, S., Pradhan, R., & Sharma, B. (2020). An Experiment on Parameter Selection for Landslide Susceptibility Mapping using TF-IDF. Journal of Physics: Conference Series, 1712(1).

Cahen, L., Snelling, N.J., Delhal, J. and Vail, J. . (1984). The Geochronology and Evolution of Africa. Larendon Press, Oxford, 512.

Chalachew Tesfa, & Woldearegay, K. (2021). Characteristics and susceptibility zonation of landslides in Wabe Shebelle Gorge, south eastern Ethiopia. African Earth Sciences, 182(104275).

Chen, Y., Ba, Q., Wu, Q., & Li, X. (2016). Landslide susceptibility evaluation based on GIS and information value model. Nceece 2015, 1586–1591.

Chimidi, G., Raghuvanshi, T. K., & Suryabhagavan, K. V. (2017). Landslide hazard evaluation and zonation in and around Gimbi town, western Ethiopia—a GIS-based statistical approach. Applied Geomatics, 9(4), 219–236.

Cruden, D. (1991). A simple definition of a landslide. Bulletin of Engineering Geology & the Environment, 43(1), 27-29.

Dai, F. C., Lee, C. F., Li, J., & Xu, Z. W. (2001). Assessment of landslide susceptibility on the natural terrain of Lantau Island, Hong Kong. Environmental Geology, 40(3), 381–391.

Dai, F. C., Lee, C. F., & Ngai, Y. Y. (2002). Landslide risk assessment and management: An overview. Engineering Geology, 64(1), 65–87. https://doi.org/10.1016/S0013-7952(01)00093-X

Das, I., Stein, A., Kerle, N., & Dadhwal, V. K. (2012). Landslide susceptibility mapping along road corridors in the Indian Himalayas using Bayesian logistic regression models. Geomorphology, 179, 116–125.

Davidson, A. (1983). The Omo River project, reconnaissance geology and Geochemistry of part of Illubabor, Kefa, Genu Gofa and Sidamo, Ethiop. Inst. Geol. Surv, Minist. Mines Energy, 2, 1–89, 2, 1–89.

Davidson, A. (Anthony). (1983). The Omo River Project : reconnaissance geology and geochemistry of parts of Ilubabor, Kefa, Gemu Gofa and Sidamo, Ethiopia. Bulletin of Engineering Geology and the Environment, 2, 89.

Du, G. liang, Zhang, Y. shuang, Iqbal, J., Yang, Z. hua, & Yao, X. (2017). Landslide susceptibility mapping using an integrated model of information value method and logistic regression in the Bailongjiang watershed, Gansu Province, China. Journal of Mountain Science, 14(2), 249–268. https://doi.org/10.1007/S11629-016-4126-9

Ebinger, C. J., Yemane, T., Woldegabriel, G., Aronson, J. L., & Walter, R. C. (1993). Late Eocene–Recent volcanism and faulting in the southern main Ethiopian rift. Journal of. Geological Society, 150,(1), 99–108.

Ebinger, C. J. (1989). Tectonic development of the western branch of the East African Rift System. Geological Society of America Bulletin, 101(7), 885–903.

Erener, A., Mutlu, A., & Düzgün, H. S. (2016). A comparative study for landslide susceptibility mapping using GIS-based multi-criteria decision analysis (MCDA), logistic regression (LR) and association rule mining (ARM). Engineering Geology, 203, 45–55, 45–55.

Ermias, B., Raghuvanshi, T. K., & Abebe, B. (2017). Landslide Hazard Zonation (LHZ) Around Alemketema Town, North Showa Zone, Central Ethiopia - A GIS Based Expert Evaluation Approach. International Journal of Earth Sciences and Engineering, 10(01), 33–44. https://doi.org/10.21276/ijee.2017.10.0106

Firomsa, M., & Abay, A. (2018). Landslide assessment and hazard zonation in ebantu district of oromia regional state western ethiopia. Advances in Science, Technology and Innovation, 1861–1863. https://doi.org/10.1007/978-3-319-70548-4_538

Gariano, S. L., & Guzzetti, F. (2016). Landslides in a changing climate. Earth-Science Reviews, 162, 227–252. https://doi.org/10.1016/J.EARSCIREV.2016.08.011

Getachew, N., & Meten, M. (2021). Weights of evidence modeling for landslide susceptibility mapping of Kabi-Gebro locality, Gundomeskel area, Central Ethiopia. Geoenvironmental Disasters, 8, 1-22.

Girma, F., Raghuvanshi, T. K., Ayenew, T., & Hailemariam, T. (2015). Landslide hazard zonation in Ada Berga district, Central ethiopia- A GIS based statistical approach. Journal of Geomatics, 9(1), 25–38.

DR, G. (1987). Vegetation and slope stability. Slope stability, 187-230.

GSE. (1994). Etiopian Institute of Geological Surveys.

Guzzetti, F., Cardinali, M., Reichenbach, P., & Carrara, A. (2000). Comparing landslide maps: A case study in the upper Tiber River basin, central Italy. Environmental Management, 25(3), 247–263. https://doi.org/10.1007/S002679910020

Guzzetti, F., Carrara, A., Cardinali, M., & Reichenbach, P. (1999). Landslide hazard evaluation: a review of current techniques and their application in a multi-scale study, Central Italy. Geomorphology, 31(1-4), 181-216.

Hasegawa, S., Kumar, Æ. R., Nishimura, T., & Nonomura, Æ. A. (2009). DEM-Based Analysis of Earthquake-Induced Shallow Landslide Susceptibility. 419–430. https://doi.org/10.1007/s10706-008-9242-z.

Highland, L. M., & Bobrowsky, P. (2008). The landslide Handbook - A guide to understanding landslides. US Geological Survey Circular, 1325, 1–147.

Kanungo, D. P., Arora, M. K., Sarkar, S., & Gupta, R. P. (2006). A comparative study of conventional, ANN black box, fuzzy and combined neural and fuzzy weighting procedures for landslide susceptibility zonation in Darjeeling Himalayas. Engineering Geology, 85(3–4), 347–366. https://doi.org/10.1016/J.ENGGEO.2006.03.004

Kebeba, O., Shano, L., Chemdesa, Y., & Jothimani, M. (2024). Integration of geospatial analysis, frequency ratio, and analytical hierarchy process for landslide susceptibility assessment in the maze catchment, omo valley, southern Ethiopia. Quaternary Science Advances, 15(June), 100203. https://doi.org/10.1016/j.qsa.2024.100203

Kirschbaum Dalia, Thomas Stanley, & Zhou Yaping. (2015). Spatial and temporal analysis of a global landslide catalog. Geomorphology, 249, 4–15.

Kursah, M. B., Wang, Y., Bayoh, H. D., & Tarawally, M. (2021). A comparative study on the predictive ability of archived and SBAS-InSAR inventories for landslide susceptibility using frequency ratio model in Western Area, Sierra Leone. Environmental Earth Sciences, 80(10), 1–18. https://doi.org/10.1007/s12665-021-09663-x

Maina-Gichaba, C., Kipseba, E. K., & Masibo, M. (2013). Overview of Landslide Occurrences in Kenya: Causes, Mitigation, and Challenges. Developments in Earth Surface Processes, 16, 293–314.

Martínek, K., Verner, K., Hroch, T., Megerssa, L. A., Kopačková, V., Buriánek, D., Muluneh, A., Kalinová, R., Yakob, M., and Kassa, M. (2021). Main Ethiopian Rift landslides formed in contrasting geological settings and climatic conditions. Nat. Hazards Earth Syst, 3465–3487.

Mebrahtu, T. K., Hussien, B., Banning, A., & Wohnlich, S. (2021). Predisposing and triggering factors of large-scale landslides in Debre Sina area, central Ethiopian highlands. Bulletin of Engineering Geology and the Environment, 80(1), 365–383. https://doi.org/10.1007/s10064-020-01961-1

Mengistu, F., Suryabhagavan, K. V., Raghuvanshi, T. K., & Lewi, E. (2019). Landslide Hazard Zonation and Slope Instability Assessment using Optical and InSAR Data: A Case Study from Gidole Town and its Surrounding Areas, Southern Ethiopia. Remote Sensing of Land, 3(1), 1–14. https://doi.org/10.21523/GCJ1.19030101

Mersha, T., & Meten, M. (2020a). GIS-based landslide susceptibility mapping and assessment using bivariate statistical methods in Simada area, northwestern Ethiopia. Geoenvironmental Disasters, 7(1). https://doi.org/10.1186/s40677-020-00155-x

Meten, M., Bhandary, N. P., & Yatabe, R. (2015). Application of GIS-based fuzzy logic and rock engineering system (RES) approaches for landslide susceptibility mapping in Selelkula area of the Lower Jema River Gorge, Central Ethiopia. Environmental Earth

Sciences, 74(4), 3395–3416. https://doi.org/10.1007/s12665-015-4377-8

Meten, M., PrakashBhandary, N., & Yatabe, R. (2015). Effect of Landslide Factor Combinations on the Prediction Accuracy of Landslide Susceptibility Maps in the Blue Nile Gorge of Central Ethiopia. Geoenvironmental Disasters, 2(1), 1–17. https://doi.org/10.1186/S40677-015-0016-7/FIGURES/9

Pradhan, B. (2010). Landslide susceptibility mapping of a catchment area using frequency ratio, fuzzy logic and multivariate logistic regression approaches. Journal of the Indian Society of Remote Sensing, 38(2), 301–320. https://doi.org/10.1007/S12524-010-0020-Z

Pradhan, B., & Lee, S. (2010). Landslide susceptibility assessment and factor effect analysis: backpropagation artificial neural networks and their comparison with frequency ratio and bivariate logistic regression modelling. Environmental Modelling & Software, 25(6), 747–759. https://doi.org/10.1016/J.ENVSOFT.2009.10.016

Jibson, R. W., Prentice, C. S., Borissoff, B. A., Rogozhin, E. A., & Langer, C. J. (1994). Some observations of landslides triggered by the 29 April 1991 Racha earthquake, Republic of Georgia. Bulletin of the seismological Society of America, 84(4), 963-973. https://doi.org/10.1785/BSSA0840040963.

Raghuvanshi, T. K., Ibrahim, J., & Ayalew, D. (2014a). Slope stability susceptibility evaluation parameter (SSEP) rating scheme - An approach for landslide hazard zonation. Journal of African Earth Sciences, 99(2), 595–612. https://doi.org/10.1016/J.JAFREARSCI.2014.05.004

Raghuvanshi, T. K., Negassa, L., & Kala, P. M. (2015). GIS based Grid overlay method versus modeling approach – A comparative study for landslide hazard zonation (LHZ) in Meta Robi District of West Showa Zone in Ethiopia. The Egyptian Journal of Remote Sensing and Space Science, 18(2), 235–250.

Schuster, R. L. (1996). Socioeconomic significance of landslides. Landslides: Investigation and mitigation, 247, 12-35.

Shano, L., Raghuvanshi, T. K., & Meten, M. (2020). Landslide susceptibility evaluation and hazard zonation techniques-a review. Geoenvironmental Disasters, 7(1), 1–19. https://doi.org/10.1186/s40677-020-00152-0

Solaimani, K., Mousavi, S. Z., & Kavian, A. (2013). Landslide susceptibility mapping based on frequency ratio and logistic regression models. Arabian Journal of Geosciences, 6(7), 2557–2569. https://doi.org/10.1007/s12517-012-0526-5

Tesfa, C. (2022). GIS-Based AHP and FR Methods for Landslide Susceptibility Mapping in the Abay Gorge, Dejen–Renaissance Bridge, Central, Ethiopia. Geotechnical and Geological Engineering, 40(10), 5029–5043. https://doi.org/10.1007/s10706-022-02197-4

Van Westen, C. J., Rengers, N., Terlien, M. T. J., & Soeters, R. (1997). Prediction of the occurrence of slope instability phenomenal through GIS-based hazard zonation. Geologische Rundschau, 86(2), 404-414.

Varnes, D. J. (1978). Slope movement types and processes. Landslides: analysis and control.

Woldemariam, K. W. (2005). Rainfall-triggered landslides in the northern highlands of Ethiopia: Characterization, GIS-based Prediction and Mitigation. na.

Woldearegay, K. (2008). Characteristics of landslides in the highlands of Ethiopia. Journal of Mountain Science, 5(1), 34–39.

Woldearegay, K. (2013). Review of the occurrences and influencing factors of landslides in the highlands of Ethiopia: With implications for infrastructural development. Momona Ethiopian Journal of Science, 5(1), 3.

WoldeGabriel, G., Yemane, T., Suwa, G., White, T., & Asfaw, B. (1991). Age of volcanism and rifting in the Burji-Soyoma area, Amaro Horst, southern Main Ethiopian Rift: geo- and biochronologic data. Journal of African Earth Sciences, 13(3–4), 437–447. https://doi.org/10.1016/0899-5362(91)90107-A

Wubalem, A., & Meten, M. (2020). Landslide susceptibility mapping using information value and logistic regression models in Goncha Siso Eneses area, northwestern Ethiopia. SN Applied Sciences, 2(5). https://doi.org/10.1007/s42452-020-2563-0

Yilmaz I. (2009). Landslide susceptibility mapping using frequency ratio, logistic regression, artificial neural networks and their comparison: a case study from Kat landslides (Tokat—Turkey). J Comput Geoscience, 35, 1125–1138.

Yin, K. L. (1988). Statistical prediction model for slope instability of metamorphosed rocks. In Proceedings of the 5th International Symposium on Landslides (Vol. 2, pp. 1269-1272).

APPENDIX 1.1 Annual Rainfalls Six Station

Precipitation of Bonneia

Year	Jan	Feb	Mar	Apr	May	Jun	Jul	Aug	Sep	Oct	Nov	Dec	Annual
2010	31.64	47.46	105.47	121.29	110.74	68.55	52.73	47.46	26.37	52.73	26.37	5.27	696.09
2011	0	0	15.82	31.64	94.92	58.01	26.37	26.37	42.19	42.19	163.48	10.55	511.52
2012	0	0	5.27	221.48	121.29	15.82	84.38	158.2	89.65	58.01	36.91	52.73	843.75
2013	15.82	0	84.38	221.48	94.92	79.1	100.2	68.55	58.01	116.02	89.65	0	928.12
2014	0	31.64	68.55	116.02	105.47	63.28	79.1	47.46	73.83	126.56	52.73	21.09	785.74
2015	0	0	47.46	195.12	147.66	94.92	47.46	15.82	26.37	142.38	179.3	15.82	912.3
2016	0	15.82	58.01	174.02	126.56	52.73	21.09	26.37	31.64	142.38	47.46	5.27	701.37
2017	0	5.27	42.19	147.66	105.47	63.28	31.64	10.55	47.46	189.84	63.28	0	706.64
2018	0	5.27	58.01	131.84	126.56	47.46	31.64	36.91	63.28	205.66	89.65	0	796.29
2019	0	36.91	116.02	395.51	105.47	36.91	5.27	31.64	36.91	36.91	21.09	31.64	854.3
2020	0	0	36.91	184.57	158.2	42.19	31.64	26.37	26.37	189.84	100.2	36.91	833.2
2021	26.37	5.27	116.02	279.49	158.2	105.47	36.91	58.01	58.01	121.29	15.82	242.58	1223.44
2022	42.19	5.27	26.37	207.7	202.6	28.16	63.66	44.55	39.81	60.61	174.55	14.68	910.13
Average													**826.19**

Precipitation of Sermaile

Year	Jan	Feb	Mar	Apr	May	Jun	Jul	Aug	Sep	Oct	Nov	Dec	Annual

2010	32.64	47.46	105.47	121.29	110.74	68.55	52.73	47.46	26.37	62.73	96.37	5.27	796.09
2011	0	0	15.82	31.64	94.92	58.01	26.37	26.37	42.19	42.19	163.48	10.55	511.52
2012	0	0	5.27	221.48	121.29	15.82	84.38	158.2	89.65	58.01	36.91	52.73	843.75
2013	16.82	0	84.38	221.48	94.92	79.1	100.2	68.55	58.01	116.02	89.65	0	928.12
2014	0	31.64	68.55	116.02	105.47	63.28	79.1	47.46	73.83	126.56	52.73	21.09	785.74
2015	0	0	47.46	195.12	147.66	94.92	47.46	15.82	26.37	142.38	179.3	15.82	912.3
2016	0	15.82	58.01	174.02	126.56	52.73	21.09	26.37	31.64	142.38	47.46	5.27	701.37
2017	17.76	15.31	58.97	360.2	137.08	39.44	35.65	30.03	36.02	80.73	13.25	9.5	833.93
2018	0	5.27	42.19	147.66	105.47	63.28	31.64	10.55	47.46	189.84	63.28	0	706.64
2019	0	36.91	116.02	395.51	105.47	36.91	5.27	31.64	36.91	36.91	21.09	31.64	854.3
2020	0	0	36.91	184.57	158.2	42.19	31.64	26.37	26.37	189.84	100.2	36.91	833.2
2021	26.37	5.27	116.02	279.49	158.2	105.47	36.91	58.01	58.01	121.29	15.82	242.58	1223.44
2022	42.19	5.27	26.37	207.7	202.6	28.16	63.66	44.55	39.81	60.61	174.55	14.68	910.13
Average													**833.88**

Precipitation of Burji

Year	Jan	Feb	Mar	Apr	May	Jun	Jul	Aug	Sep	Oct	Nov	Dec	Annual
2010	5.27	42.19	116.02	179.3	121.29	52.73	42.19	73.83	5.27	58.01	21.09	0	717.19
2011	0	0	5.27	42.19	126.56	47.46	36.91	0	36.91	31.64	158.2	10.55	495.7
2012	0	0	0	263.67	100.2	5.27	47.46	163.48	73.83	63.28	10.55	15.82	743.55

2013	0	0	131.84	274.22	100.2	110.74	94.92	68.55	36.91	131.84	94.92	0	1044.14
2014	0	10.55	47.46	110.74	142.38	31.64	58.01	52.73	63.28	121.29	42.19	31.64	711.91
2015	0	0	36.91	184.57	174.02	147.66	89.65	26.37	47.46	126.56	126.56	42.19	1001.95
2016	0	5.27	58.01	200.39	131.84	84.38	26.37	36.91	21.09	126.56	52.73	15.82	759.38
2017	17.76	15.31	58.97	360.2	137.08	39.44	35.65	30.03	36.02	80.73	13.25	9.5	833.93
2018	0	58.01	184.57	279.49	179.3	47.46	0	58.01	21.09	79.1	47.46	5.27	959.77
2019	0	0	21.09	131.84	168.75	94.92	21.09	52.73	63.28	205.66	89.65	47.46	896.48
2020	15.82	15.82	100.2	263.67	221.48	163.48	47.46	47.46	94.92	168.75	21.09	31.64	1191.8
2021	21.09	5.27	26.37	208.72	190.36	34.88	62.35	79.35	54.87	103.79	292.22	19.13	1098.4
2022	26.76	13.63	46.64	413.94	102.74	73.35	61.39	55.17	42.51	73.97	23.49	11.25	944.83
Average													**873.95**

Precipitation of Amaro

Year	Jan	Feb	Mar	Apr	May	Jun	Jul	Aug	Sep	Oct	Nov	Dec	Annual
2010	5.27	100.2	174.02	258.4	237.3	121.29	79.1	126.56	58.01	116.02	15.82	0	1291.99
2011	0	0	10.55	98.01	226.76	68.55	73.83	15.82	52.73	63.28	253.12	10.55	833.2
2012	0	0	5.27	427.15	158.2	10.55	116.02	348.05	142.38	100.2	36.91	26.37	1371.09
2013	5.27	5.27	189.84	442.97	226.76	189.84	179.3	121.29	105.47	263.67	131.84	0	1861.52
2014	0	36.91	68.55	258.2	232.03	89.65	121.29	79.1	147.66	226.76	73.83	68.55	1302.54
2015	0	5.27	42.19	295.12	258.4	247.85	137.11	73.83	89.65	147.66	163.48	94.92	1455.47
2016	10.55	10.55	73.83	332.23	247.85	121.29	94.92	68.55	58.01	216.21	68.55	21.09	1323.63
2018	0	21.09	63.28	205.66	205.66	89.65	105.47	100.2	121.29	290.04	121.29	5.27	1328.91

2017	0	5.27	42.19	147.66	105.47	63.28	31.64	10.55	47.46	189.84	63.28	0	706.64
2019	5.27	84.38	210.94	384.96	247.85	105.47	10.55	116.02	63.28	89.65	73.83	10.55	1402.73
2020	0	0	5.27	126.56	184.57	174.02	58.01	116.02	147.66	200.39	116.02	94.92	1223.44
2021	36.91	26.37	116.02	332.23	363.87	295.31	84.38	126.56	168.75	295.31	26.37	47.46	1919.53
2022	84.38	15.82	31.64	275.53	191.19	50.28	104.52	162.77	129.14	197.92	345.65	30.41	1619.26
Average													**1401.83**

Precipitation of Maddale

Year	Jan	Feb	Mar	Apr	May	Jun	Jul	Aug	Sep	Oct	Nov	Dec	Annual
2010	31.64	47.46	105.47	121.29	210.74	68.55	52.73	97.46	26.37	162.73	90.37	5.27	1020.08
2011	0	0	65.82	31.64	94.92	98.01	26.37	26.37	42.19	42.19	163.48	10.55	601.54
2012	26.37	5.27	116.02	279.49	158.2	105.47	36.91	58.01	58.01	121.29	15.82	242.58	1223.44
2013	21.09	0	94.92	374.22	368.75	131.84	142.38	110.74	94.92	158.2	221.29	0	1718.35
2014	0	31.64	100.2	258.2	184.57	89.65	116.02	100.2	116.02	189.84	89.65	31.64	1307.63
2015	0	5.27	58.01	289.84	247.85	252.93	116.02	42.19	63.28	274.22	390.04	73.83	1813.48
2016	0	10.55	68.55	300.59	195.12	79.1	82.19	89.65	68.55	189.84	79.1	15.82	1679.06
2017	0	21.09	68.55	147.66	237.3	79.1	79.1	58.01	126.56	263.67	84.38	0	1165.43
2018	0	21.09	68.55	147.66	297.3	99.1	79.1	58.01	126.56	263.67	84.38	31.64	1577.06
2019	0	52.73	126.56	411.33	274.02	94.92	5.27	68.55	73.83	100.2	79.1	21.09	1307.6
2020	0	10.55	73.83	447.85	189.84	94.92	68.55	94.92	84.38	263.67	216.21	89.65	1634.37
2021	36.91	42.19	226.56	464.06	321.68	174.02	73.83	105.47	126.56	174.02	73.83	311.13	2130.26
2022	110.74	15.82	36.91	343	291.34	73.68	106.69	107.63	101.21	253.64	214.53	31.35	1686.54
Average													**1534.32**

Precipitation of Soyama

Year	Jan	Feb	Mar	Apr	May	Jun	Jul	Aug	Sep	Oct	Nov	Dec	Annual
2010	31.64	47.46	105.47	121.29	110.74	68.55	52.73	47.46	26.37	52.73	26.37	36.91	696.09
2011	0	0	15.82	31.64	94.92	58.01	26.37	26.37	42.19	42.19	163.48	242.58	511.52
2012	0	0	5.27	221.48	121.29	15.82	84.38	158.2	89.65	58.01	36.91	14.68	943.75
2013	27.3	35.4	0	125.85	383.1	55.65	20.6	88	97.4	252.6	97.4	36.91	1183.3
2014	5.8	52.6	0	81.6	304.8	105.9	29.4	127.2	162.8	276.8	104	242.58	1254.9
2015	0	3.4	54.8	151.6	247.2	88.2	72.2	12.6	42.2	112.8	138	14.68	978.6
2016	2.3	13.6	44.4	187.2	122.6	102.8	100.6	48	81.6	189.6	36.3	36.91	950.3
2017	0	5.27	42.19	147.66	105.47	63.28	31.64	10.55	47.46	189.84	63.28	0	706.64
2018	0	44.4	97.6	0	242	24.8	47.4	150.4	79.4	74.4	29.2	242.58	789.6
2019	0	46.4	48.6	0	97	33.2	45.8	33.2	26.3	38	30.6	14.68	413.5
2020	0	29.5	7.2	48.8	126.8	202.1	118.2	45.45	50.8	59	18.3	36.91	750.55
2021	43	12.6	16.2	53.4	49	31.8	84.4	57.7	45.7	53.2	6	242.58	953
2022	27.55	8	16	42.2	78.8	3.2	74	55.5	32.95	18.2	17.95	14.68	374.35
Average													**816.62**

APPENDEX 1.2 Logistic Regression

Variables Entered/Removed [a]

Model	Variables Entered	Variables Removed	Method
1	Lithology, Rainfall, Aspect, Stream, Lineament, Curvature, Landuse, Slope[b]	.	Enter

a. Dependent Variable: LS

b. All requested variables entered.

Model Summary

Model	R	R Square	Adjusted R Square	Std. Error of the Estimate
1	.819[a]	.670	.663	.291

a. Predictors: (Constant), Lithology, Rainfall, Aspect, Stream, Lineament, Curvature, Landuse, Slope

ANOVA [a]

Model		Sum of Squares	df	Mean Square	F	Sig.
1	Regression	62.353	8	7.794	92.317	.000[b]
	Residual	30.647	363	.084		
	Total	93.000	371			

a. Dependent Variable: LS

b. Predictors: (Constant), Lithology, Rainfall, Aspect, Stream, Lineament, Curvature, Landuse, Slope

Variables in the Equation

		B	S.E.	Wald	df	Sig.	Exp(B)
Step 0	Constant	.075	.104	.000	1	1.000	1.000

Variables in the Equation

		B	S.E.	Wald	df	Sig.	Exp(B)	95% C.I.for EXP(B)	
								Lower	Upper
Step 1[a]	Slope	0.283	1.043	16.713	1	.000	71.063	9.203	548.750
	Lithology	0.214	.886	6.351	1	.012	9.323	1.643	52.917
	Lineament	-0.029	.726	33.669	1	.000	67.492	16.269	279.985
	Rainfall	0.064	.010	.005	1	.943	1.001	.981	1.021
	Aspect	0.314	.000	.002	1	.963	1.000	.999	1.001
	Curvature	0.058	1.109	.926	1	.336	2.908	.331	25.569
	Stream	0.275	4.870	1.723	1	.189	597.098	.043	8336386.630
	LULC	0.085	.609	11.313	1	.001	7.768	2.352	25.652
	Constant	0.557	.586	7.328	1	.007	.204		

a. Variable(s) entered on step 1: stream, aspect, curvature, lineament, lithology, LULC, RF, slope.